INVESTIGATION OF TRANSVERSE DEPRESSION FORMATION DURING THE CONTINUOUS CASTING OF STEEL USING REAL-TIME MOULD THERMAL DATA

By

Hanson Mark Adjei-Sarpong

B.Sc, The University of Science and Technology, Ghana, 1989

A THESIS SUBMITTED IN PARTIAL FULFILLMENT OF THE

REQUIREMENTS FOR THE DEGREE OF MASTER OF APPLIED SCIENCE

in

THE FACULTY OF GRADUATE STUDIES

(Department of Metals and Materials Engineering)

We accept this thesis as conforming

to the required standard

THE UNIVERSITY OF BRITISH COLUMBIA

August 1994

© Hanson Mark Adjei-Sarpong, 1994

In presenting this thesis in partial fulfillment of the requirements for an advanced degree at the University of British Columbia, I agree that the Library shall make it freely available for reference and study. I further agree that permission for extensive copying of this thesis for scholarly purposes may be granted by the head of my department or by his or her representatives. It is understood that copying or publication of this thesis for financial gain shall not be allowed without my written permission.

Department of Metals and Materials Engineering

The University of British Columbia
Vancouver, Canada

Date August 29, 1994

ABSTRACT

With the need to achieve defect-free steel increasing, traditional methods of billet quality evaluation in the cold state are becoming inadequate as corrective actions can only be taken after the fact. Real-time monitoring of the billet casting process using signals from thermocouples embedded in the wall and other mechanical sensors has become attractive in predicting the occurrence of defects and controlling the appropriate operating parameters to minimize the generation of quality problems on-line. This study examined the formation of transverse depressions in the continuous casting of steel billets using real-time mould thermal data.

A plant trial involving an instrumented mould was carried out at a mini mill designated as Company G. Signals from thermocouples installed in the mould wall, as well as from casting speed and metal level controllers, were sampled at 100 Hz during the casting of steel grades ranging from 0.12 to 0.83 %C with oil lubrication. Three billet samples corresponding to the beginning, middle and the end of each heat were collected and later subjected to metallographic analysis for cracks and solidification structures. Two different shapes of the depressions; "nose"- and smooth-type were identified during the billet samples analysis.

Analysis of the mould thermal data revealed that a transverse depression is manifested as a drop in mould temperature as the depression passes by a given thermocouple position. The depressions were seen to initiate close to the meniscus, and travel down the mould length at the speed at which the strand is withdrawn. A rise in metal level was found to precede the formation of a depression. A mechanism has been proposed to explain these observations. Metal level fluctuations, oil flow rate, and casting speed (relative to section size), are critical parameters to the

generation of the depressions. The mechanism of depression formation and other findings from this study conform to other related observations made in various steel plants. Other factors that were seen to influence the formation of the depressions include steel composition and mould taper.

Table of Contents

List of Tables

List of Figures

ACKNOWLEDGEMENT

I would like to express my sincere gratitude to my supervisors, Professors J.K. Brimacombe and I.V. Samarasekera for their invaluable support and guidance throughout the course of this work.

Mr. P. K. Agarwal organized the plant trial, and his role in this and other areas of the work is greatly appreciated. My gratitude goes to Mr. Neil Walker for his technical assistance in the instrumentation of the mould and the metallographic examinations of the billet samples. My sincere thanks to Mr. P. Wenman for his help in printing the photographs used in this thesis. The fruitful discussions and co-operation of all the "Smart Mould" group members is sincerely appreciated.

I am very grateful to my GOD for HIS protection and blessings, my family, best friend - Evelyn Donkor, and colleagues for their continuing support and encouragement.

Chapter 1: Introduction

The continuous casting of steel billets involves pouring of molten steel at a controlled rate into a water-cooled copper mould and continuous withdrawal of the solidifying strand as shown in Figure 1.1. The withdrawal of the strand is aided by oscillation of the mould and a constant supply of lubricating oil onto the mould wall. The process has been established worldwide due to its higher yield, enhanced productivity, and better quality compared to the conventional ingot casting process.

Within the entire context of the process, the mould is considered to be the heart of the operation since it controls the two most fundamental processes: heat transfer and solidification [1]. The efficiency of heat extraction is ultimately responsible for surface, internal, and shape quality of the cast product, and the productivity of the machine.

Numerous investigations have been undertaken in the past few decades to study the effect of mould design and operating parameters on mould heat transfer, solidification and billet defects. The studies have led to significant improvements in mould operation and product quality.

Despite these achievements, the casting of defect-free billets on a routine basis remains an elusive goal. However, steelmakers are being driven to achieve new levels of quality, owing to competition, increasingly stringent product specifications, and the need to conserve energy by adopting hot-charging and direct rolling practices.

Thus, there is a move to shift from the traditional quality control which has been performed on the cast product in the cold state. Generally, surface quality has been assessed by visual inspection, and internal quality has usually been assessed by sulphur prints or macroetches of

sections cut from the cast product. However, these methods are inadequate because they are performed "after the fact" and do not allow on-line corrective actions to be taken. Considerable effort worldwide has therefore been directed towards the development of systems for monitoring the operation and cast quality on-line so that corrective actions can be taken before it is too late.

This philosophy forms the basis of the present work which is part of an on-going project to develop an "intelligent mould" capable of identifying operational upsets and billet defects and taking corrective actions on-line. The present work was undertaken to investigate the formation of transverse depressions during the continuous casting of plain carbon and boron steels using real-time mould thermal data, and to establish a link between the mould thermal response and the defect.

Transverse depressions (see Figure 1.2) are mould-related surface defects which form either at the midface or at the off-corners of billets. Severe transverse depressions are potential sites for breakouts, and may also result in laps on the billet surface during rolling. In addition, internal cracks that form at the base of the depressions may penetrate to the surface, and cause significant quality problems in the rolled product.

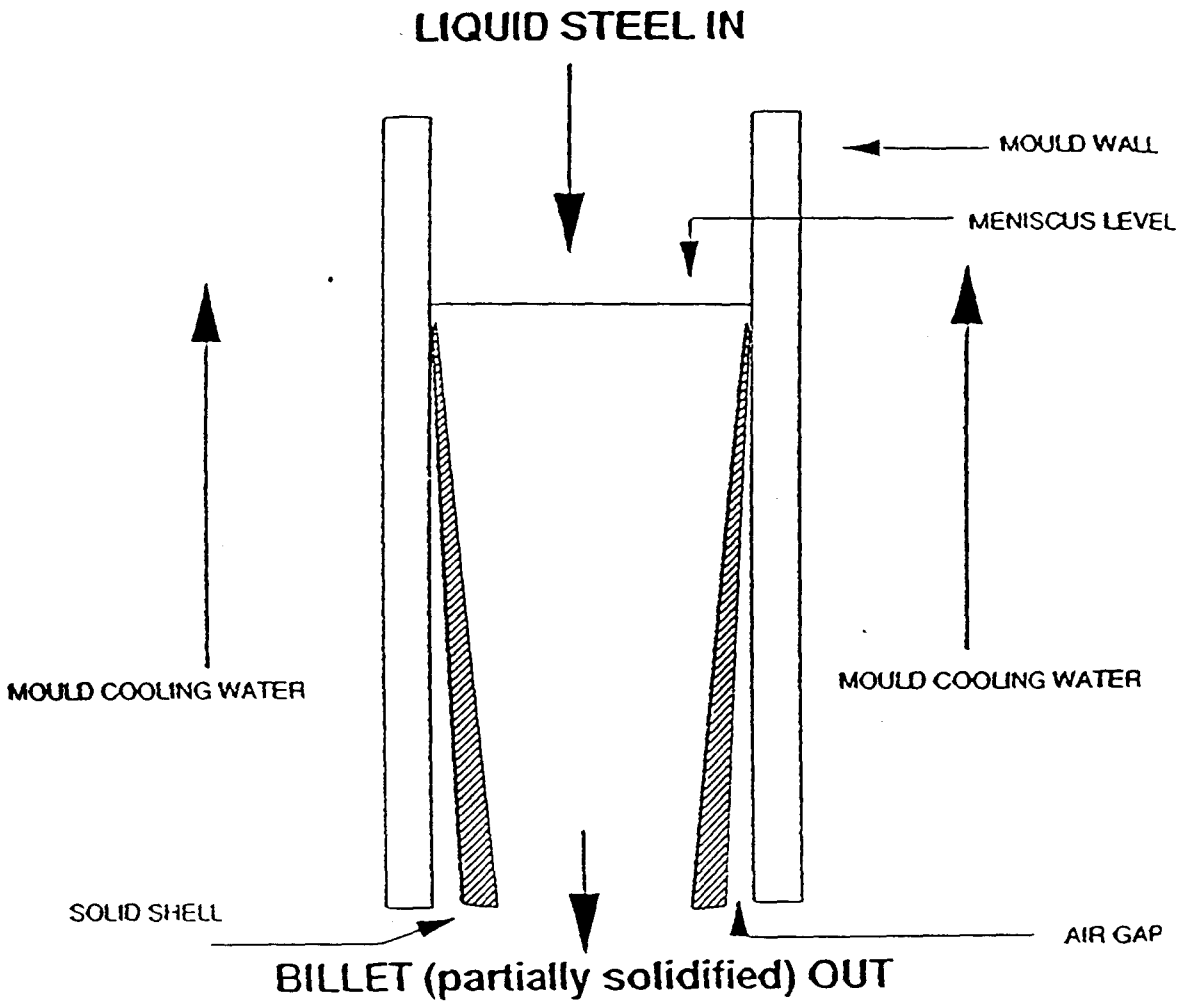

Figure 1.1: Schematic diagram of a casting set-up for the continuous casting of steel billets [2].

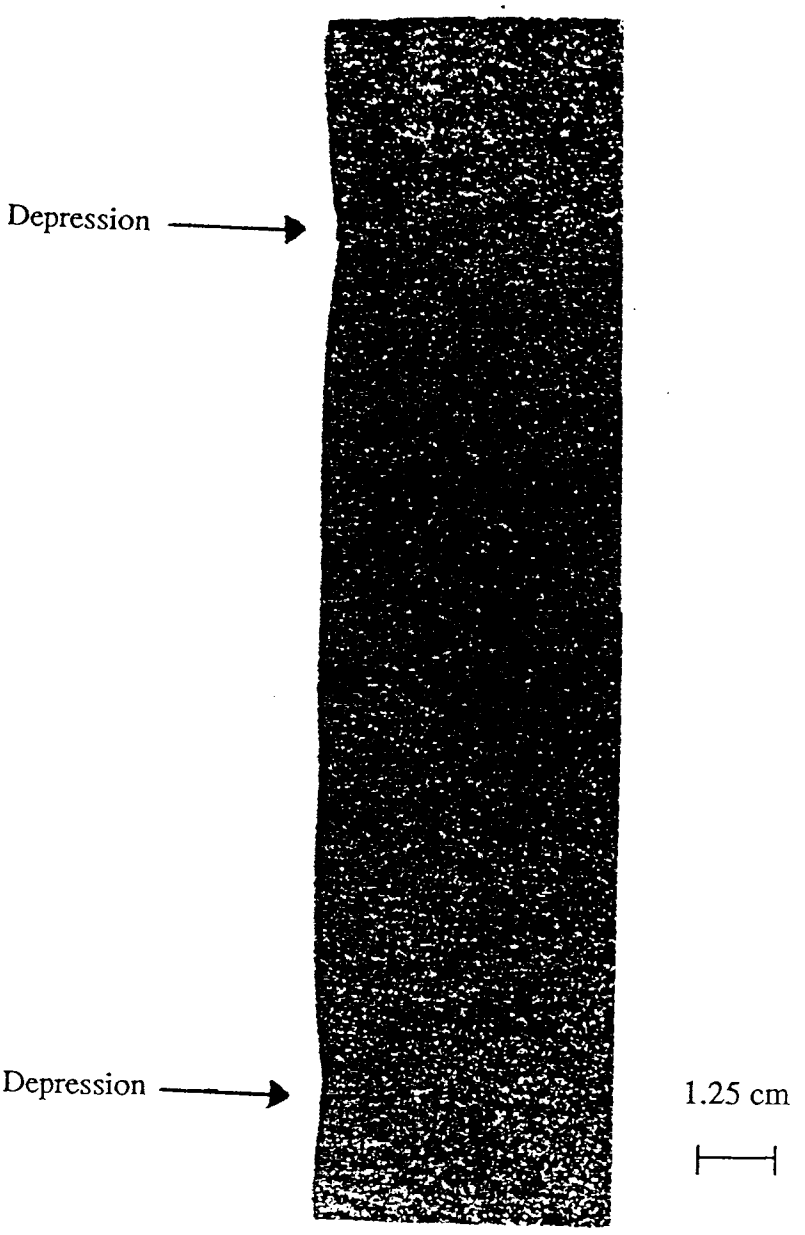

Figure 1.2: Longitudinal section of a billet showing transverse depressions, [2].

Chapter 2: Literature Review

2.1 Transverse Depressions.

In a study of heat transfer in billet moulds, Samarasekera and Brimacombe [3] indicated the significance of mould heat extraction and taper in the formation of transverse depressions. They have linked depressions to sticking and/or binding in the mould as shown schematically in Figure 2.1, and postulated the following mechanism for its formation.

When there is high local mould-shell friction, under conditions of sticking or binding, the shell is subjected to axial tensile strain due to the mechanical pulling of the withdrawal system. Depending on the magnitude of the strain, the shell can begin to flow plastically and form a neck similar to a specimen in an Instron testing machine. The reason is that, at temperatures typically in the mould, between 1150°C and 1430 °C, steel has a high ductility [4]. The necking is manifested as a depression on the billet surface. However, close to the solidification front within about 50 °C of the solidus temperature, the steel has virtually zero ductility so that, under the influence of tensile strain, a transverse crack forms.

Depending on the shell thickness at the time of the crack formation, as well as the extent of necking, the crack may penetrate to the surface. Thus it is common for transverse cracks to be found at the base of transverse depressions. It could be discerned from Figure 2.1 that a crack which has not penetrated to the surface gives a rough measure of the shell thickness at the time of crack formation.

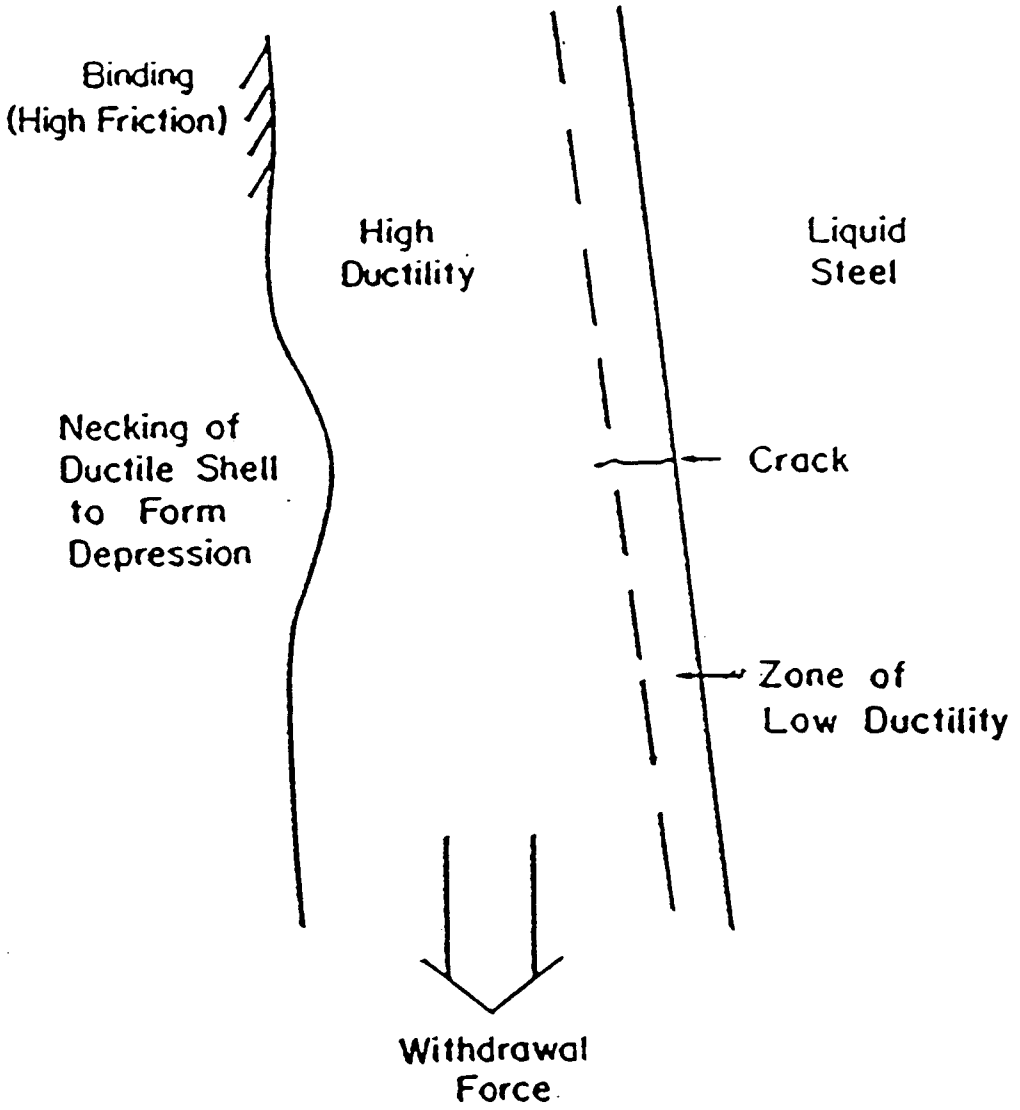

Figure 2.1: Schematic diagram showing the formation of transverse depressions and cracks in a billet due to sticking or binding in the mould [3].

Evidence of the validity of this mechanism has been seen in load cell data analyzed respectively by Brendzy [5], and Chandra [2] in studies where load cells were used to measure mould friction. They observed that the steel grades which exhibited transverse depressions had a higher mould load which fluctuated with time, indicating greater mould-strand interaction.

Excessive taper is therefore crucial to the formation of transverse depressions/cracks, as the strand is more likely to bind in the mould. In addition, factors such as casting speed, steel grade, and oscillation marks which influence heat extraction and shrinkage of the shell are critical.

2.1.1 Taper and Shell Shrinkage.

Solidification begins in the mould, and the resultant shrinking of the shell causes the strand to pull away from the mould wall thereby opening up an air gap between the strand and the mould which consequently influences heat transfer and billet quality. It has been indicated that, among the following steps through which heat is transferred from the liquid steel to the cooling water (convection in the liquid steel pool, conduction through the solid shell, conduction, and to a lesser extent, radiation across the air gap, conduction in the mould and convection at the mould-cooling water interface), the air gap accounts for as much as 84% of the total thermal resistance to heat transfer [6].

Continuous casting moulds are tapered inwardly to compensate for the billet shrinkage; and the resulting reduction in the air gap improves the rate of heat extraction. However, excessive taper can cause difficulty in the withdrawal of the strand [8,9], which promotes mould wear [8,10], and, in extreme cases, causes the billet to jam in the mould [7] leading to the generation of transverse

depressions. On the other hand, lack of sufficient taper can lead to bulging of the shell in the mould, which in turn, generates other quality problems such as off-corner internal cracks [32]. Thus an optimum taper is important to minimize or eliminate many mould-related defects.

Billet moulds may either be single or multiple tapered, and each of the designs has implications for quality. The key element to mould design is to be able to define clearly the mould-strand gap which in simple terms depends on the distortion of the mould [11,12] and shrinkage of the strand. The analysis of the gap is, however, complex since the shrinkage of the shell and the distortion of the mould depend on many variables such as steel composition, casting speed, metal level variations, and cooling water velocity. Further complications result from the fact that the gap varies in width in the transverse plane [13].

The effect of steel composition on taper requirements have been reported in earlier studies [7,14] , which noted that the mould taper desired to compensate for the air gap is influenced by the carbon content. A detailed study of the effect of steel grade on mould taper requirements was undertaken by Chandra [2], and he concurred that it is impossible to design a universal mould through which all steel grades can be cast, due to the dissimilar shrinkage characteristics of different grades of steel.

Significantly, he pointed out some fundamental misconceptions in previous taper design relating to heat transfer. Measurements of mould heat transfer at several mini-mills has shown that, a steep upper taper design aimed at enhancing heat transfer actually ends up reducing heat transfer at the meniscus due to decreasing mould-strand interaction. A steep upper taper prevents the mould wall from acquiring a net negative taper during casting thereby reducing mould-strand interaction and heat transfer. It has also been shown that excessive mechanical interaction can lead to deep

and non-uniform oscillation marks, off-squareness, off-corner internal cracks and laps [2,32,72]. This work has led to better estimation of taper requirements for casting low- and high-carbon grades for improved quality.

At the meniscus, grades with long freezing range (C>0.6%), have thinner shells and are susceptible to tearing. If lubrication is not adequate, sticking of the shell to the mould can lead to tearing, and bleeds and laps. Since lubrication is affected adversely when the hot face temperature of the mould is high enough to vaporize the oil, such grades need to be cast in moulds with steep upper taper designed to reduce heat transfer in the meniscus area, to ensure that a liquid film of oil is present on the mould wall.

The effect of casting speed on billet moulds taper requirements, and its influence on transverse depression formation was studied by Samarasekera and Brimacombe [3]. They reported that when employing double-taper moulds a larger taper is required in the upper zone for the casting of large sections at low casting speeds, whilst in the lower zone the taper requirements are much less than for smaller sections cast at higher speed. This stems from the reduced heat extraction in the lower part of the mould, owing to thermal resistance of a thicker shell associated with relatively low casting speeds. Thus, in relation to billet quality, sticking or binding could occur when casting large sections at low speeds in moulds with steep tapers in the lower region which may lead to the formation of transverse depressions and cracks.

Mould cooling water velocity was also found to affect mould distortion, and consequently taper requirements [9]. It was found that, the use of low cooling water velocity resulted in greater distortion of the copper mould tube because of higher operating temperatures.

2.1.2 Lubrication.

Mould heat transfer and friction have been found to be influenced to a great extent by lubrication. Mineral or vegetable oils, and occasionally a blend of the two are used during casting. The effectiveness of oil lubrication is related to the oil type, flow rate, and some important characteristics as: viscosity, flash point, fire point, and boiling point. The liquid lubricant is pumped to the top of the mould into an oil channel from which it weeps through a narrow slot onto the mould hot face. The velocity of the oil down the mould wall is dictated by the oil feed rate and the viscosity which is a function of the mould wall temperature [5].

Oil viscosity determines the resistance to oil flow down the mould wall. The flash point is the temperature at which the oil burns off before it reaches the metal level, while the boiling point of the oil refers to the temperature at which it vaporizes. To ensure proper lubrication it is important that the peak hot face temperature of the mould is lower than the boiling and flash points of the oil.

When the lubricating oil comes in contact with the liquid steel at the meniscus it vaporizes and pyrolyzes, and part of it escapes as gas while some of it is trapped in the gap between the mould and the solidifying shell during the downstroke of the mould [15,16,17]. The gas trapped in the mould-strand gap is reported to enhance heat transfer [2]. In an experiment to study the effects of oil type and flow rate on an operating caster, Chandra [2] found that mould temperatures were higher for vegetable-based oils than mineral oils at low flow rates. This was due to the enhancement of thermal conductivity in the air gap by the presence of hydrogen gas. It caused an observed increase in heat flux when oil flow rate was increased from 0 ml/min to 25 ml/min. The no-oil

experiment had little or no hydrogen gas in the air gap. It was, however, reported that an increase in flow rate from 25 to 100 ml/min did not yield a significant increase in heat flux compared to an increase in oil flow from 0 to 25 ml/min.

Mould lubrication is known to affect billet surface quality. Adverse lubrication conditions in the meniscus area causes sticking of the strand to the mould. Saucedo and Blazek [18] reported the significance of lubrication when they observed that mould oscillation without a lubricant could not prevent sticking. Sticking hinders smooth removal of the strand from the mould and leads to the generation of quality problems in billet quality - transverse depressions and breakouts. Insufficient lubrication increases the tendency for sticking. It is thus essential to have proper lubrication to ensure good billet surface quality. Excessive supply of oil however is uneconomical [2] and leads to entrapment of hydrogen and pinhole formation in the billet.

The sensitivity of mould-strand interaction to oil-type and flow rate was reported by Brendzy [5]. Load cells employed as friction measuring devices revealed an increased mould-strand interaction resulting from a reduction in oil flow rate. However, in a similar work, Chandra [2], reported that there was no influence of either oil type or flow rate on mould friction as indicated by load cells. This may be attributed to the reported high operating hot-face temperature (approximately 350 °C - above the boiling point of the lubricating oil). In this case oil type and flow rate may have little or no influence because the oil vaporizes and very little will be left for lubrication.

2.1.3 Oscillation Characteristics.

The concept of mould oscillation was first introduced by Junghans [19], and was responsible for the commercialization of continuous casting. Without it mould-strand friction is excessive, and smooth withdrawal of the shell without tearing is nearly impossible.

During operation, the mould is oscillated up and down with a stroke of 5 to 20 mm and a frequency of 2 to 4 Hz. During the downstroke, the maximum downward speed of the mould becomes higher than the withdrawal speed of the strand and this period of time is known as "negative strip". This is a concept originally proposed by Halliday [21] as a means to overcome shell tearing due to the drag effect associated with the initial design which did not ensure relative velocity between the mould and strand and resulted in excessive shear force [17]. In addition to negative strip, there is another concept known as mould lead which is basically the displacement of the mould relative to that of the strand during negative strip. Figure 2.2 is a schematic diagram of the components of mould oscillation. Mathematically negative strip time, t_N, and mould lead, L_M, are respectively expressed as follows:

$$t_N = \frac{1}{\pi f}\cos^{-1}\left(\frac{v_c}{\pi f S}\right) \tag{2.1}$$

$$L_M = S\sin(\pi f t_N) - V_c t_N \tag{2.2}$$

where V_c, S, and f are respectively casting speed, stroke length, and oscillation frequency.

The oscillation influences the formation of oscillation marks on the strand at regular intervals which have significant effect on billet quality as will be discussed later. For sinusoidal oscillation, the distance d between the oscillation marks is related to the casting speed and oscillation frequency as follows:

$$d = \frac{V_c}{f} \tag{2.3}$$

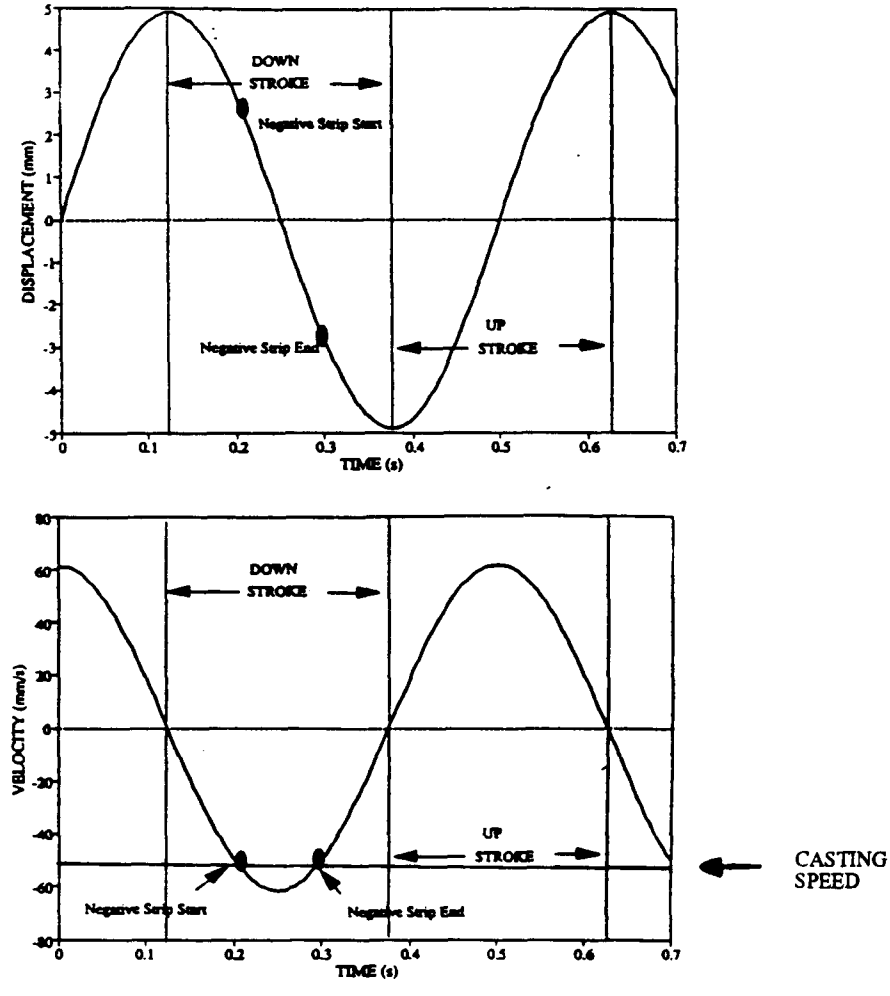

Figure 2.2: Schematic diagram showing the components of mould oscillation [2].

2.1.4 Tundish Streams

Recently, it is becoming evident that the quality of the final product is affected by tundish stream character. The nature of tundish streams are influenced by ladle streams, and the design of the tundish. In turn, tundish streams affect liquid steel flow patterns in the mould and metal level fluctuations. The stream character influences the degree of re-oxidation which occurs by atmospheric contact during pouring operation.

Tundish streams may be shrouded or not depending on the application of the final product and the level of quality required. Shrouding of the stream prevents interaction of atmospheric air with the liquid stream, and decreases the entrainment of oxygen. When liquid steel is poured through air, re-oxidation can take place at several different locations; it can occur between the tundish and mould as a result of contact between the stream and air, or in the mould due to reaction between air entrained in the falling stream.

A rough stream has a higher surface to volume ratio and entrains more air causing increased turbulence in the mould and excessive splashing. With a turbulent pool, new liquid is continuously brought to the surface where further contact with air can occur. Turbulent pools give little opportunity for proper separation of re-oxidation products. These oxides, in the form of mould scum are displaced to the outside of the mould where they can be entrapped in the freezing interface of the strand.

The effect of ladle stream position in the tundish on the surface condition of billets was studied by Maddever and co-workers [22,23]. The experiment employed open stream pouring from ladle-to-tundish, and tundish-to -mould. The tundish had three nozzles located in the bottom within

square-shaped wells, and a dam at the pouring box to minimize turbulence produced by the incoming ladle stream. In order to simulate the irregularities of tundish streams, the ladle stream was closed and opened after every 10-20 seconds. They observed that, the two streams closest to the pouring box were always turbulent anytime the ladle stream was turned on, while the other stream farther away from the pouring box was smooth and pencil-like. On the other hand, when the ladle stream was off, the two streams closest to the pouring box had a smooth pencil-like behavior as the other one. Examination of billet samples revealed that billets from the strands closest to the pouring box had a higher percentage of surface slag patches. By experimenting with various nozzle configurations, they noted that the nature of the tundish streams was influenced by nozzle configuration, and that, stable streams which are unaffected by turbulence in the tundish could be obtained with proper nozzle design. A similar deleterious effect of turbulence generated in the entry region of ladle stream on tundish streams was also reported by Heaslip et al. [24]. Figure 2.3 (a,b) schematically show the influence of tundish stream character on the pattern of flow within billet moulds.

Smooth streams entrain very little air within the pool, while rough streams entrain a considerable amount of air within the pool. Penetration was found to be shallow, with strong upward currents caused by the rising bubbles in the case of rough streams, and was associated with considerable surface activity.

Flow studies carried out by Kemeney and co-workers [25] indicated that tundish flow patterns are controlled under all conditions when weirs and dams are used in combination. "Weirs" and "dams" are partial dams covering the complete width of the tundish from above and below the liquid pool surface respectively. They noticed that flow patterns in the tundish with no flow modifications

had some stagnant regions, which were found to lower the retention time of fluid in the tundish. The effect was that separation of non-metallic inclusions from the molten steel was hindered, and more inclusions were carried into the mould. In contrast, the use of weirs and dams increased the minimum retention time by slowing the flow, thereby providing maximum opportunity for inclusion separation. In addition, on exiting the weir the fluid is forced toward the surface of the liquid pool by the dam, and thus increasing the probability of non-metallic separation. As opposed to the use of weirs only, the flow pattern was observed to be insensitive to changes in flow rates, tundish level, or casting speed. Figures 2.4 (a,b) depict schematically the flow patterns in a tundish with and without flow modifications.

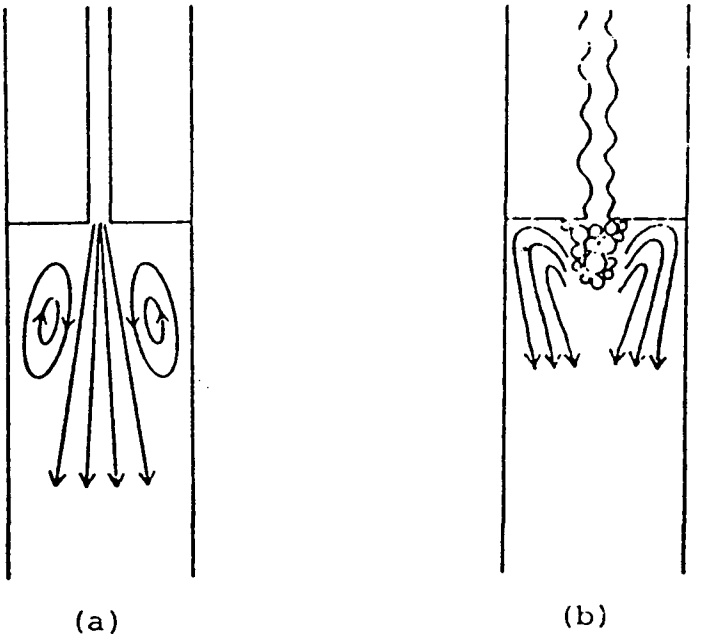

Figure 2.3: Schematic diagram showing the influence of tundish stream character on flow patterns within billet moulds (102 X 102 mm or greater in cross-section); a) flow pattern produced by a smooth stream, b) flow pattern produced by a rough stream. [22,23]

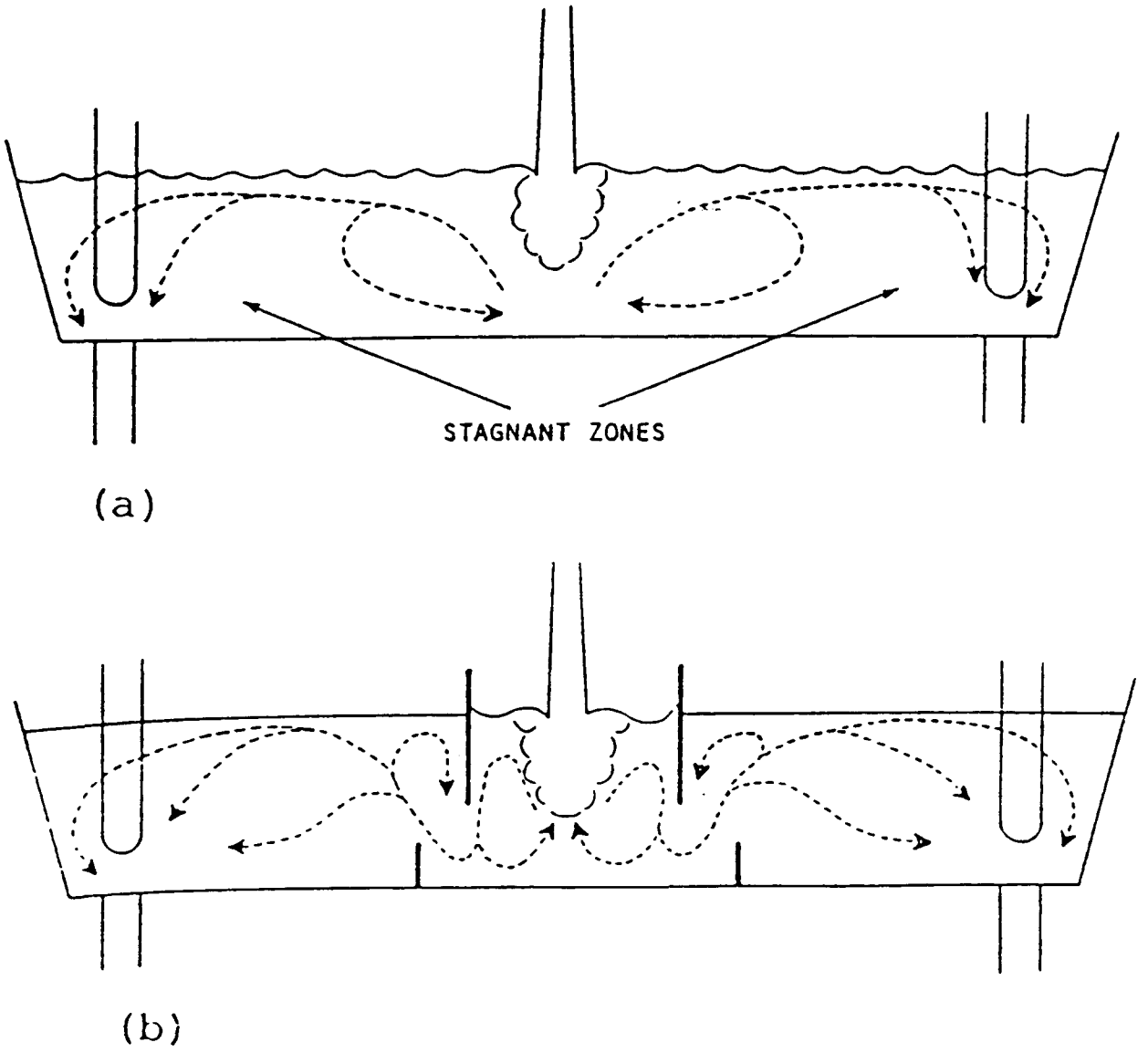

Figure 2.4: Schematic diagram showing flow patterns with and without flow modifications; a) flow pattern in a conventional tundish with no flow controls, b) flow pattern in a tundish with weirs and dams. [25]

2.1.5 Effect of Steel Composition on Transverse Depression Formation.

The mechanism for transverse depression formation as discussed previously indicates that, for the same taper and casting conditions, the steel grades which shrink the least are likely to bind in the mould and lead to the generation of transverse depressions. Heat transfer and solidification studies of plain carbon steels in the past have indicated that low carbon steels are susceptible to transverse depression formation compared to medium and high carbon grades [2,3,5]. The reason is that low carbon grades, containing about 0.10 to 0.14 %C, have wrinkled surfaces due to shrinkage associated with the $\delta \rightarrow \gamma$ solid state phase transformation; this results in lower heat transfer to the mould as a result of which cooling and shrinkage of the shell are reduced.

With regard to boron grades, there are reports in the literature on the benefits such as increased hardenability [79,80] and problems such as nozzle clogging and transverse cracking associated with continuous casting of boron-containing steels [71,78] , mostly in slab casting. There are however no reports of transverse depression formation in these grades of steel.

2.2 Other Mould-Related Quality Problems

The thermo-mechanical behavior of the mould has been reported to be the origin of most mould-related quality problems [11,12,14,26-34]. Samarasekera and co-workers [11] reported that, during operation, the mould distorts and changes shape in response to internally generated thermal stresses. The distortion of the mould arises from a combination of thermal expansion due to non-uniform heating of the mould wall, the restraint of the free expansion of the copper tube by the mould support system and the geometric configuration of the mould itself. Thus, the mould tube bulges with the maximum bulge occurring at about 50 to 100 mm below the meniscus where

the mould is hottest. This results in a region of negative taper above the point of maximum bulge, and a positive taper below it. Furthermore, it was shown that the bulge was not static, but changes dynamically in response to mould temperature fluctuations caused by metal level fluctuations and nucleate boiling in the cooling channel. If the stresses in the mould wall exceed the yield stress of the copper, permanent distortion occurs.

Other variables which influence the magnitude of the bulge and its position relative to the top of the mould are the cooling water quality and velocity, mould tube alignment and tolerances, position of the mould tube constraint relative to the top of the mould, and mould wall thickness.

Poor water quality due to high hardness level, the presence of corrosion products, oil, grease or biological fouling stemming from algae and moss, has been identified to affect the thermal field and the distortion of the mould tube. This is linked to the deposition of scale from the cooling water on the cold face of the mould tube. The presence of even a relatively thin layer of scale introduces a large resistance to heat flow locally and raises the mould temperature. The consequence is an increase in the bulging of the mould tube [26].

The mould cooling water velocity strongly affects thermal distortion of the mould tube. It has been established that lower water velocity leads to an increase in both the magnitude of the negative taper below the metal level and the peak distortion [26]. Low cooling water velocity (<8m/s) promotes nucleate boiling in the cooling channel, which causes the heat transfer coefficient at the mould-cooling water interface to fluctuate resulting in dynamic changes to mould temperature and shape. Water velocity in excess of 12 m/s is required to prevent boiling [33].

It is essential to maintain uniform water flow around the periphery of the mould to avoid localized excessive heating of the mould and associated distortion of the mould tube. Maintaining proper mould tube alignment, and close tolerances on the dimensions of the water jacket are key to ensuring uniform water flow in the channel [33]. Small changes in the water gap dimensions can lead to a drastic change in the cooling water velocity.

With regard to mould wall thickness, it has been determined that thicker mould walls give rise to smaller negative taper at the meniscus [33].

A four-sided constraint to support the mould tube has been found to be superior to two-sided constraint. The two-sided constraint system gives rise to non-uniform mould distortion and greater bulging at the off-corners relative to the midface [33]. The constrained sides deform more than the unconstrained sides.

2.2.1 Oscillation Marks

Oscillation mark on the surface of billets increase the air gap between the mould and the solidifying shell, thereby influencing heat transfer and solidification. Control of the depth and uniformity is therefore important from the view point of billet quality.

Samarasekera et al. [34] proposed that oscillation marks form because of the mechanical interaction between the mould and the strand during negative strip period. It was postulated that during the period of negative strip, when the mould is moving faster than the strand, the mould, owing to its negative taper at the meniscus bears down on the newly solidifying shell near the meniscus and cause the solid to buckle to form an oscillation mark.

It was, however, indicated in a later study in which the mould did not acquire a negative taper that oscillation marks form primarily as a result of the relative velocity between the mould and the strand during negative strip period at the meniscus [72]. The relative motion causes the strand to decouple from the mould through buckling of the newly forming shell leading to the formation of an oscillation mark as shown in Figure 2.5. An observed smooth decompression of load cell response during negative strip period was explained to have resulted from the relative motion between the mould and the strand during the negative strip period. As originally reported by Samarasekera et al [34], the extent of interaction was found to be influenced by the shape of the mould at the meniscus. They observed that billets cast through a shallower taper (2.75 %/m) which assumed a negative taper during operation had deeper oscillation marks than those from a steeper taper (4.9 %/m) which did not assume a negative taper. The minimum load (decompression) was found to be related to casting speed. As casting speed increases, negative strip time decreases, and the minimum load recorded during the downstroke increases because there is less time for the decoupling

Another theory based on mechanical deformation was also proposed by Wray [35]. He proposed that the first solid forms against the mould wall, and once formed, it "wrinkles" away due to internal thermal-mechanical stresses induced by the severe temperature gradients existing in the shell. This wrinkling effect is considered responsible for the formation of oscillation marks.

The theory based on mould-strand interaction has also been reported by other authors [36,37], and seems to have more credence compared to the latter owing to the following observations [34,38]:

(i) negative strip time and factors that influence the distortion of the mould tube have been identified to affect the depth and uniformity of the oscillation marks [34,38]

(ii) a reduction in the negative strip time from 0.21-0.12 s reduced the depth and improved the uniformity of oscillation marks on the billet surface. The recommended optimum range for negative strip to minimize sticking, as well as problems associated with deep and non-uniform oscillation marks, is 0.12 to 0.15 s.

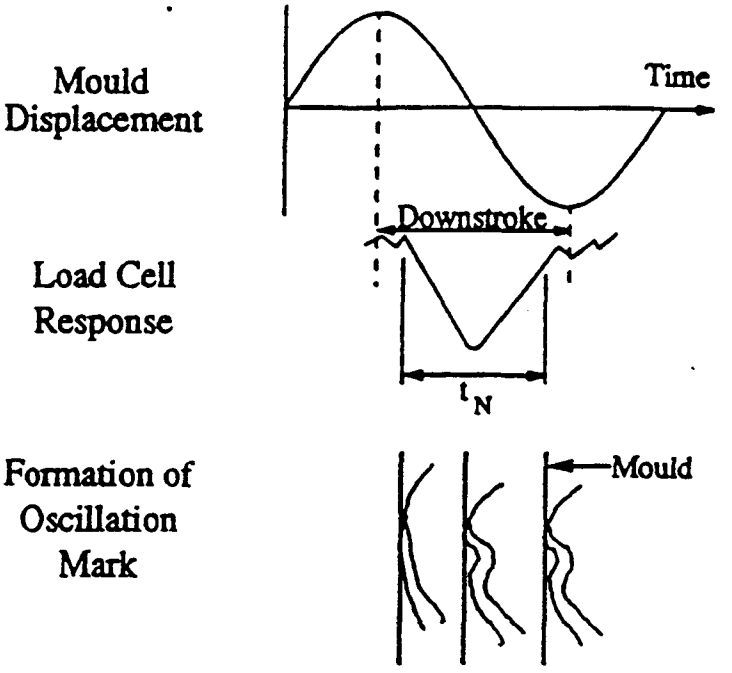

Figure 2.5: Mechanism of oscillation mark formation [72].

2.2.2 Off-Corner Internal Cracks.

Off-corner internal cracks, also referred to as hinge cracks, are usually found at one or several of the eight off-corner locations of a billet. They may be observed in the transverse sections of the billet. They occur roughly at a distance of about 15 mm from a given corner, and 4 to 6 mm from the surface. In most cases the outer tips of the cracks overlap with white solidification bands (in macroetches), a feature which has been described as due to the disturbance of interdendritic liquid [32]. This suggests that both phenomena originate at the same time as the bulging of the shell. The bulging of the shell disturbs the interdendritic liquid.

The mechanism put forward by Brimacombe and co-workers [32] indicates that off-corner internal cracks are generated by bulging of a face or faces of the billet in the lower part of the mould where the mould-strand gap is large especially with single tapered moulds. This leads to generation of tensile strains at the solidification front in those regions leading to internal cracks as shown in Figure 2.6. Thus cracks can form and continue to grow inwards following the solidification front, as it advances, as long as the strain is maintained.

It is clear from the above mechanism that sites which have the deepest oscillation marks are prone to off-corner internal cracks. It was reported that deep oscillation marks in the off-corner regions reduce the rate of heat extraction and the shell growth as the strand passes through the mould [32]. Design parameters such as taper, and steel chemistry are critical to the incidence of cracking. Furthermore, operating variables such as mould cooling water velocity, casting speed and oscillation characteristics may influence the bulging and the extent of cracking.

2.2.3 Rhomboidity

Rhomboidity is a shape problem. In square billets the term "off-squareness" is often used to describe it whereas in rounds this shape problem is referred to as "ovality". The difference between the two diagonals is a measure of the severity of the problem in square or rectangular shapes. In rounds, the difference between the longest and shortest diameters is used as the measure. An upper limit of 6 mm has been imposed for this difference in diagonals. Severely rhomboid billets pose problems in pusher type reheat furnaces and also during rolling where the corners may roll and generate seams in the final product.

The mechanism for the generation of rhomboidity, as in off-corner cracking has been linked to oscillation mark formation and non-uniform heat extraction, in the mould and in the sprays. The problem usually begins with the formation of deep and non-uniform oscillation marks around the periphery of the billet. In the vicinity of deep oscillation marks, the rate of heat extraction is low due to a wide mould-strand gap. On the other hand, regions of the billet having shallow oscillation marks experience higher heat extraction. Thus the presence of non-uniform oscillation marks gives rise to non-uniform heat extraction rates around the periphery of the billet which ultimately leads to a solid shell having non-uniform thickness. The situation is further exacerbated by regions of the shell that are cooling more rapidly, shrinking and pulling the obtuse-angle corners farther from the mould wall. Although the billet exiting the mould is reasonably square, it may have a non-uniform solid shell as shown in Figure 2.7 [32]. In the sprays, the colder portions of the billet having a thicker solid shell tend to cool faster than the hotter regions because of the longer thermal path and the effects of unstable boiling, consequently leading to non-uniform shrinkage of the billet and generation of rhomboidity.

The above mechanism is supported by the following observations made on square billets during casting:

i) the obtuse angle of rhomboid billets have the deepest oscillation marks.

ii) the billets emerging from the mould when observed through a peep-hole showed that, of the two corners in view, one was cold(dark), and the other was hot(bright). Subsequent billet inspection of the cooling bed indicated that the acute-angle corners in the billet corresponded to the colder corners whereas the hot corners formed the obtuse angle of the billet.

Asynchronous intermittent boiling of the cooling water channel has also been linked to the generation of rhomboidity in the billet [63]. It is proposed that mould distortion varies with time as the boiling events change asynchronously on different faces and cause non-symmetrical cooling of the billet due to changing air-gap width. The orientation and severity of the rhomboidity varies during the heat due to this phenomenon which supports the above mechanism. Further, this observation is useful as it can be employed to distinguish rhomboidity due to asynchronous intermittent boiling from that caused by other factors such as machine alignment, wobbly mould oscillation, or poor spray cooling. In the absence of any mould effects, rhomboidity must be caused by asymmetric spray cooling.

Factors relating the thermo-mechanical behavior of the mould and the nature of the mould-strand interaction are critical, since the problem has been linked to deep and non-uniform oscillation marks on the billet surface. Hence, mould distortion, taper, oscillation characteristics, and lubrication parameters are important. The use of adequate cooling water velocity, good quality water, close tolerances with respect to the water gap, and proper mould tube alignment are essential in minimizing or eliminating the incidence of asynchronous boiling.

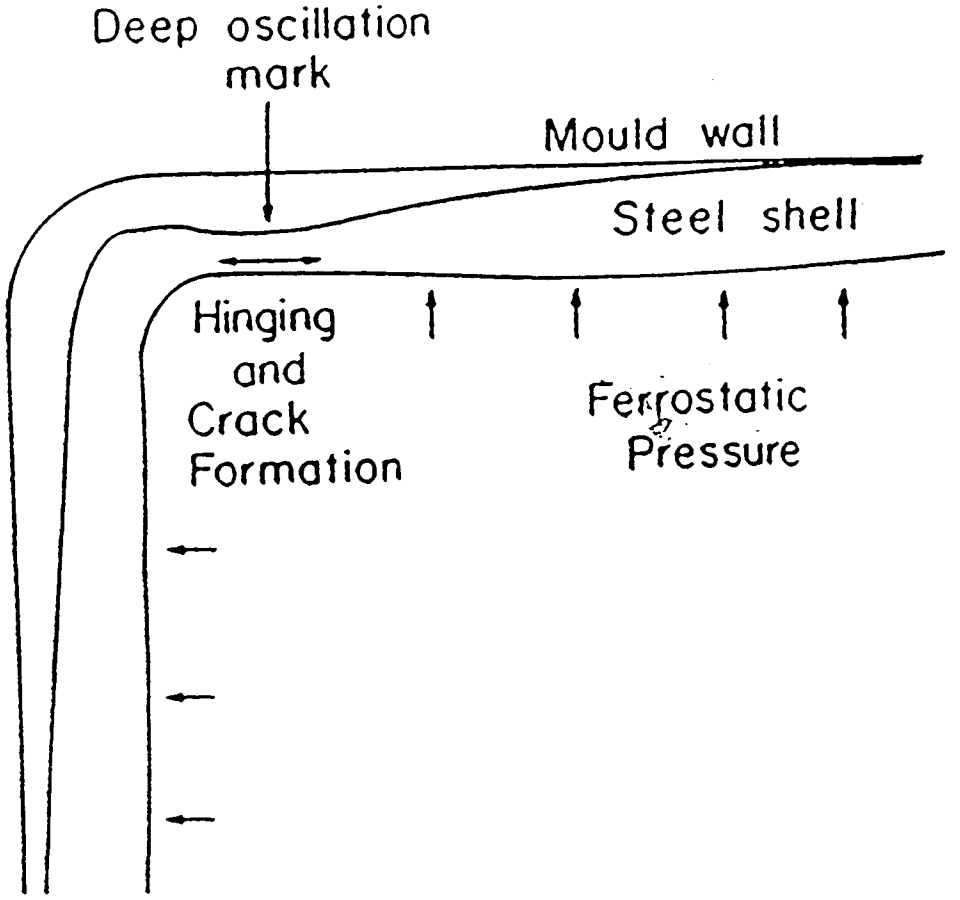

Figure 2.6: Schematic diagram illustrating the mechanism for generation of off-corner internal cracks due to bulging and hinging of the shell [32].

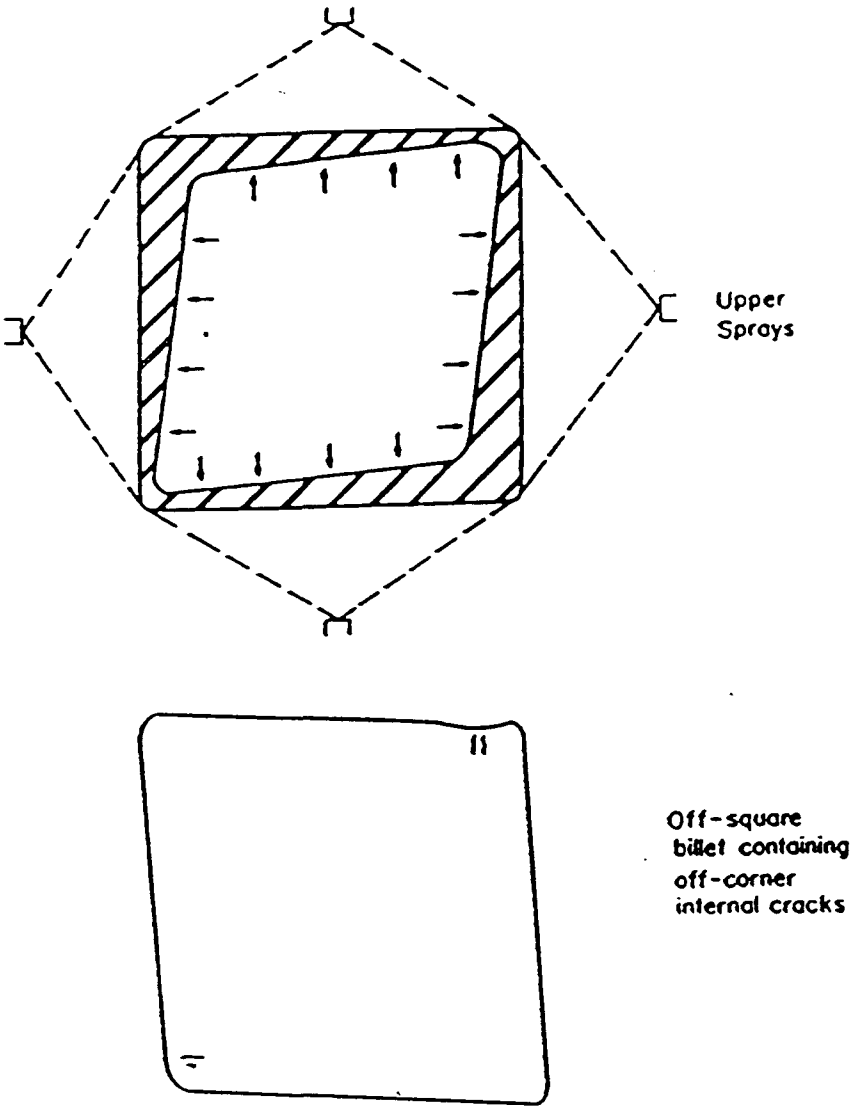

Figure 2.7: Schematic diagram showing a billet with non-uniform shell thickness being distorted into a rhomboid shape by spray cooling [32].

2.2.4 Breakouts.

Breakouts occur when there is rupture of the shell as a result of which molten metal flows out beneath the mould. This is a serious problem because, not only does it hamper productivity but it is also a safety hazard. Breakouts are linked to the presence of a thin weak solid shell at the mould exit. The shell may be thin at localized regions or all round the billet periphery. The presence of cracks may also lead to breakouts, particularly if the cracks act as stress concentration sites and aid the rupture of the shell.

Samarasekera and Brimacombe [39] have indicated that, in billet casting, breakouts sometimes occur close to transverse depressions (with cracks), and very close to the obtuse corners which are hotter and have thinner solid shell. The presence of depressions or deep oscillation marks on the billet surface increases the mould-strand air gap which, in turn, influences the generation of thin shells especially in those regions of the mould where thermal resistance of the air gap dominates the mould heat extraction.

They also related breakouts to sticking in the mould due to poor lubrication. About 79% of breakout occurrence is reported to be caused by shell sticking [40]. The following mechanism have been proposed for sticking related breakouts [41]. When a portion of the shell adheres to the mould wall, the continuing withdrawal of the strand causes it to tear. Molten steel then fills the gap, and upon contacting the mould wall forms a new shell at this location. This new, and very thin, shell is subsequently ruptured as described above, due to the opposing forces of the upward oscillation stroke and the downward strand withdrawal. As described earlier, another thin shell is formed due to the inflow of molten metal. This sequence is repeated continuously as a function of the oscillation

frequency. The tear often referred to as "pseudo-meniscus", gradually moves down the mould with a speed reported to be 50-95% of the casting speed. The variability of the speed is due to differences in steel chemistry, casting speed, and oscillation parameters [42-44].

Scum entrapment between the shell and the mould wall, has also been linked to breakouts especially in slab casting. This leads to the formation of an extremely thin shell such that once the strand exits the mould, this region of the shell may rupture to create breakout.

2.2.5 Bleeds and Laps

As the name implies this defect is basically bleeding of liquid steel from a torn shell which rapidly solidifies and forms laps on the strand. It is attributed to adverse lubrication conditions that usually arise in moulds with hot face temperature higher than the boiling point of the lubricating oil. Strands with an initial shell that is thin are highly susceptible, particularly grades with carbon content exceeding 0.6% as noted by Chandra [2].

2.3 Friction and Temperature Measuring Devices.

2.3.1 Friction Measuring Devices.

Mould friction can be monitored by accelerometers, load cells, or by strain gauges.

2.3.2 Accelerometers

Accelerometer-based friction monitoring systems center around piezoelectric transducers attached directly to the mould wall. The mechanical vibrations transmitted through the mould are

converted to discrete electrical pulses by the accelerometer, and these electrical signals are in turn recorded by a computerized data acquisition facility. The most widely known use of accelerometers for mould friction monitoring is the ML TEKTOR developed at C.R.M. [45-47]. Accelerometers have also been used to monitor the motion of the mould, and it was indicated that mechanical faults not easily detected by routine visual inspection could be identified [48].

2.3.3 Load Cells

As far as mould friction measurements are concerned, load cells have probably been the most widely used. Unlike accelerometers which can be located directly on the vertical mould wall, load cells are usually located between the mould and the oscillator table [5,49,50], with one load cell usually at each of the four corners. Load cells have also been installed on the two supporting arms beneath the oscillating table.

Since load cells are highly dependent on the type and flow rates of mould lubricants many load cell applications are restricted to the evaluation of casting parameters, and the mechanical performance of the machine [51]. The problems associated with load cells are the mould inertial forces and the distribution of load between the sensor and other mechanical components such as bolts securing mould to the oscillator table. Signals from load cells located adjacent to the water O-rings have been reported to be dampened [5].

2.3.4 Strain Gauges

In comparison to accelerometers and load cells, strain gauges are generally located on the oscillator shaft. While this remote location provides ease of installation and protection from the

hostile mould environment area, it simultaneously dampens the sensitivity, and in the presence of bearing wear or slight misalignment of the oscillator, the absolute mould friction may be distorted [52]. Nonetheless, strain gauges have been used successfully to monitor casting parameters and to detect the onset of breakouts.

2.3.5 Temperature Measuring Devices.

There are several temperature measuring devices, but for practical reasons thermocouples are used in preference to the others. Since temperature measurements by thermocouples are based on changes in contact potential between two dissimilar metals they may be manufactured by joining two dissimilar metals. Over the years various standards have evolved with proper documentation of voltage-temperature relationships for each thermocouple type. The choice of one is dictated by the range of temperature to be measured, required accuracy, and cost.

In practice, the thermocouple junction needs protection and rigidity, and these are provided by a sheath which will give a fast response. The actual junction can be arranged in one of the following options: insulated junction, grounded junction, and exposed junction and again, the choice of one is determined by the application. The fastest response is obtained from the exposed junction; but this is only used when the atmosphere does not attack the thermocouple wires [53].

The main problem encountered with thermocouples is the low signal level. Since electrical noise on the signal lines is usually of several orders higher than the temperature signal itself, they must have high input impedance, and very high common mode noise rejection. Furthermore, particular care needs to be taken with regard to screening and the avoidance of ground loops.

2.4 Monitoring and Control Systems.

As pointed out in the introduction, recent focus for steelmakers has been the direct linking of casting and primary rolling operations. To attain the highest productivity, emphasis has been placed on high speed casting, which consequently leads to reduced shell thickness at the bottom of the mould. Furthermore, many of today's high productivity machines routinely change tundishes or submerged entry nozzles, as in slab casting, on the fly during normal operations. These transient operations inevitably lead to unstable periods of casting speed and mould level control which enhance the probability of sticking [54]. These and other challenges, already mentioned, require on-line control of casting variables within set limits to achieve the required level of quality. Again, on-line detection of events and/or defects such as sticking, binding, transverse depressions, and breakouts are important in order to effect corrective actions.

The objectives of control systems are many and varied and may be one, or a combination, of the following:

i) to monitor and control casting parameters such as casting speed and metal level.

ii) to monitor events and/or defects and effect corrective actions automatically or manually.

iii) to predict on-line the quality of the as-cast product in order to separate out defective billets.

iv) to monitor the mechanical performance of the caster, for example mould dynamics [48].

As far as monitoring and control systems are concerned, the majority of the work done in the past has been focused on the development of breakout prevention systems [57]. Generally, breakout prevention schemes may employ one or a combination of the following: mould heat transfer relationships, friction monitoring, and mould thermal monitoring.

2.4.1 Breakout Prevention Scheme Using Friction Monitoring.

The concept of monitoring mould friction to detect and prevent breakouts stems from the basic relation between increased friction and breakouts. As with mould heat transfer, mould friction is affected by a variety of casting parameters - lubrication, taper design, steel composition, casting speed, steel cleanliness, steel superheat, metal level control, and mould oscillation. The relationships have been addressed in various publications [5,45,46].

Mould friction may be monitored by either accelerometers, or load cells usually attached directly to the mould, and strain gauges on the oscillator.

While friction monitoring has been effective in detecting the events which can contribute to sticking, the interaction of these events have made it very difficult for sticker-type breakout detection and prevention [40,55,56]. Blazek and co-workers [56] indicated the difficulty of using mould friction to predict the occurrence of sticker-type breakouts. They found that the time variation of mould friction for heats interrupted by sticker-type breakouts was similar to that for heats unaffected by sticker-type breakouts. Nonetheless, breakouts which gradually develop due to scum or slag entrapment have successfully been detected by friction monitoring devices [55,59].

2.4.2 Breakout Prevention Scheme Using Mould Heat Transfer Relationships.

Basically, breakout prevention schemes employing heat transfer relationships are established through monitoring the amount of heat removed through the mould walls. Based on historical data, a minimum heat removal criterion can then be determined such that an adequate shell thickness is

established prior to strand withdrawal. The heat flux for each mould face, Q_A, as a function of temperature rise of the mould cooling water, ΔT, for each face and flow rate, W, may be expressed as follows [57]:

$$Q_A = \frac{C_p \rho_w W \Delta T}{A} \tag{2.4}$$

Figure 2.8 shows a breakout induced by insufficient heat transfer preceded by a period of several minutes in which the heat removal gradually declines. This approach was recognized as early as 1972 by Koening [58]. It must however be noted that while this method can provide an effective means of detecting the gradual development of breakout conditions, the response time is insufficient to indicate a rapid onset of steel shell ripping or tearing [57]. Again, detection is limited to breakouts caused by progressive decline in heat removal.

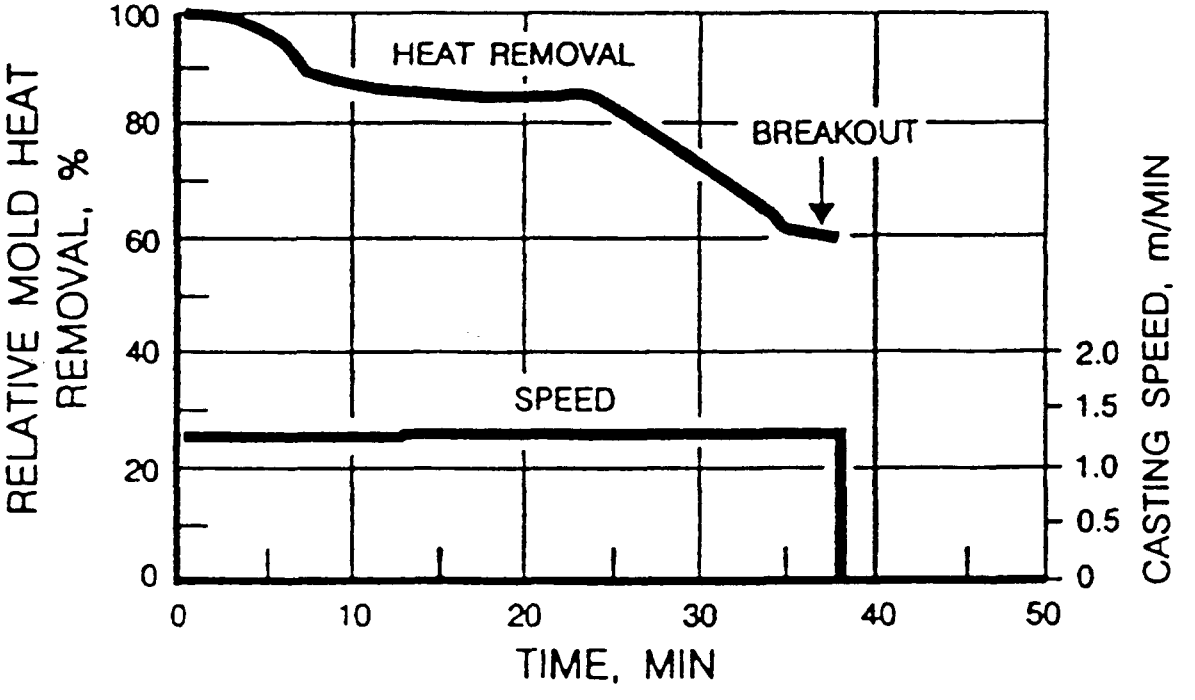

Figure 2.8: Decline of heat removal prior to a breakout during steady state operation [64]

2.4.3 Breakout Prevention Scheme Using Mould Thermal Monitoring.

Sticker-type breakout detection by thermal analysis works on the principle that localized heat transfer variation can easily be recognized by temperature measuring devices. This is based on the relationship of sticker-type breakouts and increased heat flux through the mould adjacent to the sticker as was recognized as early as 1954 by Savage and Pritchard [59].

The localized thermal monitoring is usually done with embedded thermocouples or heat flux sensors [60]. These have proven more effective than the friction-based detection system as they are based on a more direct measurement technique, and can detect a greater number of breakouts.

Figure 2.9 schematically describes the propagation of a sticker-type breakout, and Figure 2.10 shows the detection of a sticker-type breakout using thermocouples in the vertical plane. As has been described earlier, the movement of the "pseudo-meniscus" causes a significant increase in temperature at the sensor. The portion of the strand above the tear is not withdrawn and therefore increases in thickness due to the high heat transfer. As this relatively thick portion passes the sensor, a rapid decline of mould temperature is registered.

2.4.4 Other Uses of Thermal Monitoring Systems.

Thermocouples have also been employed to characterize events such as: leaky or misaligned submerged nozzles, insufficient argon flow and inadequate mould flux lubrication in powder casting [52]. This system is based on a "temperature variability index", determined by averages and standard deviations of signals from a thermocouple located about 80 mm below the meniscus scanned every second. Details of the computations were not reported.

Thermocouples located near the bottom of the mould have been used by Koyama et al [62] to study the uniformity of mould flux inflow. They related the product of mould flux viscosity, η, and casting speed, V_c, to mould temperature fluctuations. It was shown that for specific operating conditions, there exists a value, ηV_c, for which temperature fluctuations is a minimum.

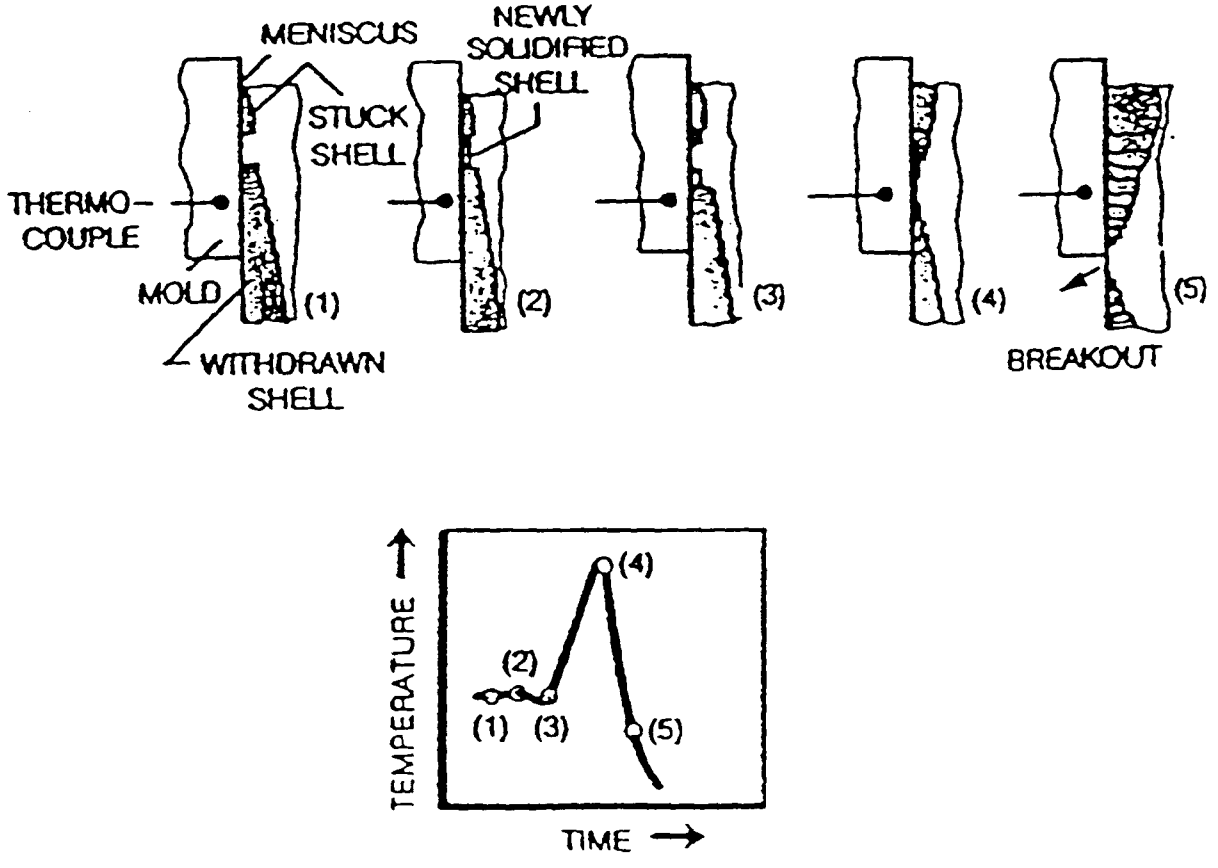

Figure 2.9: Propagation of a mould sticker [65]

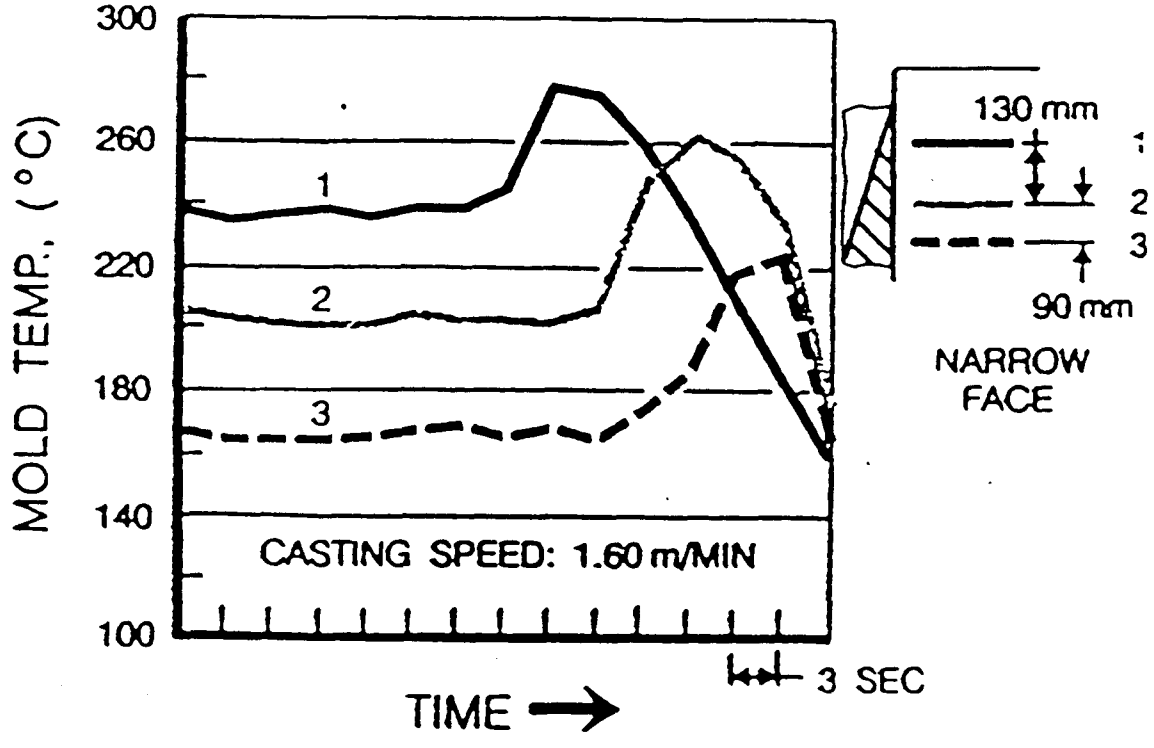

Figure 2.10: Detection of sticker-type breakout using three thermocouples in the vertical plane [66]

Chapter 3: Scope and Objectives

As mentioned in the previous chapter, transverse depressions are mould-related defects, and in order to monitor and control their formation on-line, knowledge of the events leading to their formation is required. Laboratory experiments are not a viable means of obtaining such knowledge due to the complicated nature of the continuous casting process; and hence a plant trial, in which an operating mould was instrumented with mechanical sensors and thermocouples, was carried out. Data from the sensors, and billet samples from the heats monitored, were collected for analysis. The heats monitored were plain carbon and boron-containing steel, ranging from low to high carbon grades. The data analysis, primarily in real-time focused, on the mould thermocouple signals.

The billet samples collected during the trial were subjected to a complete metallographic examination. Specifically, longitudinal sections were taken of samples containing transverse depressions and macroetched to determine the presence of cracks and their depth beneath the depressions.

It was anticipated that the outcome of the analysis would achieve the following objectives:

a) to establish correlations between mould thermal response and transverse depressions.

b) to investigate the causes of the formation of transverse depressions during the continuous casting of boron and non-boron steels.

Chapter 4: Experimental Work and Results

A plant trial was conducted at a steel plant designated as Company G. This involved casting trials and data acquisition on an operating mould instrumented with thermocouples, load cells, accelerometers, and linear variable displacement transducers (LVDTs). Billet samples were collected from the heats monitored and analyzed later for surface and internal quality. Since the analysis was focused on the mould thermal data, discussions on instrumentation and data acquisition will centre on the thermocouples.

4.1 Preparatory Work

The condition of the mould system was fully appraised in preparation for the trial. This involved evaluation of the oscillator, cooling water flow rate, lubrication oil distribution system and the mould design.

The original four-sided constraint system was re-machined to ensure tight fitting of the keeper plates in the slots on all four sides of the mould. A new oil plate based on the UBC Oil Distribution Design [67] was manufactured to ensure uniform distribution of the lubricating oil. Finally the internal and outside dimensions of the mould were measured. An equipment consisting of 3 LVDTs and a potentiometer, was used to measure the internal dimensions of the mould.

4.2 Instrumentation and Data Acquisition.

4.2.1 Thermocouple Installation

A total of 76 intrinsic Type-T thermocouples (copper-constantan) were installed on the four

sides of the mould as schematically shown in Figure 4.1. The north, south, and west faces each had 17 thermocouples out of which 8 were located at the off-corners, and 9 at the midface. The east face had the same configuration but instead of 9 thermocouples it had 18 thermocouples at the midface. The distance between the off-corner and the midface thermocouples was 80 mm.

The installation procedure adopted for this experiment had successfully been used in previous plant trials conducted by the UBC casting group [2,69]. Basically, it involved drilling holes through the baffle tube and into the copper mould wall. Care was taken to ensure that all the holes were drilled to the same depth, the details are shown in Tables 4.1 (a, b, c, d). A flat bottom drill was used to drill the hole which was then tapped with a bottom tap to ensure threading to the bottom of the hole. The hole depth was measured and recorded.

An intrinsic Type-T thermocouple was made by connecting a single constantan wire to the copper mould. The procedure involved creating a bead on a single constantan wire using a TIG welding machine. The bead was filed to produce a flat foot-like end approximately 0.30-0.40 mm thick. Heat shrinkable tube (1.6 mm in diameter) was then shrunk onto the bare constantan wire. This was then inserted through the baffle into the mould wall and held in place by a threaded copper plug screwed into the copper mould. On the baffle, the wire was also held in place by a plug; and a silicone sealant was applied at the contact between the plug and the wire to make sure that water did not leak from the cooling channel. All the wires were then tied together and drawn out through one large hole drilled in the mould housing; and again the hole was completely sealed with a silicone sealant. Finally, the mould was pressure tested to ensure there were no water leakages. Figures 4.2, and 4.3 respectively show the schematic set-up for measuring mould wall and cooling water temperatures, and a circuit diagram for the thermocouple connection.

Intrinsic thermocouples have a low thermal inertia, and are better suited for monitoring transient events. It has been established that the time taken for a 1 mm constantan wire on a copper substrate to reach 95% of the steady state e.m.f is of the order of micro-seconds [68].

In addition to the mould thermocouples, 6 commercially available extrinsic type T thermocouples were installed in the cooling water channel to monitor the bulk inlet, bulk outlet, and the outlet water temperature at the top centreline of each face of the mould, Figure 4.2.

4.2.2 Data Acquisition System.

A personal computer-based data acquisition system was used to record the data during the casting trials. The system was comprised of the following major components: a personal computer, an analog-to-digital (A/D) conversion plug-in data acquisition board, a multiplexer (expansion accessory), and an application software.

4.2.2.1 Personal Computer

An IBM PC clone with the following features - an Intel 80486 DX2-66 microprocessor, 16 MB RAM, 900 MB Toshiba hard disk, and a 2 GB Colorado tape drive - was used for the data acquisition and storage. This enabled 93 channels of data to be acquired for 400 s, at 100 Hz. Experiments carried out to check the capabilities and limitations of the data acquisition system indicated that the rate at which the buffer in the computer emptied its contents was a limiting factor with respect to the number of channels, rate and period of data of acquisition. It was found that this problem stemmed from the speed of the computer being used, and for the intended configuration (93 channels, 100 Hz), IBM clone models 286 and 386 were found to be inadequate.

4.2.2.2 Analog-to-Digital Conversion Board.

A Keithley Metrabyte analog-to-digital (A/D) conversion plug-in board, DAS-8, was used for the data acquisition. The board featured an 8-channel, 12-bit successive approximation A/D converter. The full scale input of each channel was +/- 5 volts with a resolution of 2.44 mV per bit. The A/D conversion time was 25 microseconds (35 microseconds maximum). Connection to the external multiplexer (EXP-16) was made through a standard 37-pin D male connector that projected through the rear of the computer.

4.2.2.3 Multiplexer

A Keithley Metrabyte Universal Expansion Interface, EXP-16, was used with the A/D conversion board (DAS-8). This was an expansion multiplexer which multiplexes 16 differential analog input channels into one analog input of the data acquisition board. The 16 channels were selected by 4 TTL/CMOS compatible address lines from the data acquisition board. It also incorporated an instrumentation amplifier that provided stable amplification of low level thermocouple signals before reaching the high level A/D converter.

All analog input connections were made on miniature screw connector strips. The board included cold-junction sensing and compensation for the thermocouples which was not used. Instead, the temperature at the junction was measured with a mercury-in-glass thermometer. The board had a gain switch which allowed the entire board to be configured for the gain selected. A gain of 200 was selected in order to operate within the entire input range of the thermocouple, 21 mV. The board was connected directly to DAS-8 with a Keithley Metrabyte C-1800 cable. It was powered by an external power supply.

4.2.2.4 Application Software

Keithley Labtech Notebook version 7.1.1 for Windows was used for the data acquisition. This offered the capability to collect data from 93 channels at a high acquisition rate, 100 Hz for 400 seconds. However the volume of data was such that it was not possible to display or analyze signals in real-time.

4.2.3 Experimental Setup

The thermocouple cables taken from the mould housing were connected to the data acquisition board (DAS-8) via the multiplexer (EXP-16). To ensure that ground loops were not created, the shields were the only components grounded; the grounding was done at the source (mould) while the power sources to the computer and the data acquisition system were "floated" using an isolation transformer. Figure 4.4 is a schematic diagram of the experimental set-up.

4.2.4 Details of the Trial

Five heats ranging from low to high carbon grades for both plain carbon and low alloy steels (boron-containing steels) were cast during the trial. While sequentially casting these heats, data was collected by the data acquisition system from the thermocouples, load cells, and LVDT's for each heat. Tables 4.2 to 4.5 detail the design and operating conditions, instrumentation and data acquisition, and the chemistry of the heats monitored.

Canola oil was the only lubricant used in the entire trial. Shrouding with nitrogen gas was provided for ladle-tundish, and tundish-mould transfer operations when casting the boron grades in order to prevent re-oxidation.

To study the effects of metal level position and cooling water velocity on the temperature distribution of the mould, the metal level was changed while casting from 185 mm to 160 mm (measured from the top of the mould) and the mould cooling water flow rate reduced from the norminal value (0.044 m^3/s) to 0.028 m^3/s during the casting of the last heat.

Three one-foot billet samples were taken from each heat cast for internal and surface quality assessment. The tundish stream, and the meniscus level were filmed with a hand held camcorder in the course of casting to aid in the data analysis.

In addition to the temperature measurements, casting speed, and metal level signals were acquired.

Casting speed measurement: The signal from the withdrawal roll tachometer, which is proportional to the casting speed, was used to record the latter. The signal from the tachometer is typically 0-40 or 0-200 volts D.C and was stepped down to 0-20 mV and filtered for any electrical noise (8 or 45 Hz) before being transmitted to the data acquisition system. Calibration of the signal was done on site by measuring the output voltage relative to the casting speed gauge and adjusting a variable resistor so as to produce a convenient ratio.

Metal level measurement: The 4 - 20 mA signal from the metal level controller was modified to produce a 0 - 10 mV output before it was connected to the data acquisition system. The signal was calibrated by lowering a steel billet into the mould and measuring the output signal for different lengths of the test billet in the mould.

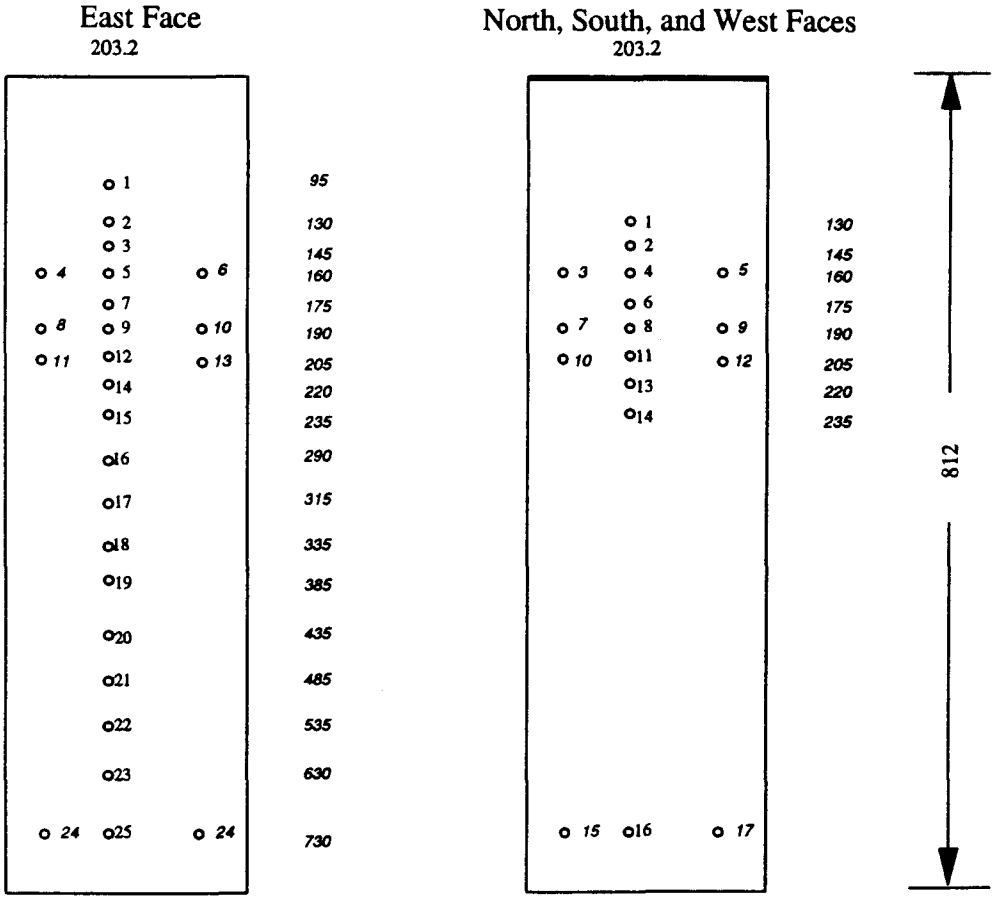

Figure 4.1 Schematic diagram of the thermocouple layout. All dimensions are in millimeters.

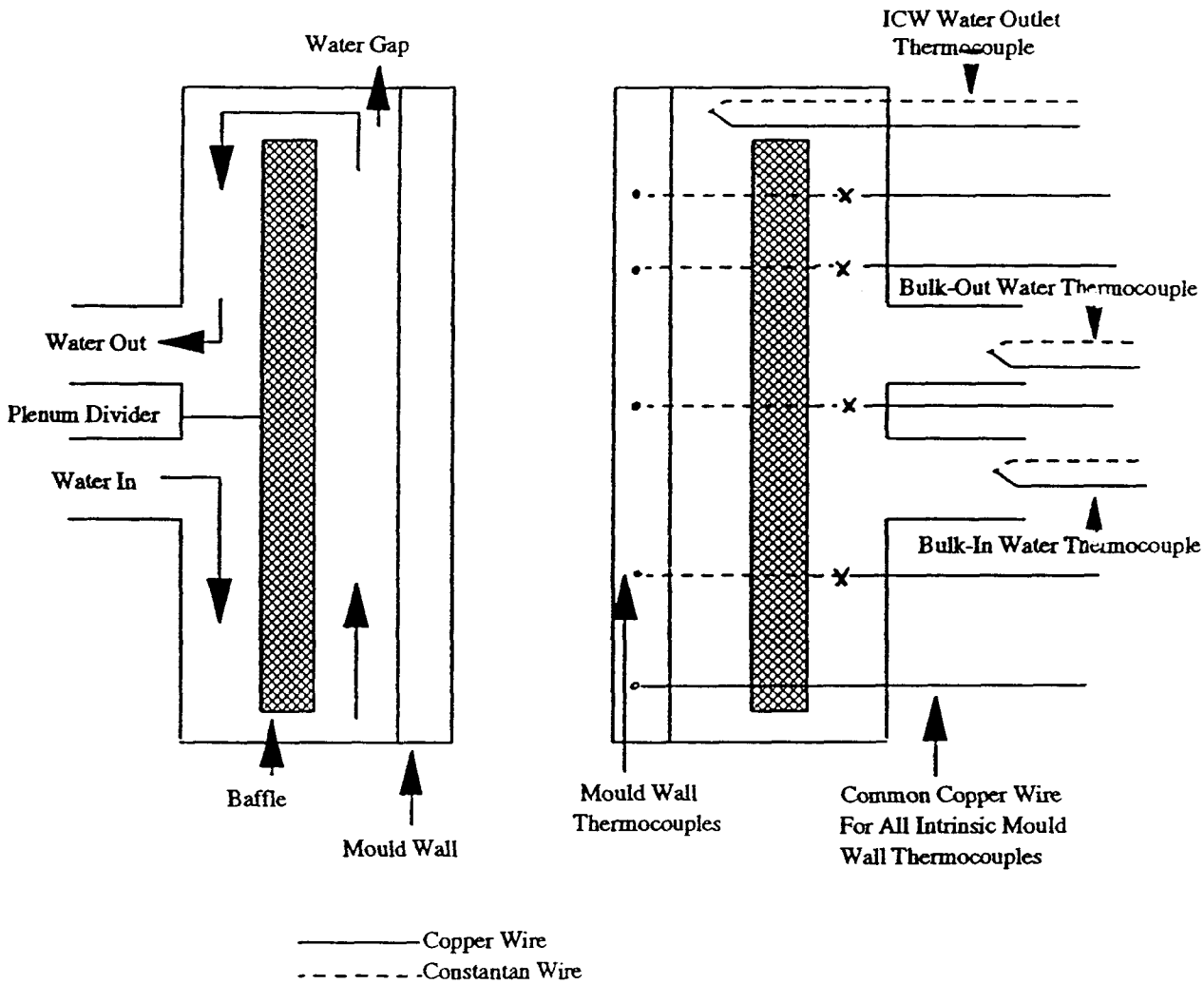

Figure 4.2 Schematic diagram showing the set-up for measuring mould wall and cooling water temperatures [2].

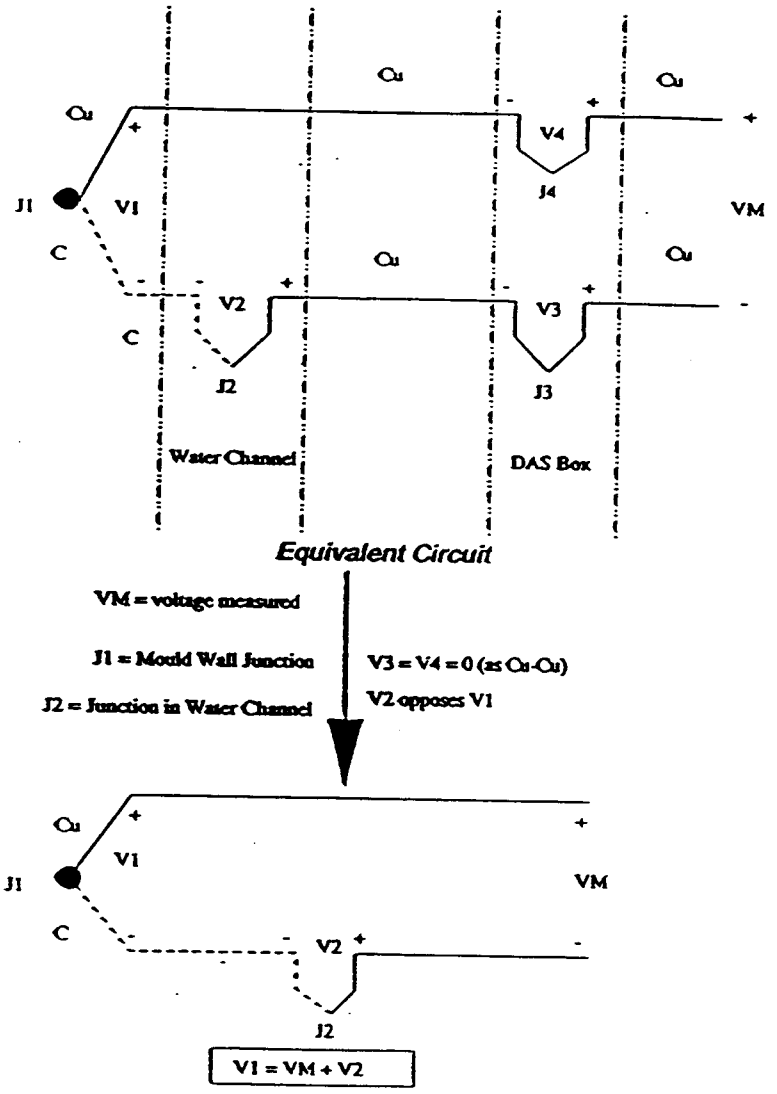

Figure 4.3 A circuit diagram for the thermocouple connection [2].

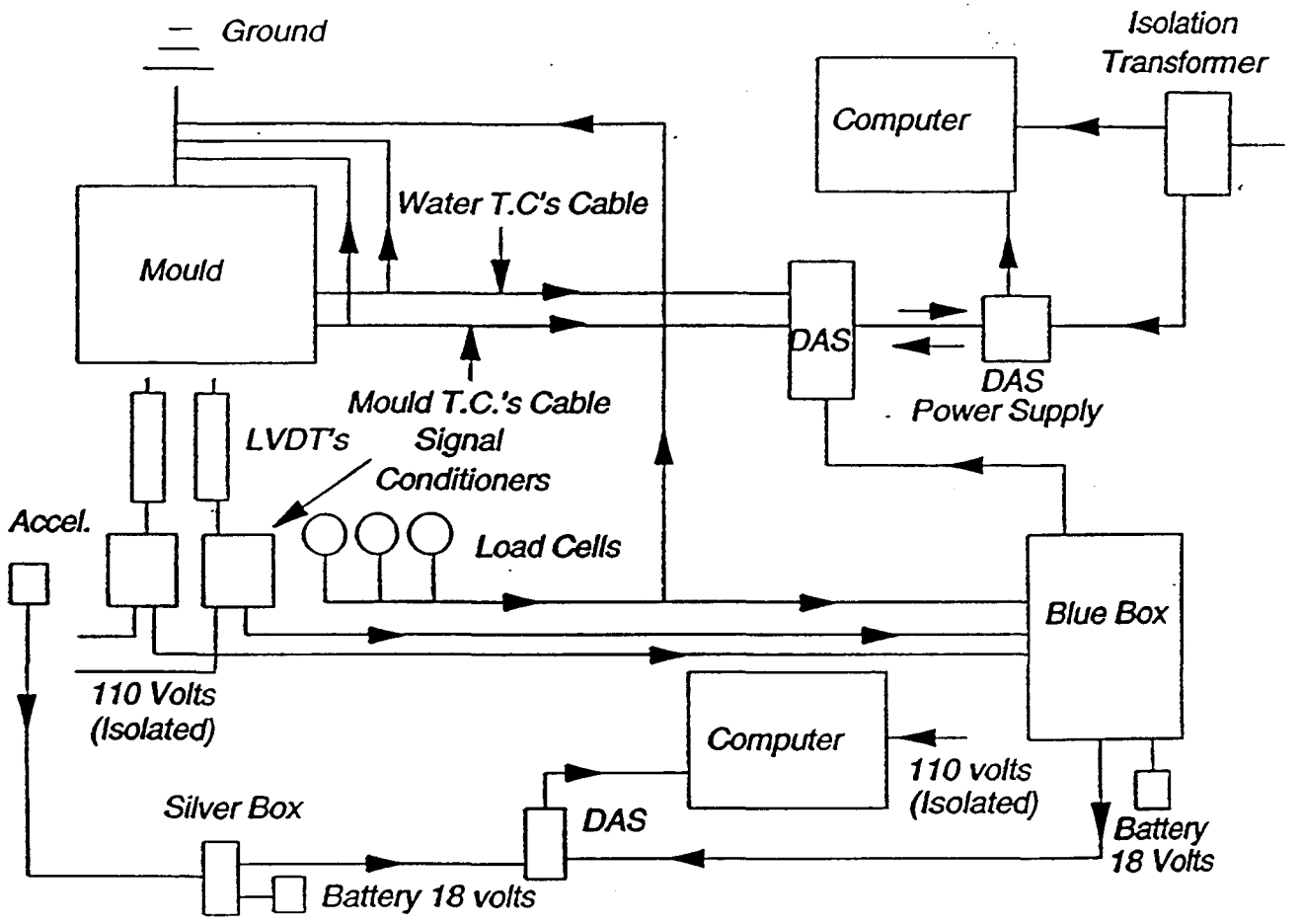

Figure 4.4 Schematic diagram of the experimental set-up.
DAS - data acquisition system.

Table 4.1 (a) Depth and axial position of thermocouples used to monitor mould wall temperature.

TC No.	Distance from top of mould (mm)	Hole depth (mm), from cold face	TC No.	Distance from top of mould (mm)	Hole Depth (mm)
East - Midface			**East - Off-corner**		
1	95.3	7.81	4	160.3	7.78
2	131.3	7.79	6	161.8	7.74
3	145.3	7.77	8	190.8	7.69
5	160.8	7.74	10	191.3	7.85
7	173.5	7.70	11	204.8	7.77
9	189.8	7.70	13	205.8	7.71
12	205.3	7.86	24	729.3	7.56
14	219.8	7.76	-	-	-
15	235.3	7.76	-	-	-
16	290.3	7.48	-	-	-
17	315.3	7.66	-	-	-
18	334.8	7.78	-	-	-
19	384.8	7.69	-	-	-
20	433.3	7.68	-	-	-
21	484.3	7.64	-	-	-
22	535.3	7.60	-	-	-
23	630.3	7.62	-	-	-
25	729.3	7.49	-	-	-

Table 4.1 (b) Depth and axial position of thermocouples used to monitor mould wall temperature.

TC No.	Distance from top of mould (mm)	Hole Depth (mm)	TC No.	Distance from top of mould (mm)	Hole Depth (mm)
North: Midface			**North: off-corner**		
1	130.3	7.85	3	160.8	8.95
2	145.3	7.78	5	161.8	7.58
4	160.3	7.91	7	189.3	8.29
6	175.3	7.63	9	190.3	7.69
11	204.8	7.57	10	204.8	8.71
13	219.8	7.57	12	205.8	7.40
14	233.8	7.63	15	730.3	7.63
16	729.3	7.33	17	730.3	7.48

Table 4.1 (c) Depth and axial position of thermocouples used to monitor mould wall temperature.

TC No.	Distance from top of mould (mm)	Hole Depth (mm)	TC No.	Distance from top of mould (mm)	Hole Depth (mm)
South: Midface			**South: off-corner**		
1	130.3	8.02	3	160.8	7.79
2	145.3	7.80	5	160.3	7.96
4	160.3	7.96	7	190.8	7.85
6	173.3	7.92	9	190.8	8.14
11	203.8	7.72	10	205.3	8.39
13	219.8	8.06	12	204.8	8.34
14	235.3	7.79	15	731.3	7.60
16	731.3	7.83	17	730.8	8.36

Table 4.1 (d) Depth and axial position of thermocouples used to monitor mould wall temperature.

TC No.	Distance from top of mould (mm)	Hole Depth (mm)	TC No.	Distance from top of mould (mm)	Hole Depth (mm)
West: Midface			**West: off-corner**		
1	130.8	7.94	3	158.3	7.64
2	143.8	8.04	5	160.3	7.82
4	160.3	7.95	7	190.3	7.73
6	175.3	8.19	9	190.3	7.84
11	205.3	8.02	10	204.8	7.88
13	22.8	8.29	12	206.3	8.01
14	235.3	8.43	15	729.3	7.78
16	730.3	8.13	17	730.3	8.30

Table 4.2 Mould Design and Operating Conditions.

Description	Details
Machine type	Curved
Mould material	DHP Copper
Constraint	Four-sided
Outside top dimension (mm)	240.2 mm
Inside top dimension (mm)	209.2 mm
Mould length	812.8 mm
Channel gap	4.99 mm
Cooling water flow rate	0.044 m^3/s
Cooling water velocity (measured)	10.44 m/s
Inlet pressure	850 kPa
Outlet Pressure	995 kPa
Oil type	Canola
Oil flow rate	55 ml/min
Casting speed	1.14 m/min
Metal level	180 - 185 mm 160 - 165 mm
Oscillation frequency	1.8 Hz
Stroke length	7 mm

Table 4.3 Summary of instrumentation and data acquisition.

Description	Detail
Thermocouple	
Type	T
Range	-270 °C to 400 °C
Accuracy	+/- 1 °C
Data Acquisition	
System	DAS-8 / EXP-16 Labtech Notebook for Windows 7.1.1
Channels	93
Rate	100 Hz
Period	400 seconds

Table 4.4 Casting conditions for the heats monitored.

Heat No.	Grade	% C	Superheat (°C)	Average (steady) metal level (mm)
142H1	C1011	0.12	44	178
146H1	C1035	0.32	62	165
146H2	C1035	0.32	53	185
147H2	15B35H	0.31	32	165
147H3	15B35H	0.31	20	165
148H1	15B30H	0.32	69	175
148H2	15B30H	0.32	53	182
149H1	C1085	0.83	40	185
149H2	C1085	0.83	23	170
149H3*	C1085	0.83		160

Note: (a) The norminal casting speed, oil type, flow rate, and oscillation frequency were the same for all heats and are shown in Table 4.2.

(b) *The cooling water flow rate was reduced to 0.028 m^3/s from the norminal value of 0.044 m^3/s.

Table 4.5 Composition of the heats monitored.

Element (Wt %)	**Heat Number**				
	142	**146**	**147**	**148**	**149**
C	0.12	0.32	0.31	0.32	0.83
Mn	0.84	0.71	0.86	1.31	0.71
S	0.028	0.023	0.009	0.006	0.022
P	0.019	0.023	0.022	0.022	0.023
Si	0.21	0.20	0.24	0.23	0.24
Cu	0.26	0.30	0.27	0.29	0.35
Cr	0.10	0.10	0.09	0.24	0.09
Ni	0.10	0.10	0.10	0.10	0.10
Mo	0.02	0.0200	0.02	0.02	0.02
Sn	0.016	0.024	0.016	0.022	0.026
Al	0.000	0.000	0.010	0.005	0.000
B	0.000	0.000	0.002	0.0032	0.000
Ti	0.000	0.000	0.033	0.033	0.000
Ca	0.000	0.000	0.001	0.002	0.000

4.3 Mould Temperature Data

This section presents raw mould temperature data obtained during the trial. The data corresponds to responses from thermocouples placed at the midface (east) of the mould (Figure 4.1).

4.3.1 Data Conversion

A large quantity of data was collected during the trial and, it could only be stored in binary form because it occupied less space on the hard disk. It was not possible to analyze the data in the binary form with the available software due to incompatibility. An existing computer program coded in Fortran 77 was used to convert the raw data to temperatures(°C) using the following power function:

$$T = a_o + a_1 x^1 + a_2 x^2 + a_3 x^3 + \ldots + a_7 x^7 \qquad (4.1)$$

where T = temperature, x = thermocouple voltage and a_o, a_1, ..., a_7 are constants, available from Omega Thermocouple Measurement and Encyclopedia.

Real-time mould thermal responses for selected thermocouples for the steel grades monitored are presented in Figures 4.5 to 4.9. For each grade there are two figures representing data from the upper and lower regions of the mould. In the meniscus region, the metal level has a significant influence on the thermocouple response. Responses from thermocouples above the meniscus were used as indicators of the metal level fluctuations instead of the metal level signals obtained from the metal level controller. This was because the metal level signal gave a global measure of the

metal level fluctuation while the thermocouples located at each face of the mould above the meniscus gave signals indicative of the local metal level fluctuations for each face. Metal level fluctuations at each face were particularly important in this analysis because it will be shown that events below the meniscus could be related to metal level phenomena.

The lower part of the mould represents the area below the meniscus where the metal level fluctuations have little or no influence on the thermocouple response. The response of the thermocouples in this region mostly reflects the strand surface profile and other events such as binding of the strand in the mould.

4.4 Billet Quality Evaluation

The billet samples were sand blasted to remove the oxide scale on the surface to facilitate visual inspection; billet surfaces were photographed. Longitudinal sections of billet samples with depressions were macroetched. Figure 4.10 is a macroetch of a longitudinal section showing transverse cracks, a feature frequently found either at the base or several millimeters below the surface. The cracks are located 8 mm below the surface. The significance of the crack depth below the surface is to locate the position in the mould where the crack formed. This will be addressed further in the next chapter. Examination of several macroetches revealed that the depressions may be categorized as follows; a "nose" and a "smooth" type, and both types could form on the same billet section as shown in Figure 4.11.

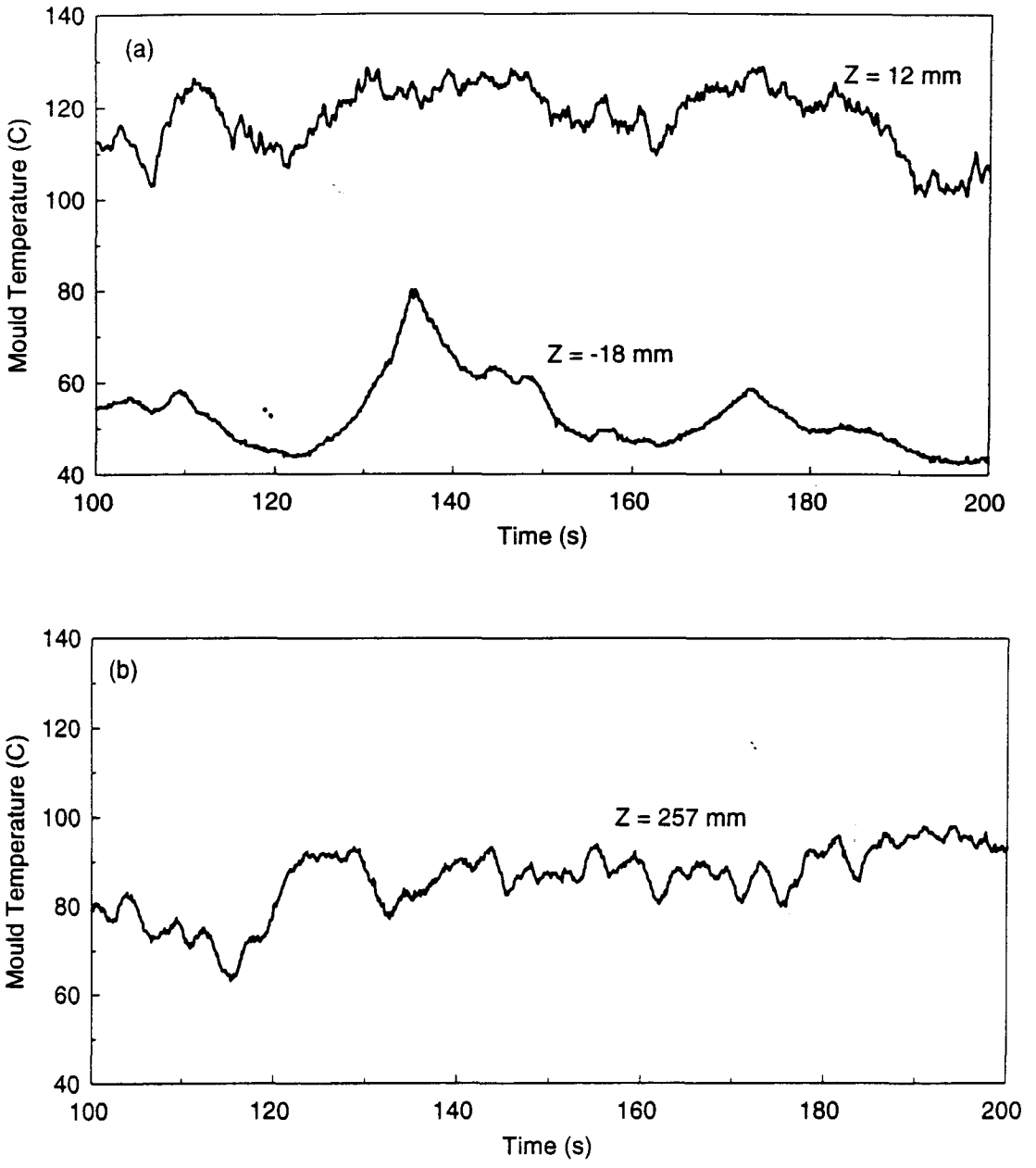

Figure 4.5: Mould thermal response. Heat 142H1 (0.12 %C), (a) upper portion of mould, (b) lower portion of mould. Z is relative to the meniscus.

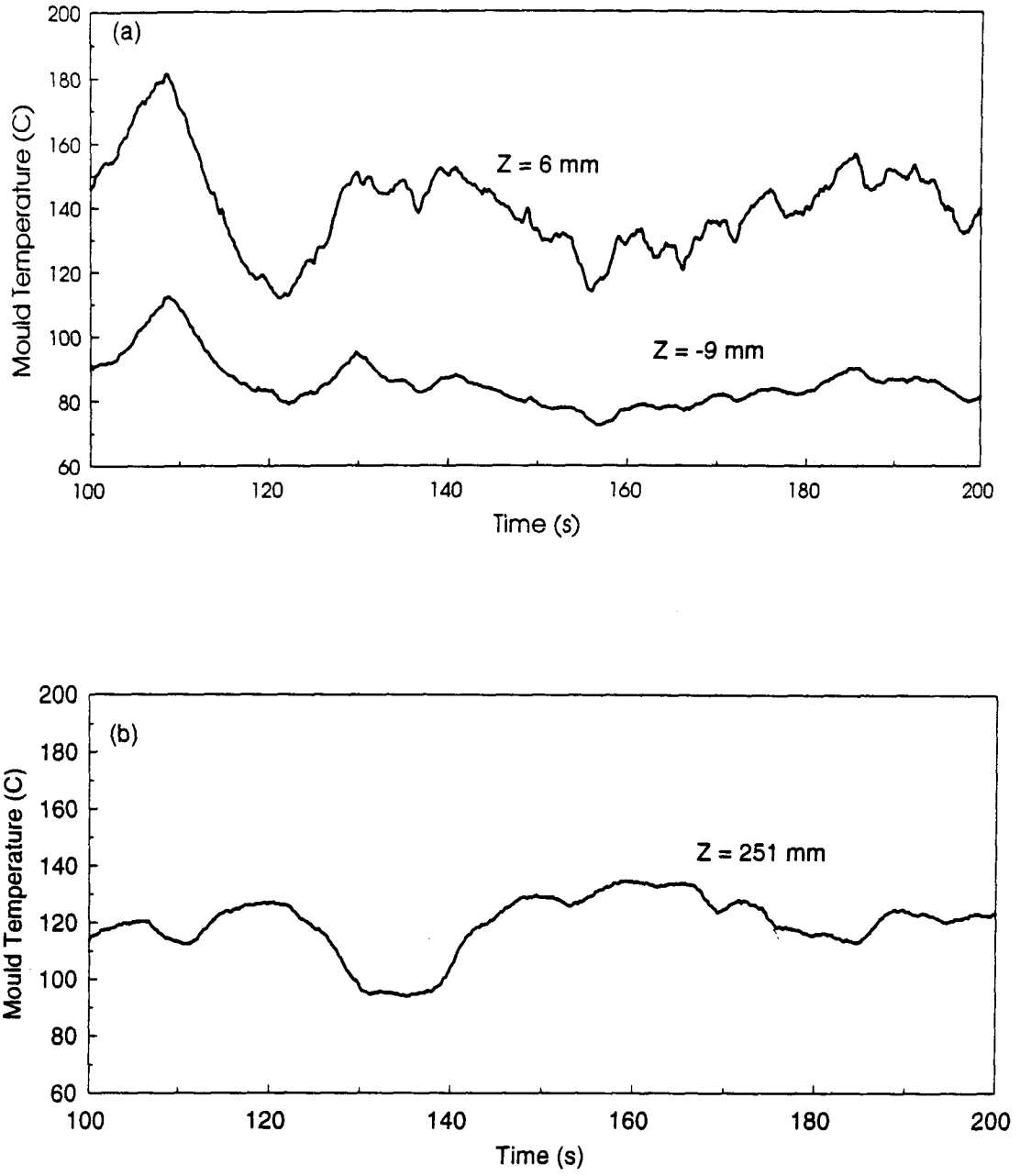

Figure 4.6: Mould thermal response. Heat 146H2 (0.32 %C), (a) upper portion of mould, (b) lower portion of mould. Z is relative to the meniscus.

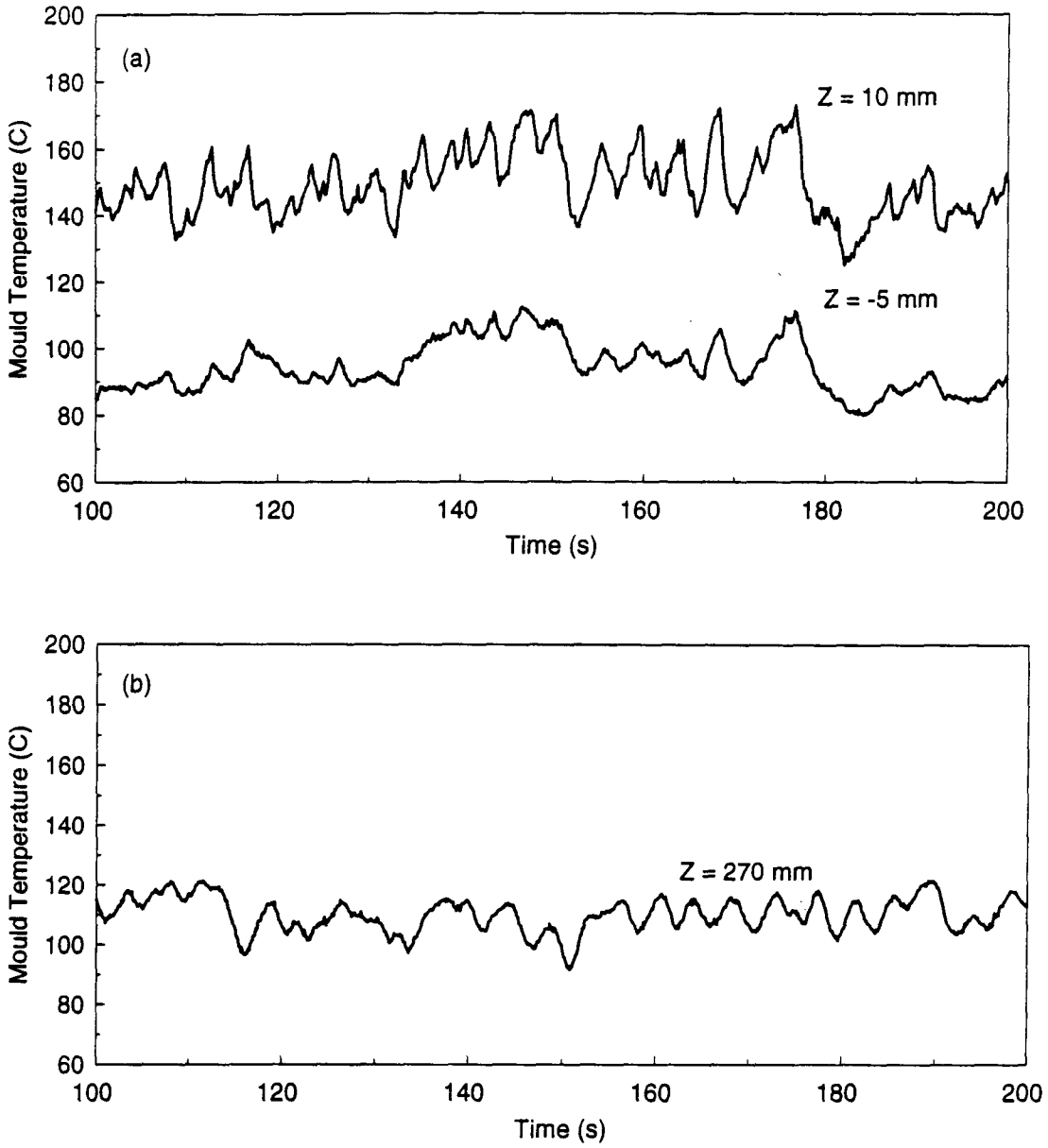

Figure 4.7: Mould thermal response. Heat 147H2 (0.31 %C, 0.002 %B, 0.033 %Ti), (a) upper portion of mould, (b) lower portion of mould. Z is relative to the meniscus.

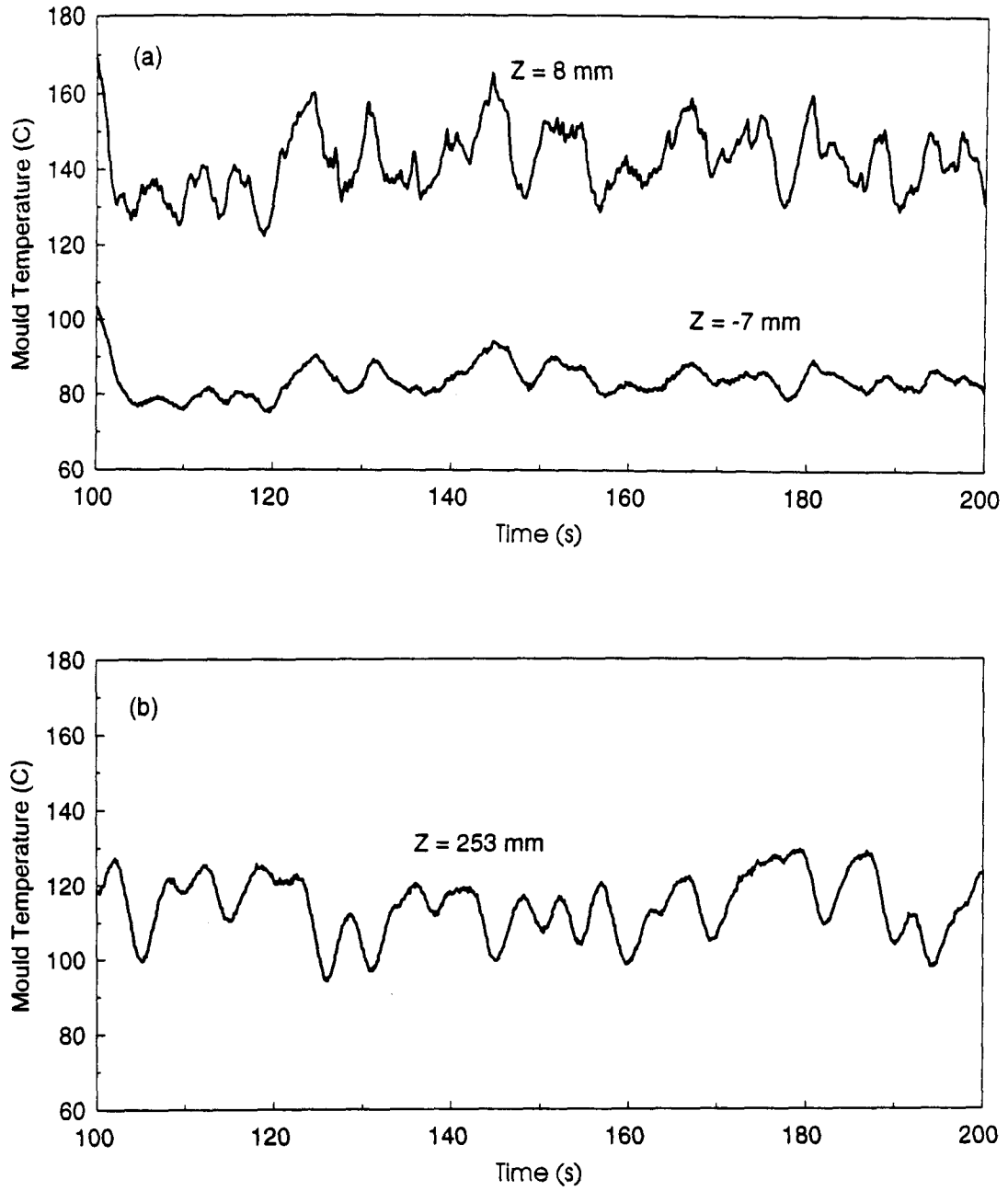

Figure 4.8: Mould thermal response. Heat 148H2 (0.32 %C, 0.0032 %B, 0.033 %Ti), (a) upper portion of mould, (b) lower portion of mould. Z is relative to the meniscus.

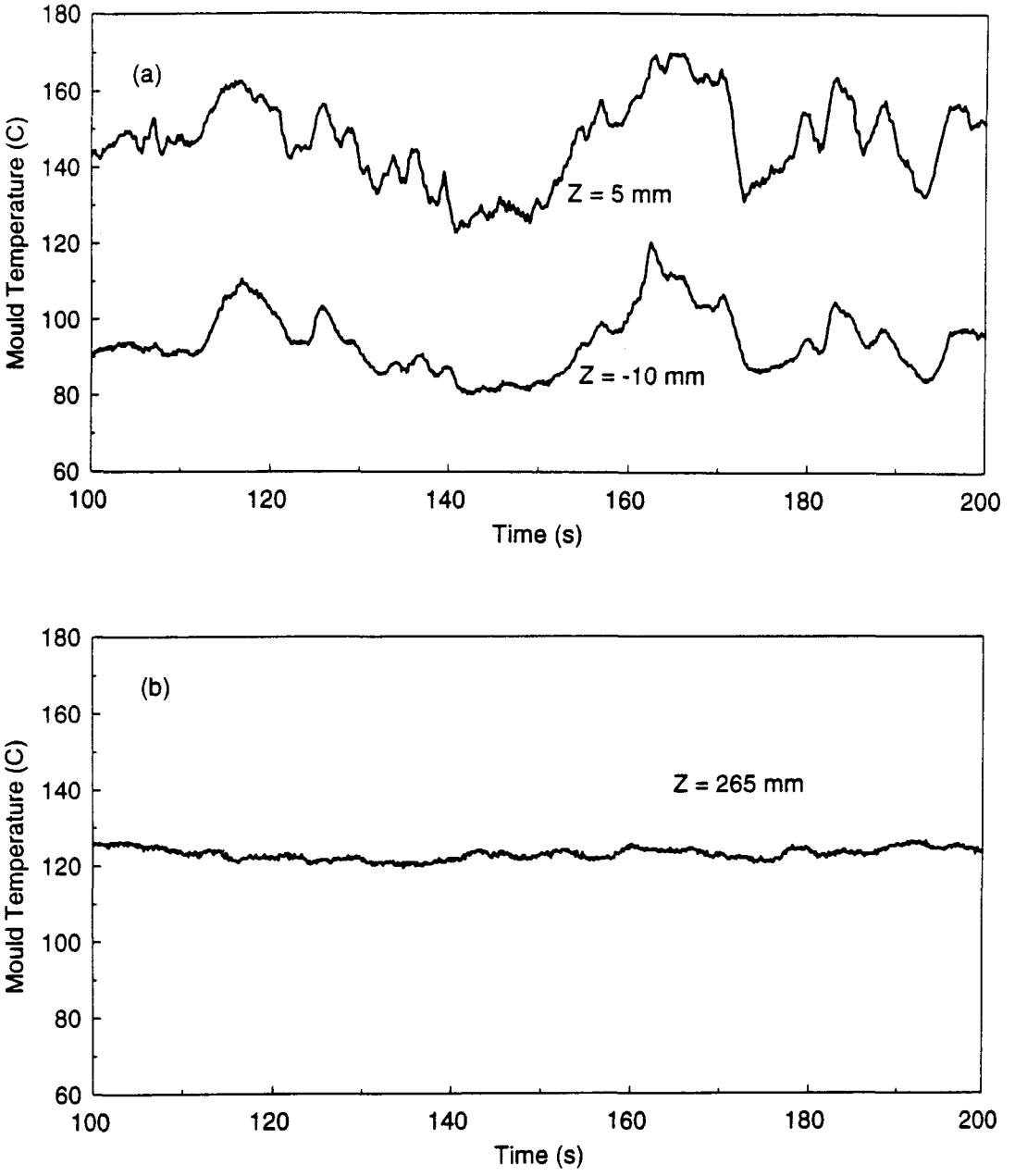

Figure 4.9: Mould thermal response. Heat 149H2 (0.83 %C), (a) upper portion of mould, (b) lower portion of mould. Z is relative to the meniscus

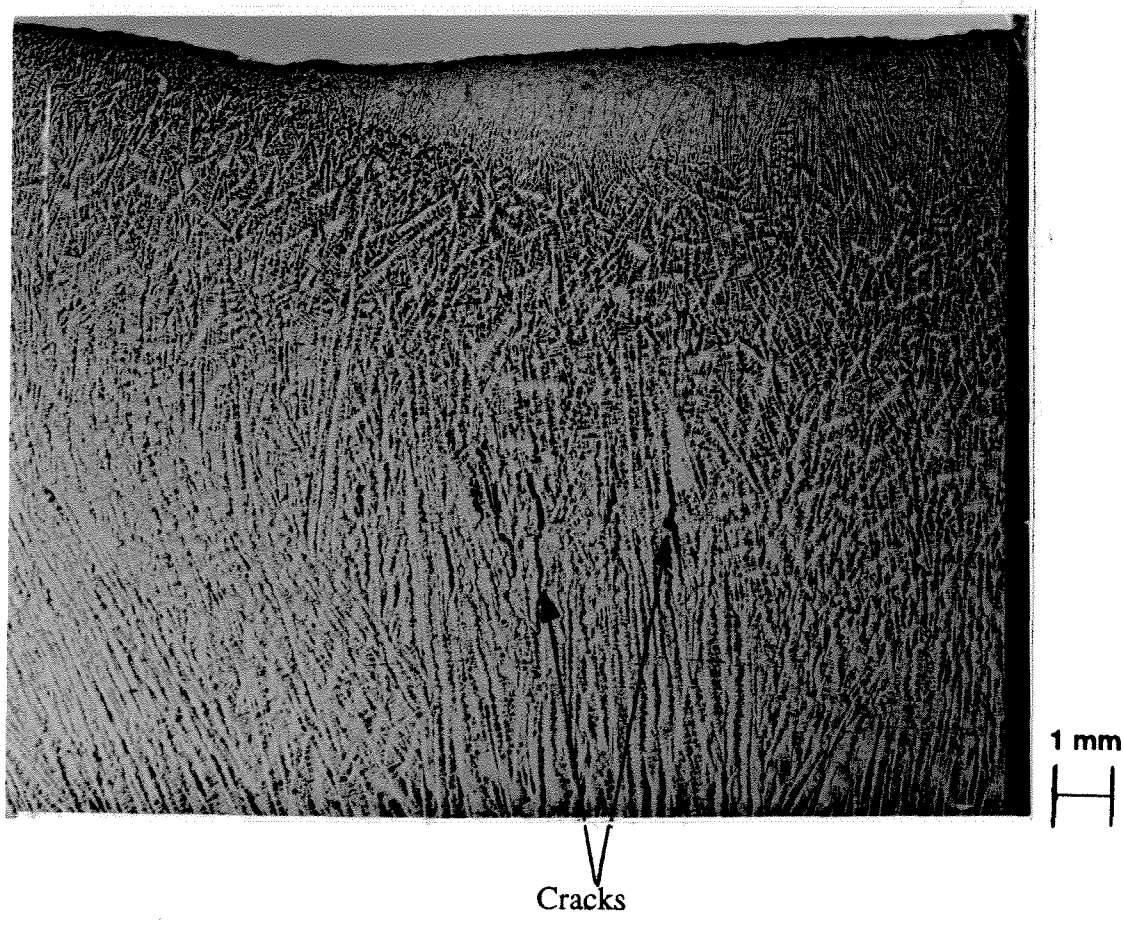

Figure 4.10 : Photograph of a longitudinal section revealing subsurface cracks; (0.32 %C, 0.0032 %B, 0.033 %Ti)

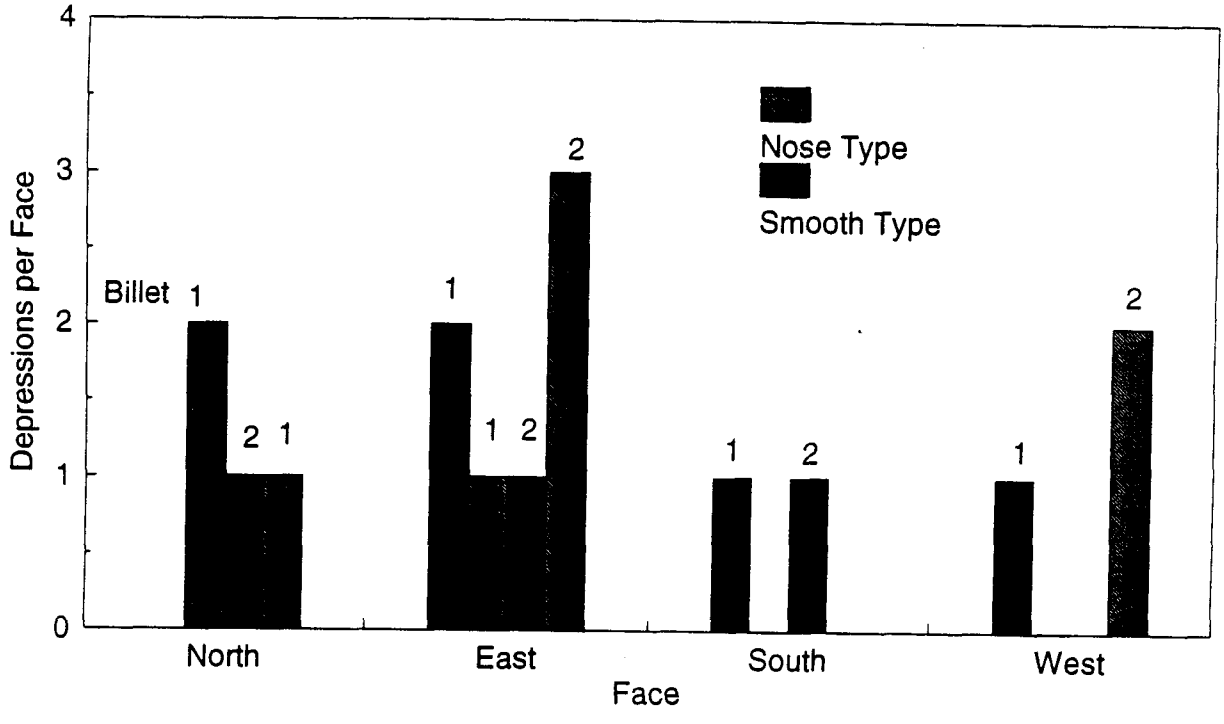

Figure 4.11 : Distribution of nose and smooth type depressions; (0.32 %C, 0.0032 %B, 0.033 %Ti)

Chapter 5: Results and Discussions

Data was gathered at a frequency of 100 Hz for a period of 400 seconds. In order to analyze it efficiently the data was plotted in short time segments, each graph containing data from 3 or 4 thermocouples which were combined to form long graphs.

5.1 Manifestation of Transverse Depressions in Mould Thermal Data

Figure 5.1 shows a pattern observed in the data which was identified to be a manifestation of transverse depressions. As mentioned earlier in Chapter 2, the air gap which forms between the strand and the mould represents about 84% of the total resistance to heat transfer from the liquid steel to the mould cooling water. Under normal circumstances a gap of less than 1 mm forms between the strand and the mould due to shrinkage associated with cooling of the strand. When there is a depression on the strand, the gap increases locally and drastically reduces heat transfer to the mould. Therefore as it passes by a thermocouple the mould temperature drops then rises locally, (Figure 5.1).

In addition to the local drop in mould temperature, the time lag between signals from successive thermocouples (longitudinally) reflects the movement with the strand of the depression down the mould length. This is evident in Tables 5.1 and 5.2 which summarize the important findings of the analysis.

It may be seen from the Tables (5.1b and 5.2b) that, over 90% of the depressions were preceded by a metal level rise, recorded as an increase in temperature at the thermocouples above the meniscus. This rise generally occurred over 2.0 ~ 6.0 s. The average speed of travel (17.7 mm/s) computed

from the spacing of successive thermocouples corresponds reasonably well with the withdrawal rate of the strand (19.1 mm/s). The axial width of the depressions as may be seen from Tables 5.1a and 5.2a varied between 40 and 110 mm. Interestingly, the width of each depression recorded by the thermocouple immediately below the meniscus (Tables 5.1a and 5.2a) appears to be proportional to the time period during which the thermocouple above the meniscus recorded a rise in temperature. This observation is important because it further links an increase in metal level to the formation of the depressions as described in later sections. No time lag was seen in the two successive thermocouples just below the metal level in most cases (see Figure 5.2b and 5.2c), indicating that, they must have seen the depressions simultaneously. It may be seen in Tables 5.1a and 5.2a that in most cases the thermocouples which first detected the depressions recorded a local drop in temperature which was shorter in duration than the drop recorded by thermocouples located below them. Thus, it is likely that the depressions must have undergone a further increase in width, axially.

A graphical representation of Table 5.2. has been shown in Figure 5.2 to illustrate the detection and travel of transverse depressions. It shows responses from thermocouples above and below the meniscus for two depressions (numbered 6 and 8). The two depressions travelling down the mould length have been presented through the responses of thermocouples located at distances 8, 23, 108, and 303 mm below the meniscus. The metal level was located at approximately 182 mm from the top of the mould. In the first figure (5.2a), which shows the response from a thermocouple located 7 mm above the metal level (TC 9), temperature increases of 7°C for a period of 4.8 s and 10 °C for 2.5 s were recorded. These temperature increases were undoubtedly associated with a rise in metal level. Following these increases, the thermocouple 8 mm below the meniscus sensed a local

drop in temperature of 20 °C corresponding to depression 6 (D6) and 16 °C for depression 8 (D8). The local drop in temperature was due to the increased gap created by the depression as explained earlier in the section.

5.1.1 Transverse Depressions and Heat Transfer in the Mould

The boron grades were found to have the largest number of depressions. This is evident in Figures 4.5 to 4.9. which show that the boron grades exhibit the greatest fluctuations in temperature, 253 and 270 mm below the meniscus. As mentioned earlier, the thermal response from the thermocouples in the lower part of the mould reflect the surface profile of the strand, specifically the depressions on the strand. As expected, the low carbon grade (0.12 %C) exhibits fluctuations in mould temperature due to the wrinkly surface. With the exception of about three "valleys" in the medium plain carbon grade (0.32 %C) the thermocouple response is fairly smooth. The high carbon grade (0.83 %C) is very smooth and indicates an absence of depressions. The explanation for these differences is given in a later section.

The influence of transverse depressions on mould heat transfer is illustrated in Figure 5.3. The lower heat flux profile for the boron grade (medium carbon) compared to the plain medium carbon grade is a clear reflection of the greater number of depressions in the boron grade - more depressions result in a larger mould-strand gap overall and therefore less heat extraction. Again, the low carbon is an exception because of the wrinkly surface as a result of the shrinkage near the meniscus associated with the solid-state $\delta \rightarrow \gamma$ transformation. The corresponding shell thickness and shrinkage profiles (external dimensions of the billet) computed from a mathematical model of billet shrinkage [76] are shown in Figures 5.4 to 5.8.

The depth of the outer tip of the cracks beneath the depressions gives an indication of the shell thickness at the time of formation of the crack; thus based on the shell thickness profiles the location in the mould where the crack formed could be estimated. A comparison of the shell shrinkage profile with the internal dimensions of the distorted mould indicate whether or not there was binding of the strand in the mould, and also where in the mould the binding occurred. It may be seen from Figures 5.4 to 5.8 that, the boron grades (medium carbon) were binding in the mould whereas the medium plain carbon grade did not. The boron grade with 0.32 %C was binding up to approximately 550 mm from the top of the mould, while the other grade with 0.31 %C was binding throughout the mould length. The low carbon (0.12 %C) and the high carbon (0.83 %C) grades were also binding up to 550 and 260 mm from the top of the mould respectively.

It may be recalled from Chapter 4 that cracks were observed about 8 mm beneath the depressions (Figure 4.10) which indicate the shell thickness at the time of crack formation. It is evident from Figure 5.7a that the shell thickness was approximately 8mm at 550 mm from the top of the mould; hence it is not surprising that binding of the strand in the mould ceases at about 550 mm from the top of the mould in Figure 5.7b.

Table 5.1a: Characteristics of Transverse Depressions Determined from Mould Thermocouples (Heat 147H2 - 0.31 %C, 0.0020 %B, 0.033 %Ti)

Depression No.		**Distance of Thermocouple from Meniscus**					
		10	**25**	**40**	**125**	**170**	**319**
1	Local Temp Drop (°C)	23	28	20	11	12	8
	Transit of Depression (s)	2.5	2.5	2.7	2.7	2.7	2.1
	Axial Width of Depression (mm)	41.8	41.8	45.1	45.1	45.1	35.1
2	Local Temp Drop (°C)	10	13	8	7	4	4
	Transit of Depression (s)	2.2	2.2	2.4	2.0	2.2	2.3
	Axial Width of Depression (mm)	37.4	37.4	40.8	34	37.4	39.1
3	Local Temp Drop (°C)	20	24	19	10	10	10
	Transit of Depression (s)	4.7	4.4	4.8	4.3	4.7	4.3
	Axial Width of Depression (mm)	76.1	71.3	77.8	69.7	76.1	69.7

Table 5.1a continued

Depression No.		Distance of Thermocouple from Meniscus					
		10	**25**	**40**	**125**	**170**	**319**
4	Local Temp Drop (°C)	15	32	33	17	18	13
	Transit of Depression (s)	3.1	3.1	3.7	4.0	4.6	3.9
	Axial Width of Depression (mm)	53.3	53.3	63.6	68.8	79.1	67.1
5	Local Temp Drop (°C)	17	24	16	10	12	10
	Transit of Depression (s)	3.0	4.2	4.4	4.1	4.0	4.0
	Axial Width of Depression (mm)	52.8	73.9	77.4	72.2	70.4	70.4
6	Local Temp Drop (°C)	11	26	24	15	12	12
	Transit of Depression (s)	2.6	2.6	3.3	3.3	3.5	3.2
	Axial Width of Depression (mm)	47.1	47.1	59.7	59.7	63.4	57.9
7	Local Temp Drop (°C)	15	17	14	14	12	12
	Transit of Depression (s)	4.4	4.4	4.2	4.4	4.5	5
	Axial Width of Depression (mm)	76.1	76.1	72.7	76.1	77.9	86.5

Table 5.1b Mould Temperature Change Above Meniscus Prior to Depression Formation and Inferred Downward Speed of Depression

Depression Number	**Thermocouple Response 5 mm Above Meniscus Prior to Depression Formation (°C)**	**Time of Response (s)**	**Average Downward Speed of Depression (mm/s)**
1	5.2	2.2	17.3
2	3.2	2.0	17.5
3	7.6	1.2	16.7
4	10	3.0	17.4
5	8	2.3	18.4
6	10	2.0	18.0
7	8	2.2	18.2

Note: (a) All depressions were first detected by the thermocouples located 10 and 25 mm below the meniscus.
(b) Norminal casting speed is 19.1 mm/s

Table 5.2a: Characteristics of Transverse Depressions Determined from Mould Thermocouples (Heat 148H2 - 0.32 %C, 0.0032 %B, 0.033 %Ti)

Depression No.		**Distance of Thermocouple from Meniscus**					
		8	**23**	**108**	**153**	**253**	**303**
1	Local Temp Drop (°C)	16	21	22	23	25	24
	Transit of Depression (s)	2.8	3.0	4.9	4.9	5.0	5.4
	Axial Width of Depression (mm)	50	54	88	88	90	97
2	Local Temp Drop (°C)	16	22	24	22	15	12
	Transit of Depression (s)	3.7	3.7	5.0	5.0	5.0	4.8
	Axial Width of Depression (mm)	65	65	88	88	88	84
3	Local Temp Drop (°C)	24	28	23	20	20	17
	Transit of Depression (s)	5.0	5.0	5.5	6.0	6.0	6.0
	Axial Width of Depression (mm)	89	89	97	106	106	106
4	Local Temp Drop (°C)	33	25	20	20	22	22
	Transit of Depression (s)	5.0	5.0	5.0	5.6	5.5	5.2
	Axial Width of Depression (mm)	90	90	90	100	99	93

Table 5.2a continued

Depression No.		Distance of Thermocouple from Meniscus					
		8	**23**	**108**	**153**	**253**	**303**
5	Local Temp Drop (°C)	22	18	19	19	19	18
	Transit of Depression (s)	5.0	6.2	6.0	6.0	6.0	6.0
	Axial Width of Depression (mm)	88	109	105	105	105	105
6	Local Temp Drop (°C)	20	20	24	22	18	20
	Transit of Depression (s)	6.0	6.0	6.0	6.0	6.4	6.4
	Axial Width of Depression (mm)	104	104	104	104	111	111
7	Local Temp Drop (°C)	24	23	22	22	22	24
	Transit of Depression (s)	5.5	4.5	4.5	4.5	4.7	5.0
	Axial Width of Depression (mm)	100	100	82	91	91	91
8	Local Temp Drop (°C)	16	20	14	14	14	12
	Transit of Depression (s)	2.6	2.6	5.0	5.0	5.0	5.0
	Axial Width of Depression (mm)	47	47	90	90	90	90

Table 5.2b: Mould Temperature Change Above Meniscus Prior to Depression Formation and Inferred Downward Speed of Depression

Depression Number	**Thermocouple Response 7 mm Above Meniscus Prior to Depression Formation (°C)**	**Time of Response (s)**	**Average Downward Speed of Depression (mm/s)**
1	5	2.5	17.9
2	2	2.0	17.5
3	9	3.0	17.7
4	13	6.0	17.9
5	-3	3.0	17.5
6	7	4.8	17.4
7	3	5.0	18.2
8	10	2.5	17.9

Note: (a) All depressions were first detected by the thermocouples located 8 and 23 mm below the meniscus.
(b) Norminal casting speed is 19.1 mm/s

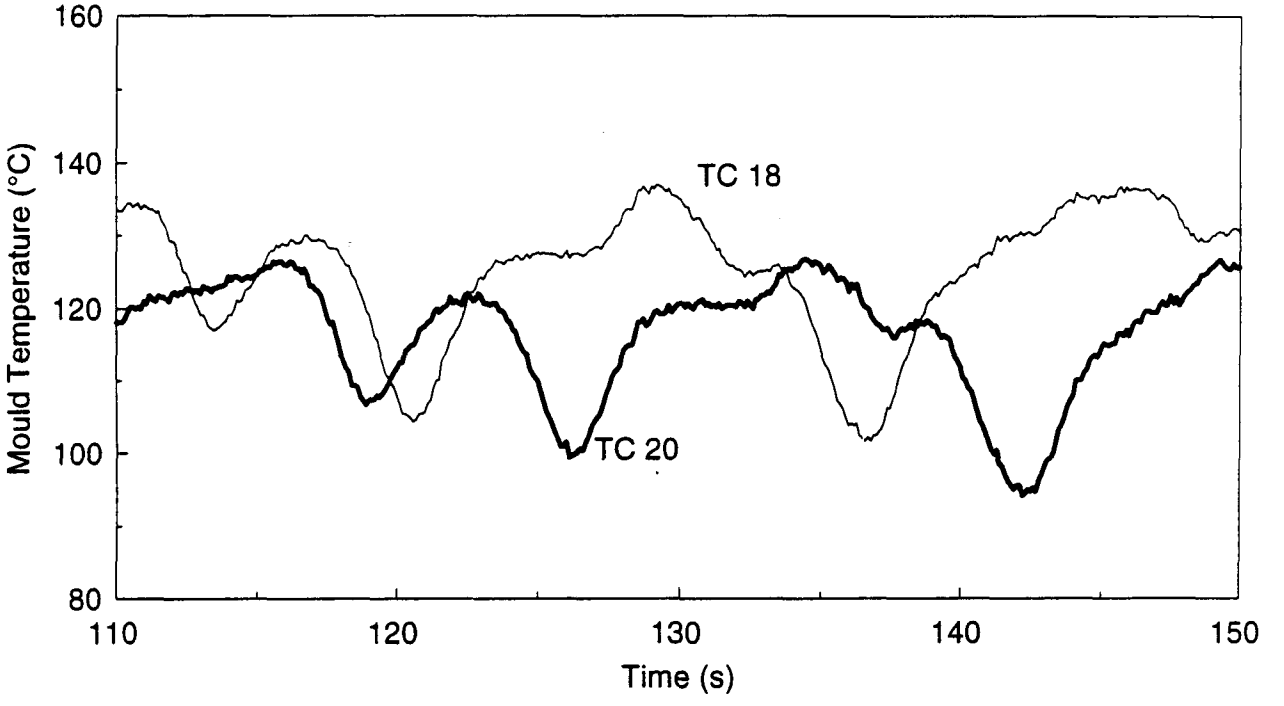

Figure 5.1: Manifestation of transverse depressions (the "valleys") in mould thermal response

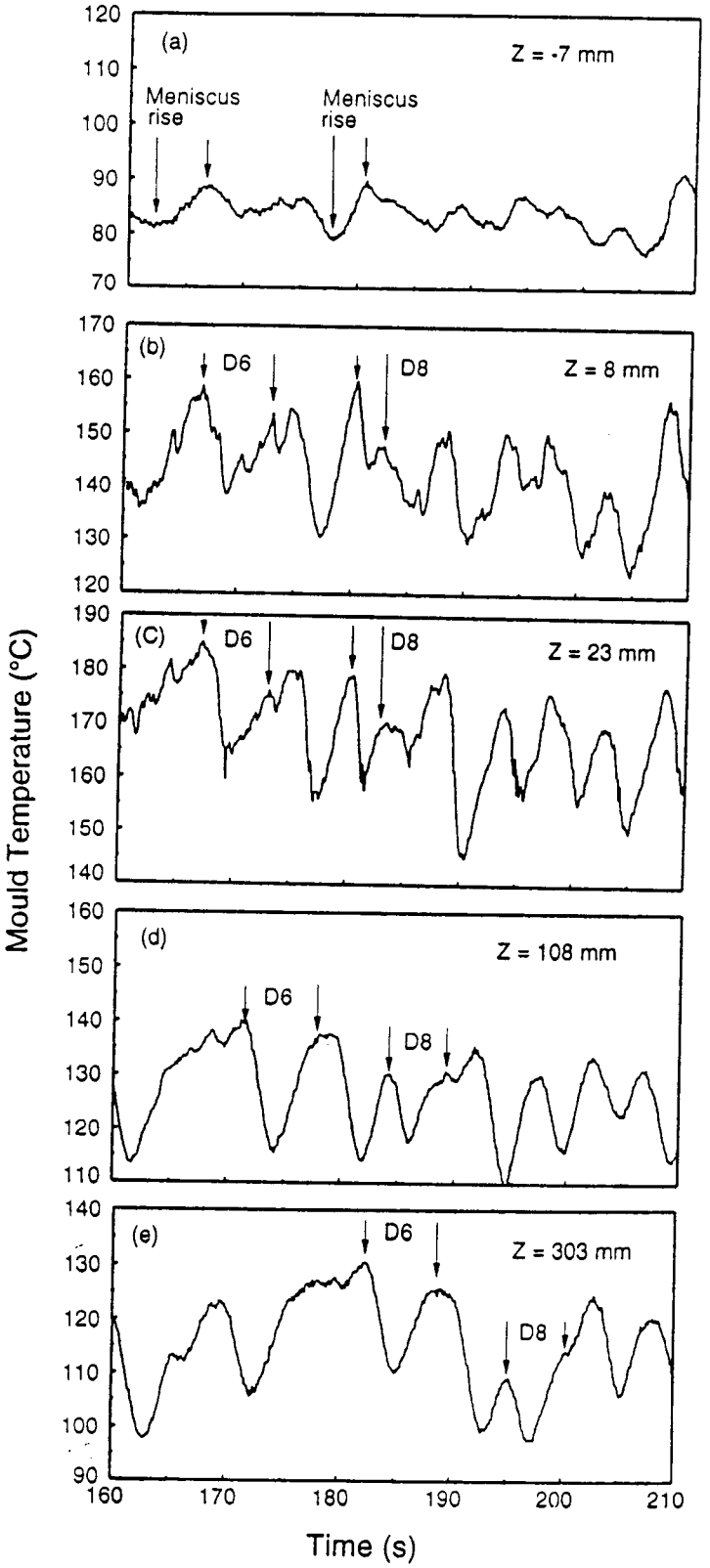

Figure 5.2: Thermal responses above (a) and below (b) - (e) the meniscus during the formation and travel of a transverse depression. All distances (Z) are relative to the meniscus. D6 and D8 represent depressions 6 and 8 respectively

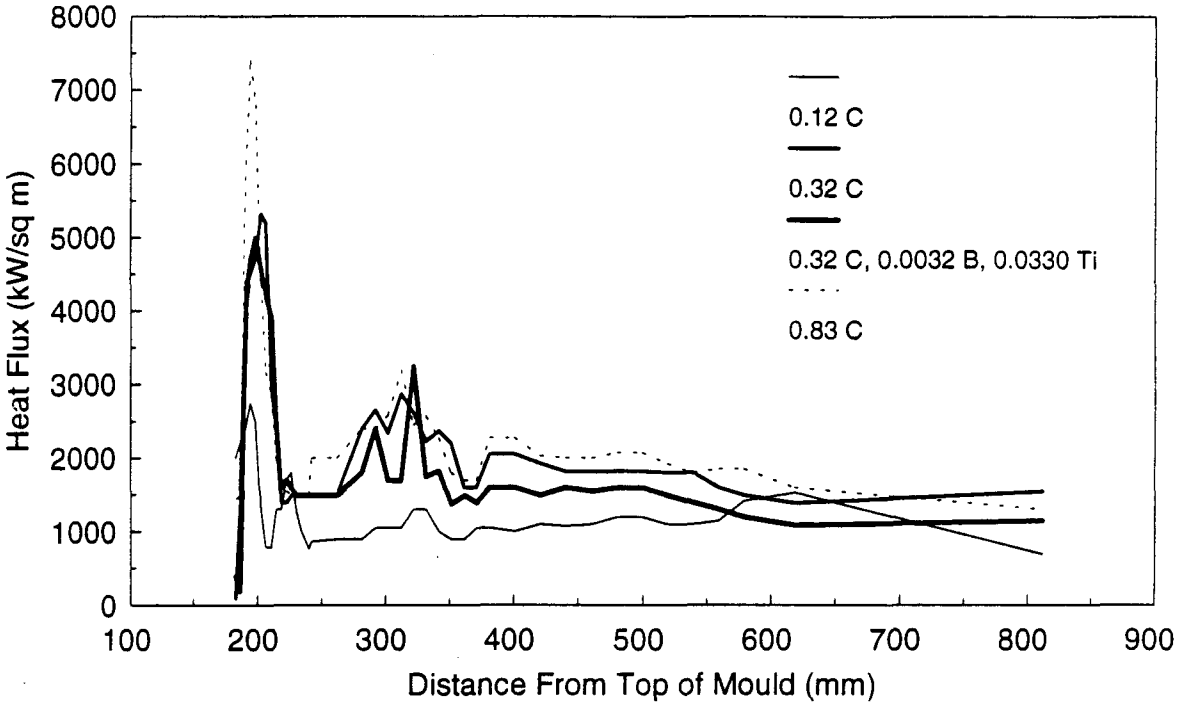

Figure 5.3 Time-averaged axial profiles of mould heat flux.

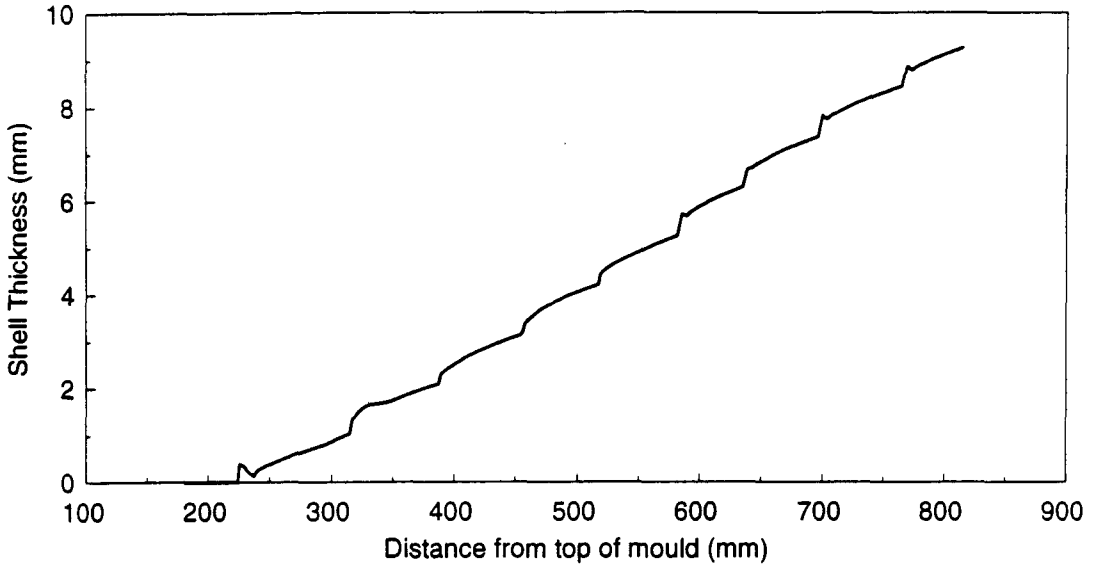

(a)

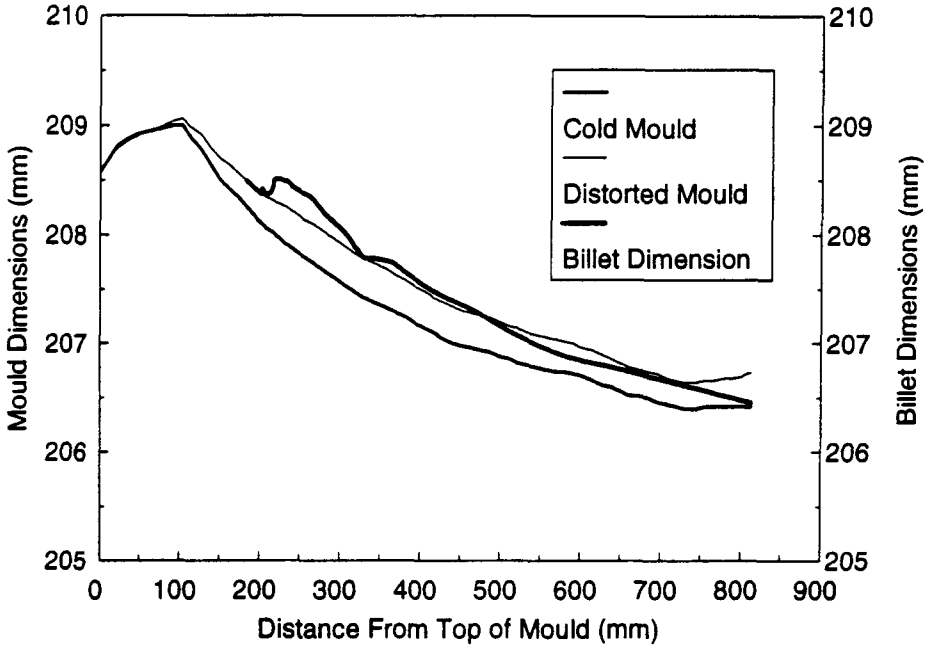

(b)

Figure 5.4: Computed axial profiles (a) shell thickness and (b) strand shrinkage; (0.12 %C)

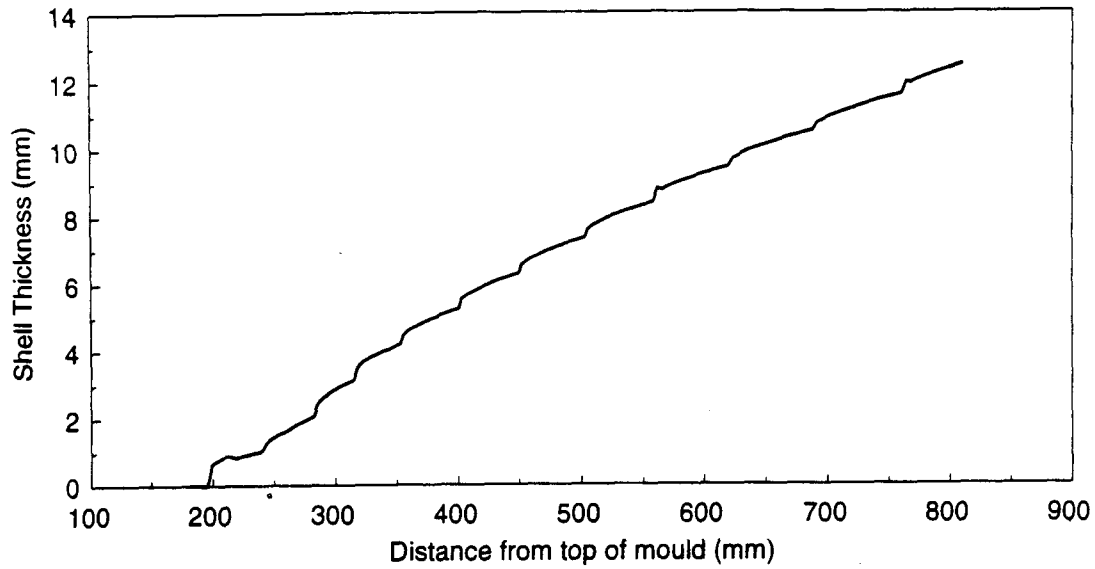

(a)

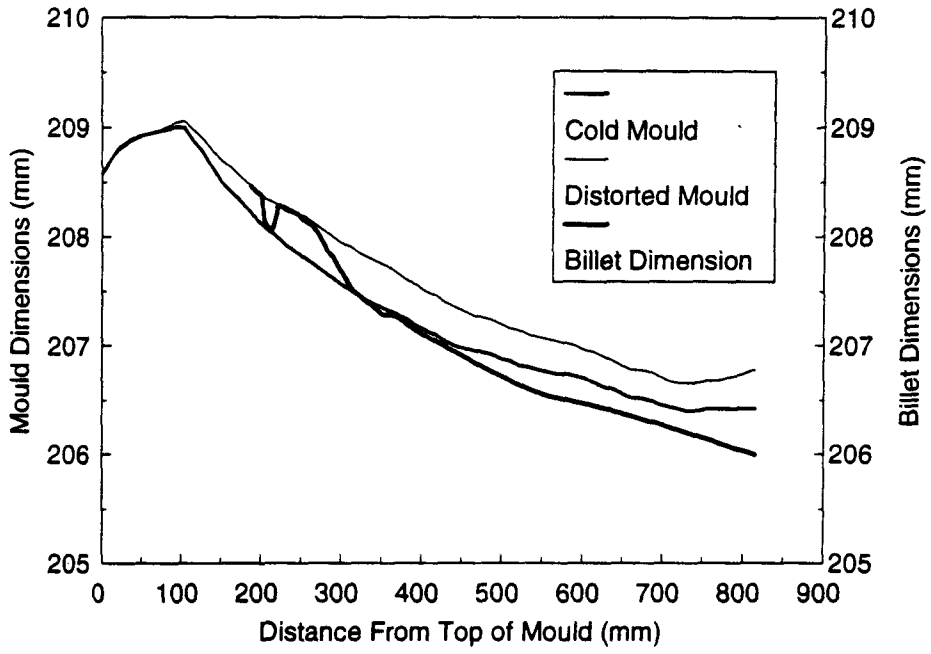

(b)

Figure 5.5: Computed axial profiles (a) shell thickness and (b) strand shrinkage; (0.32 %C)

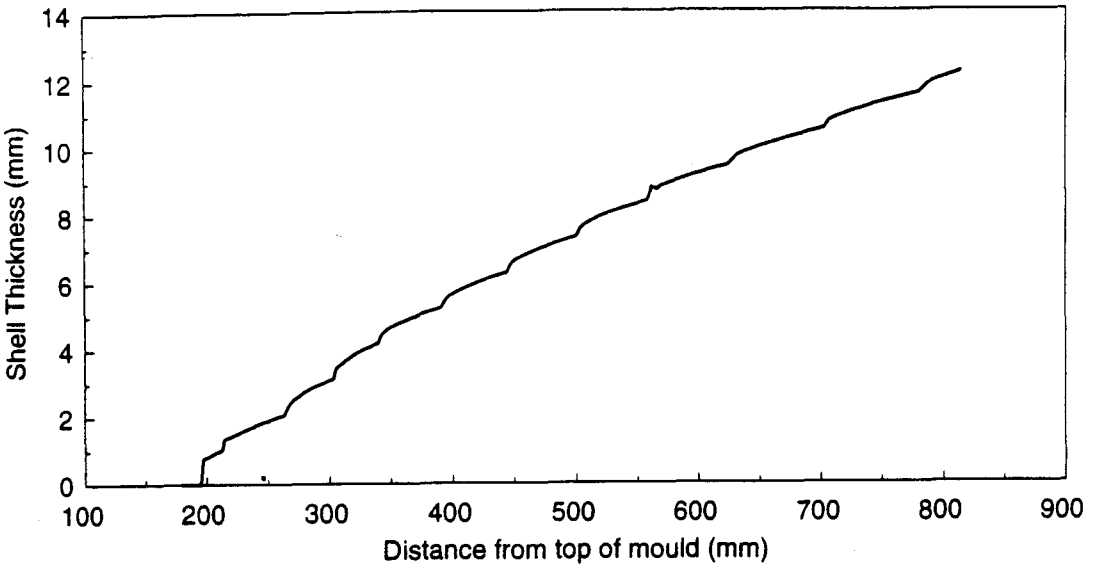

(a)

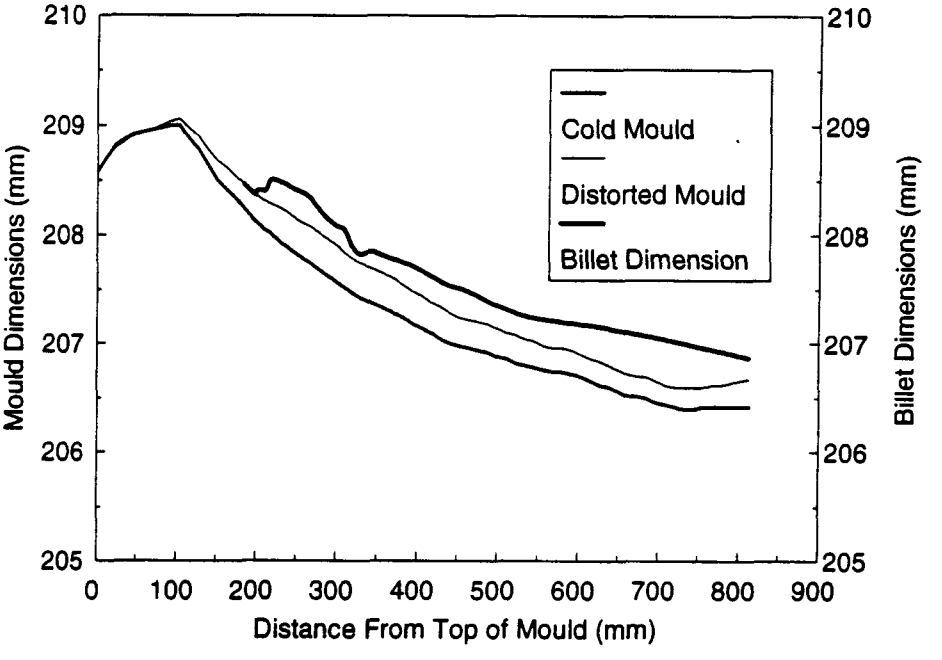

(b)

Figure 5.6: Computed axial profiles (a) shell thickness and (b) strand shrinkage; (0.31 %C, 0.0020 %B, 0.033 %Ti)

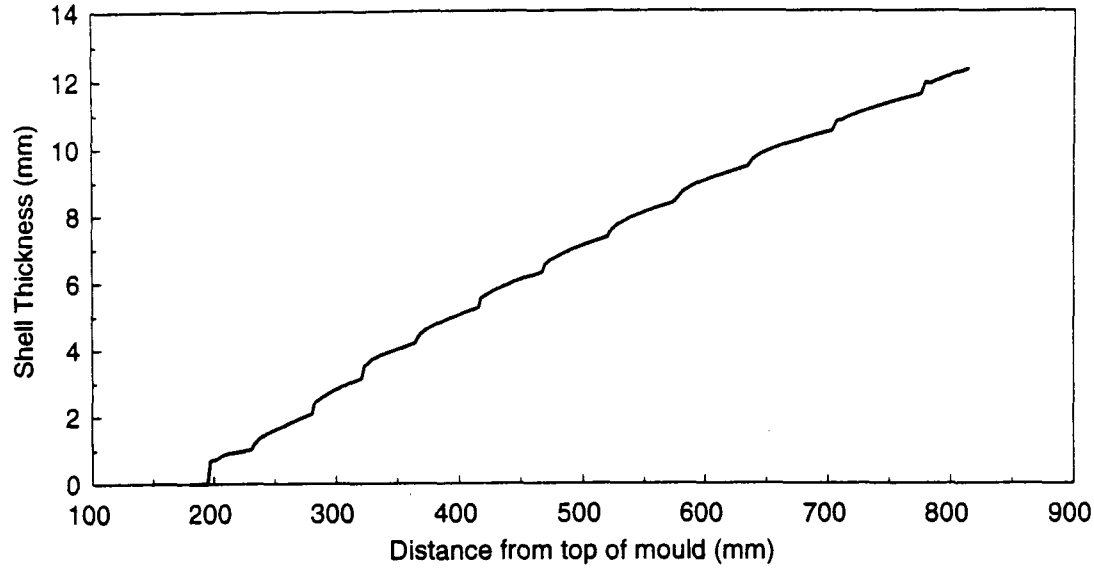

(a)

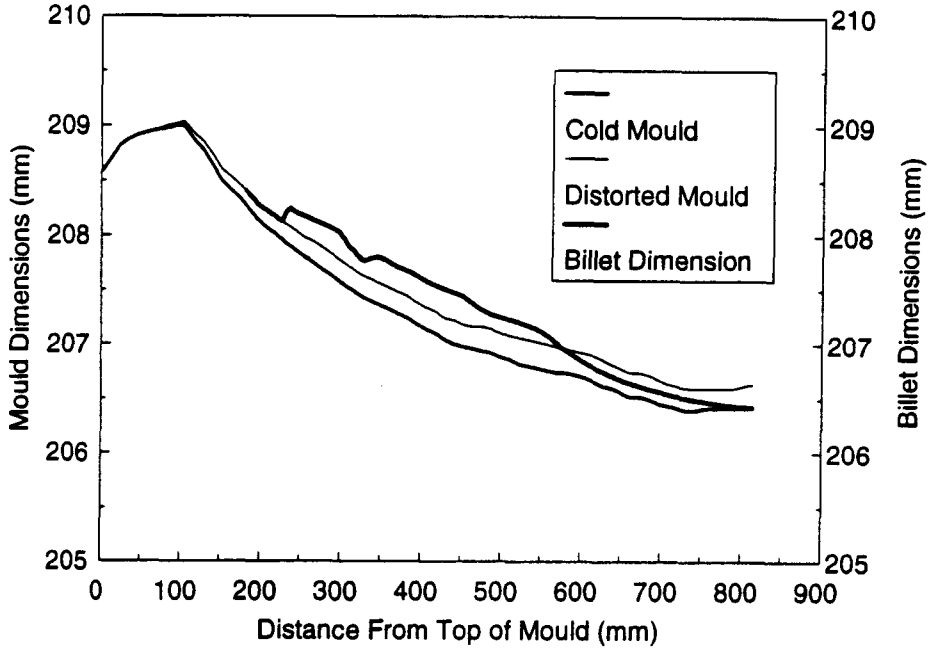

(b)

Figure 5.7: Computed axial profiles (a) shell thickness and (b) strand shrinkage; (0.32 %C, 0.0032 %B, 0.033 %Ti)

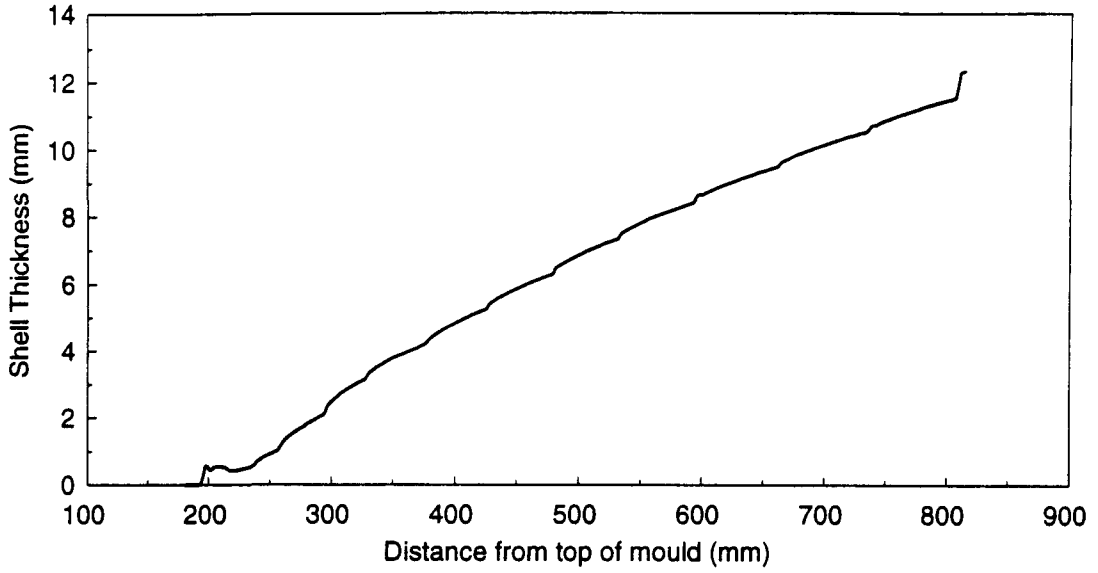

(a)

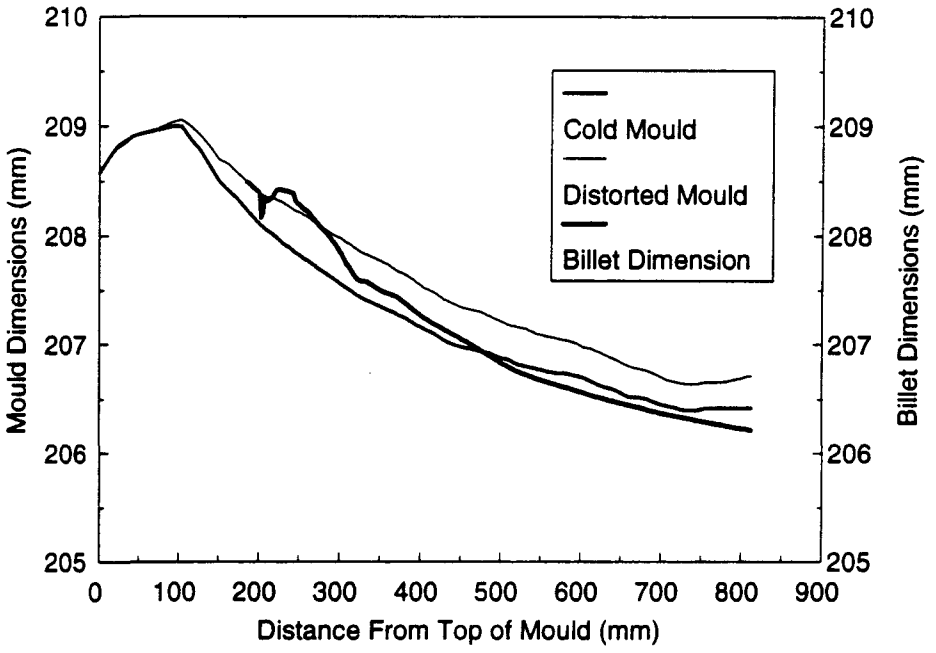

(b)

Figure 5.8: Computed axial profiles (a) shell thickness and (b) strand shrinkage; (0.83 %C)

5.2 Mechanism of Transverse Depressions

This section discusses the previous mechanism and then presents a new mechanism emerging out of this and other related work.

5.2.1 Previous Mechanism

As mentioned in Chapter 2, a mechanism explaining the formation of transverse depressions was proposed in an earlier study [3]. This mechanism, based on mould-strand interactions was specifically linked to binding of the strand in the mould. Following this, another study [72,73] which employed load cells to study mould-strand interactions reported results which were consistent with the mechanism.

The load cells registered load fluctuations with large amplitudes indicative of binding for heats which exhibited transverse depressions. Furthermore, when the heat flux data determined from thermocouples embedded in the mould wall were used to calculate the shrinkage of the billet, the outside dimension of those depression prone billets were found to be larger than the internal dimension of the distorted mould. This was particularly true in the upper part of the mould where the taper was large which caused the binding. Of considerable importance among the observations were the cracks seen below the depressions.

These cracks were undoubtedly due to tensile strains in the region of low ductility close to the solidification front, a result of the pulling action by the withdrawal rolls on the strand when it is stuck. So, clearly there was enough evidence supporting the mechanism. However, from the

findings in this work, and other related observations in mini-mills across North America, revelations of some critical parameters which were not accounted for in the previous mechanism have been made.

The use of high frequency mould temperature data has made it possible to unravel some of these parameters. The advantage of real-time mould temperature analysis is the identification of some localized events such as metal level fluctuations, sticking etc. and monitoring of the strand surface profile from the meniscus to the exit of the mould especially with high frequency data.

5.2.2 Proposed Mechanism

The most important finding in this study was detection of the location in the mould where the depressions initiate. It was found that the depressions originate close to the meniscus, about 10-15 mm below the meniscus and were preceded by a metal level rise over a period of up to 6 seconds as indicated in Tables 5.1 and 5.2. Other operating factors observed to influence the formation of transverse depressions in some independent related work are discussed below.

Casting speed:- It has been found that for a given section size there exists a critical casting speed above which depressions are absent. This is illustrated in Table 5.3 which is based on information gathered by Lorento [74] at mini-mills across North America. The critical casting speed data presented in the Table appears to bear a linear relationship to the billet size expressed in terms of the mould inside perimeter as shown in Figure 5.9

Lubricating Oil Flow Rate:- It has been found in many mini-mills that depression formation is sensitive to the oil flow rate [74]. Further evidence of the influence of oil flow rate on the

depressions may be seen in Figures 5.10 - 5.12, obtained from a previous work [72,73]. These billet sections were cast with a mineral synthetic oil at flow rates of 40, 20, and 34 ml/min respectively and it is evident that the nose-type depression is most pronounced at 40 ml/min, while at 20 ml/min depressions are smoother. It must be emphasized, however that, as both nose-type and smooth depressions could be found on the same billet section (Figure 4.11), it suggests that the conditions giving rise to a specific shape may be more likely related to the volume of oil at the meniscus rather than the mean flow rate which is an integrated average.

Metal Level Fluctuations:- The link between metal level fluctuations reported to be influenced by tundish stream quality [22,23], and transverse depression formation was observed during the trial in the present work and other studies.

It was seen during visual observations of the tundish stream quality and position, the meniscus, and the sprays (just below the mould) in the trial that the depression-prone billets were in most instances jerking as they exit the mould. The tundish streams of those heats were ropey (rough) and it was no surprise that the liquid levels were turbulent

A similar observation was made in a mini-mill in North America [74]. Following the installation of a new casting machine, transverse depressions which were accompanied by jerking of the strands, were seen to occur on 0.18 %C grades. Observations of the liquid level in the mould revealed severe turbulence and metal level fluctuations which were traced to the absence of a pour box in the tundish. A remedial action was taken by installing a temporary pour box. This remarkably improved the quality of the tundish streams, reduced the metal level fluctuations, and eliminated transverse depressions in this grade of steel.

Following these observations, a new mechanism which is shown schematically in Figure 5.13 is proposed. Thus under desired operating conditions with a reasonably stable metal level, lubricating oil vaporizes as it weeps down the mould wall and approaches the molten steel (Figure 5.13a). As the mould descends in the negative strip period of each oscillation cycle, oil wetting the chromium-plated copper surface is drawn into the gap between the mould wall and the meniscus. The oil, which has a boiling range of 200 to 350 °C, vaporizes (and pyrolyzes) as the molten steel at the meniscus presses against the mould wall releasing gas upwardly into the mould freeboard. In the absence of inert gas shielding of the tundish stream, the oil vapors combust in contact with air and flares.

However, if owing to turbulence in the mould pool, the metal level rises, as shown conceptually in Figure 5.13b, the oil vaporization rate may be insufficient to remove the wetted oil film beneath the meniscus such that some oil is trapped between the solidifying shell and the mould wall. The sudden release of vapor from the trapped oil may generate sufficient pressure to push on the shell solidifying at the meniscus and force it briefly away from the mould wall to create a depression.

This mechanism is supported by two observations. First, the simultaneous detection of the depressions by the two thermocouples just below the meniscus suggests a sudden formation of the depressions as would be the case for a sudden exertion of external pressure on the shell. Second, the fact that transverse depressions are dramatically eliminated in powder casting [81] confirms the fact that metal level fluctuations and lubricating oil play important roles in the formation of depressions.

5.2.2.1 Effect of Process Variables

If the above concept is true then the severity of the formation of transverse depressions will depend on the extent of metal level fluctuations and oil flow rate and the strength of the skin freezing at the meniscus.

Metal Level Fluctuations:- As noted above, severe metal level fluctuations which are linked to ropey tundish streams, gas entrainment in the mould pool, and a turbulent meniscus may trigger the formation of the depressions.

Lubricating Oil Flow Rate:- With respect to lubricating oil, flow rates over about 0.05 ml/min per mm of perimeter [75] can lead to entrapment of enough oil vapor beneath the meniscus to cause depressions

Steel Composition:- The observed effect of steel composition on transverse depressions may be via its influence on the strength of the thin shell solidifying at the meniscus. The carbon content strongly alters the freezing range of steel, as is well known. Thus the broader mushy zone of high carbon steel (C>0.6%) is unlikely to behave as a solid skin close to the meniscus; consequently any pressure buildup beneath the meniscus due to oil entrapment is released by a vertical escape of the vapor rather than the creation of a cavity, that is, transverse depressions, between the mould wall and the semi-solid steel skin. At lower carbon levels, with a narrower freezing range, the skin behaves more as a solid such that a sudden generation of trapped oil vapor pushes on the skin to form a transverse depression. The sensitivity of boron-containing steels to transverse depressions may be related to the presence of titanium which is added to combine with nitrogen dissolved in the steel, to form TiN, and thereby protect the boron from being consumed

as BN. It is well known that TiN is stable at steelmaking temperatures, and is probably dispersed as a solid phase in the solidifying shell. The TiN precipitates could strengthen the shell allowing the creation of sub-meniscus cavities due to trapped oil vaporization.

Casting Speed:- A summary of the effect of casting speed and section size on transverse depressions has been presented in Table 5.3. Again, this influence may be through the solid or semi-solid nature of the skin close to the meniscus, as just described. Increasing the casting speed, V_c, at a constant steel temperature entering the mould, T_o, proportionately raises the rate at which superheat, Q_{sh}, flows into the mould as follows:

Q_{sh} = [mass flow rate of steel] x [specific heat content of steel above the liquidus temperature]

$$= V_c A_M \rho x C_{pl}(T_o - T_l) \qquad (5.1)$$

where A_M is the cross-sectional area of the mould (mm^2)

ρ is the liquid steel density (g/mm^3)

C_{pl} is the average heat capacity of liquid steel (J/g°C)

T_o is the pouring temperature (°C)

and T_l is the liquidus temperature of the steel (°C)

Thus increasing the casting speed by 50% elevates the superheat by the same amount. On the other hand, the extraction of the superheat by the mould, Q_M, especially at the meniscus, depends on the local steel-to-mould heat flux, q_M (typically 3 to 7 MW/m^2 [77]), and the area through which the heat is transferred, A_M, as follows:

$$Q_M = q_M A_M$$

$$= q_M(P_M.1) \tag{5.2}$$

where A_M can be equated to the inside perimeter of the mould, P_M, times a unit length. It is reasonable to expect that increasing the casting speed and thereby the superheat into the mould may delay skin formation close to the meniscus with similar effect overall on depression formation as raising the carbon content of the steel. On the other hand, increasing the section size and thereby P_M, while maintaining the superheat input rate constant enhances the extraction which should have an opposite effect on skin formation at the meniscus, that is, accelerating solidification and the propensity to form transverse depressions. Thus the ratio of Q_{sh} to Q_M, which can be termed the Lorento Number,

$$L_o = \frac{Q_{sh}}{Q_M} \tag{5.3}$$

should be a useful criterion to characterize the critical conditions in the mould leading to transverse depressions. Then the critical Lorento Number, Lo^*, should be the same, at least approximately, at different billet producers. Thus for companies A through F in Table 5.3.

$$Lo_A^* = Lo_B^* = Lo_C^* = \ldots = Lo_F^* \tag{5.4}$$

and if q_M, T_o and T_l can be taken to be the same in the different operations (ρ and C_{pl} are properties of the molten steel)

$$\frac{V_c A_M}{P_{M\ A}} = \frac{V_c A_M}{P_{M\ B}} = ... = \frac{V_c A_M}{P_{M\ F}} \tag{5.5}$$

This ratio of variables for Companies A to F is presented in Table 5.3. Although there is some variability in the values, given the approximate method of determining the critical casting speed in plant, there is surprising constancy in the ratio; the average value of 1084 mm^2/s. These results are shown graphically in Figure 5.14 where the critical volume flow rate of the molten steel ($V=V_cA_M$) is plotted against P_M for the six companies.

Taper:- The mould taper influences transverse depressions in at least two ways. Firstly, the inside dimensions of the mould, relative to the shrinkage of the cooling solid shell, may result in binding of the strand in the mould as revealed in the shell shrinkage profiles in Figures 5.4 to 5.8. The axial tensile strain imposed on the shell by the withdrawal force, may act to widen transverse depressions initiated close to the meniscus because they are hotter and weaker owing to the local reduction in heat transfer. This is evident in Tables 5.1a and 5.2a where it is noted that in most cases the thermocouples which first detected the depressions recorded a local drop in temperature for shorter duration than the drop recorded by the ones located below them, indicating widening of the depressions, a consequence of binding. The reduced shell thickness outlined by the white solidification band as seen in Figure 5.11 is also evidence of binding. The pulling action of the withdrawal rolls under conditions of binding may result in a disturbance of the interdendritic liquid, seen as the white solidification band, and also lead to reduction in the shell thickness as the depression widens.

The mould taper at the meniscus has also been found to change the mould heat extraction significantly [77]. Reduction of the local taper from 2.7 to 0.4 %/m raises the heat flux at the meniscus from 3 to 7 MW/m^2. From the arguments presented above the steeper taper should exacerbate the formation of depressions because of the low hot-face temperature which might lead to excess lubricating oil at the meniscus. It must be noted, however, that a high hot-face temperature (above the boiling point of lubricating oil) too will cause depletion of oil for lubrication at the meniscus and lead to other quality problems such as laps and bleeds.

Table 5.3 Critical Casting Speeds and Section Sizes Influencing Depressions in Billets

Company	Section Size (mm x mm)	Mould Perimeter, P_M (mm)	Cross-Sectional Area, A_M (mm^2)	Critical Casting Speed, u_c (mm/s)	Critical Volume Flow Rate of Steel, V_c (x 10^5 mm^3 /s)	V_c/P_M (mm^2/s)
A	203 x 203	812	41,209	21.2	8.74	1080
B	127 x 178	610	22,606	28-30	6.33-6.78	1038-1110
C	203 x 203	812	41,209	25.4	10.5	1290
D	160 x 160	640	25,600	26.7	6.84	1070
E	229 x 413	1283	94,580	11.9-14.4	11.26-13.62	878-1062
	203 x 356	1118	72,270	14.4-17.8	10.41-12.86	931-1150
	203 x 254	914	51,560	21.2	10.93	1196
F	127 x 305	864	38,735	19.1-23.3	7.40-9.03	856-1045

Note: Critical ratio = 1084 $mm/^2$

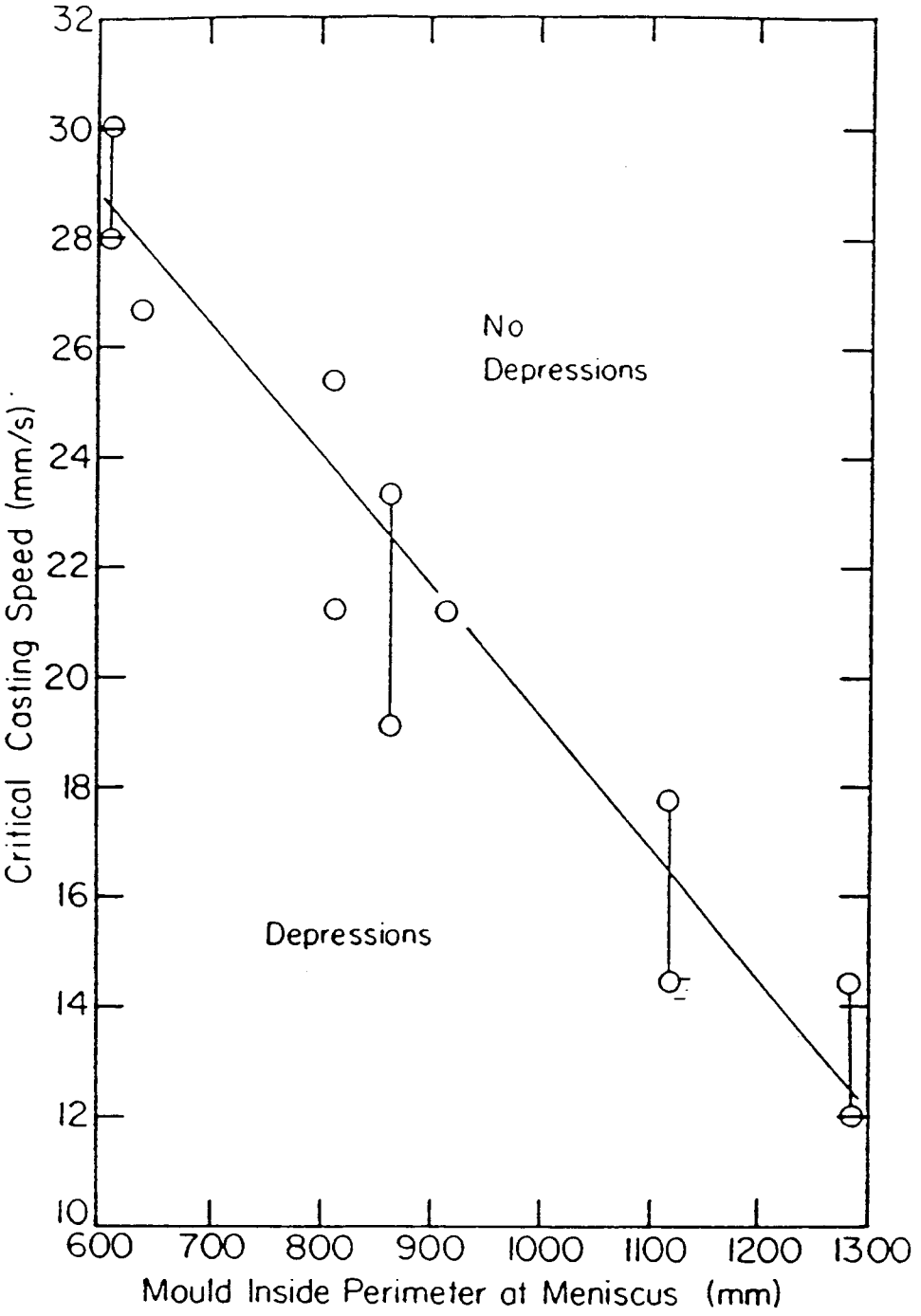

Figure 5.9: Relationship between critical casting speed for depression formation and mould inside perimeter[74].

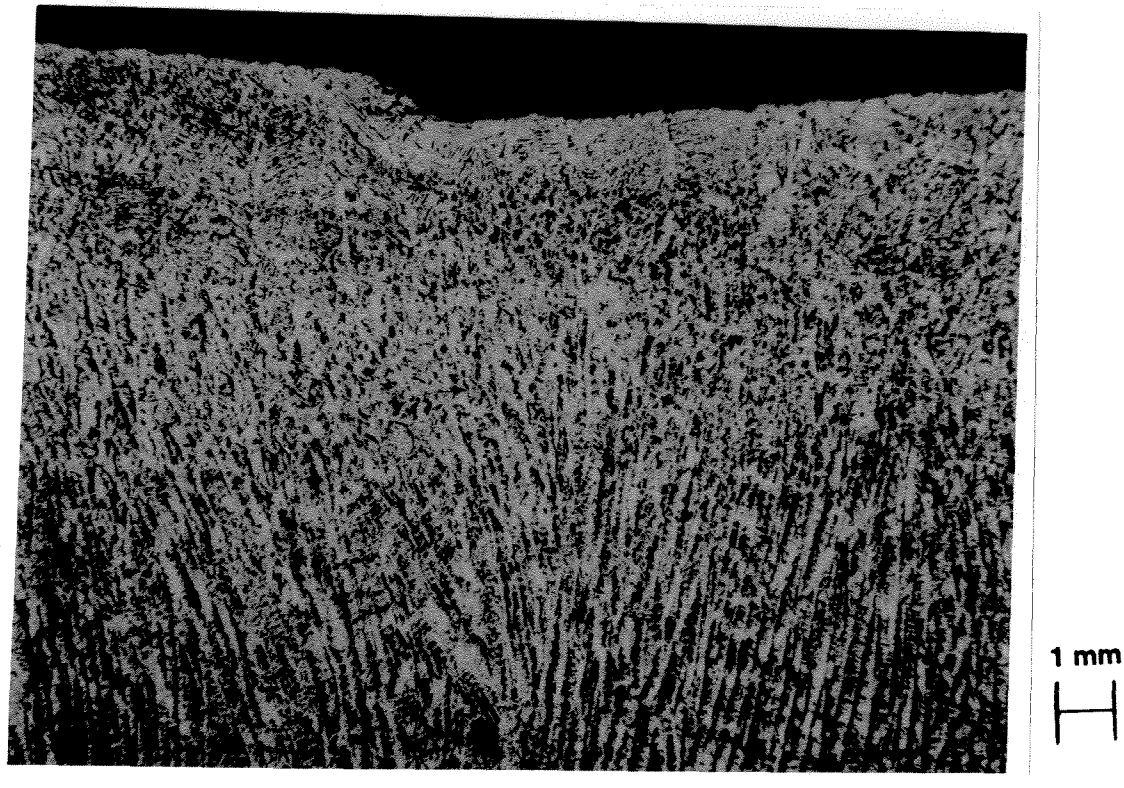

Figure 5.10: Photograph of a longitudinal section of a 0.09 pct carbon billet showing a nose-type depression. Oil flow rate = 40 ml/min.

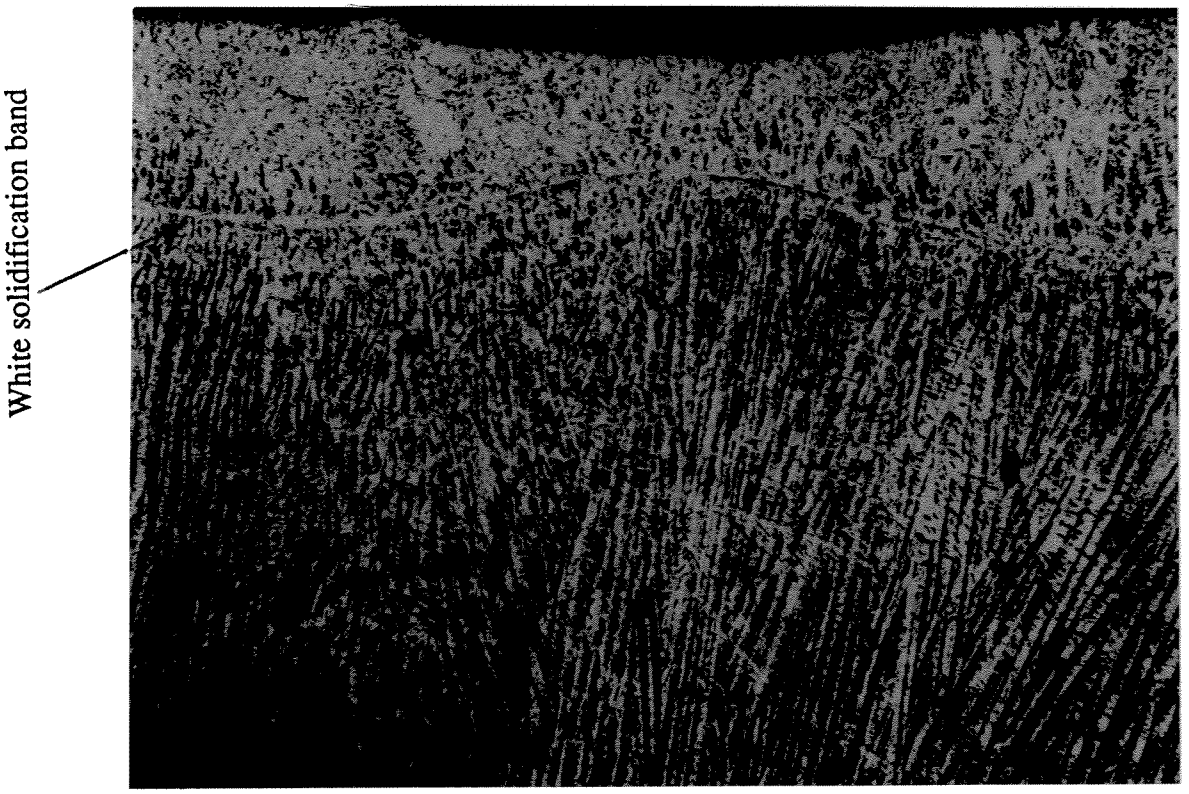

Figure 5.11: Photograph of a longitudinal section of a 0.09 pct carbon billet showing smooth depression. Oil flow rate = 20 ml/min.

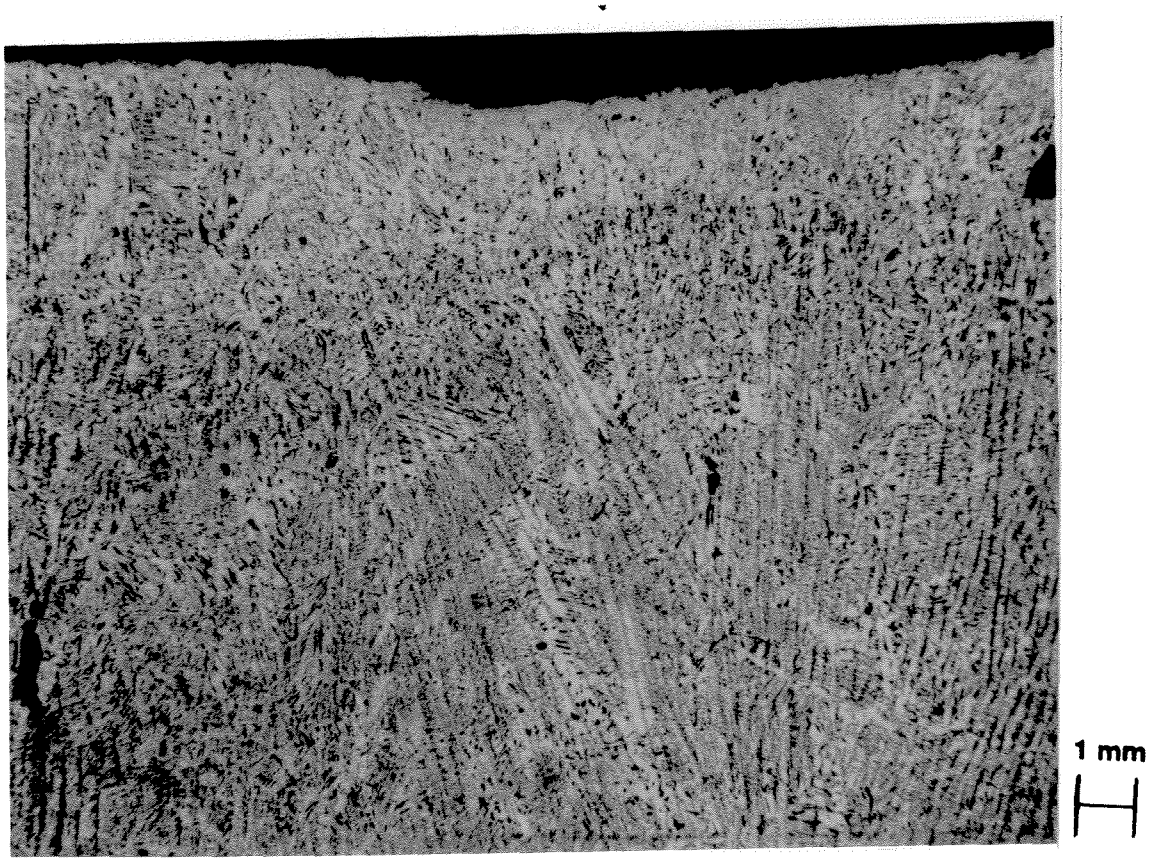

Figure 5.12: Photograph of a longitudinal section of a 0.09 pct carbon billet exhibiting a depression. Oil flow rate = 34 ml/min.

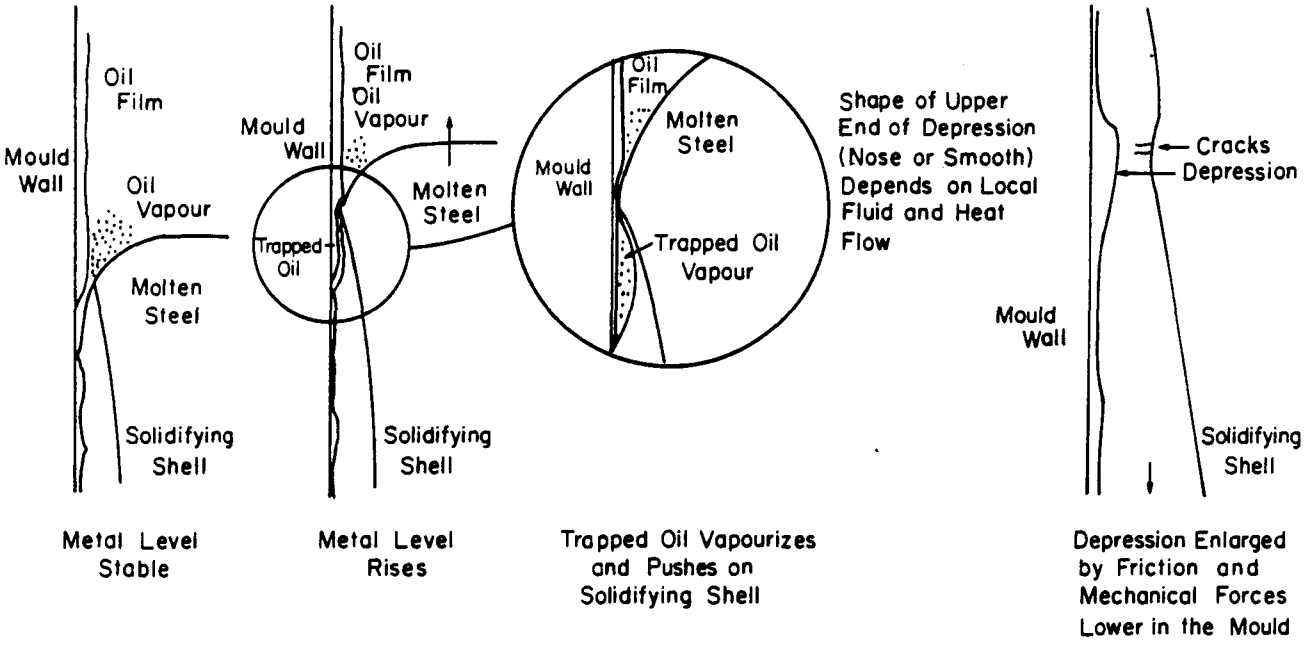

Figure 5.13: Proposed mechanism of transverse depression formation near the meniscus due to metal level rise and trapped oil vaporization.

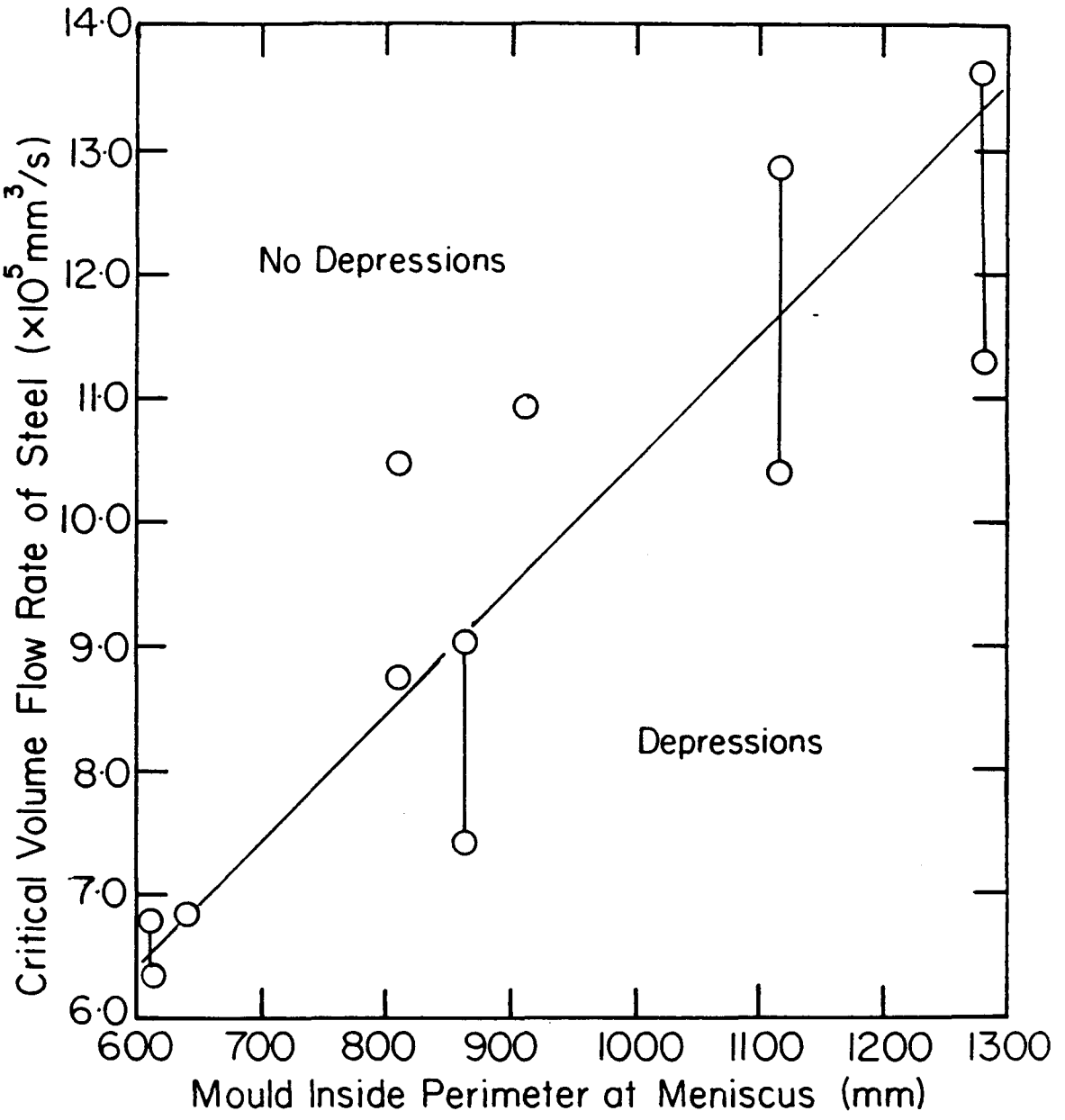

Figure 5.14: Transverse depression diagram based on the critical Lorento Number[74].

Chapter 6: Summary and Conclusions

The character of transverse depressions, their manifestation in mould thermal data, and a mechanism for their formation have been elucidated. In order to establish a link between the defect and the temperature data, a plant trial was carried out at a Canadian mini steel mill involving an instrumented operating mould. Signals from thermocouples installed along the mould length, as well as that from casting speed and metal level controllers, were recorded by a PC-based data acquisition system at a rate of 100 Hz for 400 s per heat. Both plain and boron-containing steels with carbon contents ranging from 0.12% to 0.83% were monitored.

Real-time analysis of the mould thermal response was performed using spreadsheet and computer programs coded in FORTRAN 77. Billet samples collected during the trial were subjected to metallographic analysis to determine the solidification structure and cracks beneath the depressions. To investigate binding in the mould, existing mathematical models for billet shrinkage and mould distortion were used to compute the external and internal dimensions of billets and the mould respectively. Finally the findings from the analysis together with information gathered by Lorento [74] across mini-mills in North America were used to formulate a mechanism for transverse depressions formation.

From the results of the study the following conclusions can be drawn:

(i) Thermocouples located longitudinally below the meniscus are capable of detecting transverse depressions. Responses from thermocouples located above the meniscus provide a better means of monitoring localized metal level fluctuations than signals from a metal level controller which give a global measure of metal level fluctuations.

(ii) Transverse depressions initiate close to the meniscus, about 15 - 20 mm below the meniscus, and travel down the mould at the same speed at which the strand is withdrawn.

(iii) Due to the gap created between the strand and the mould by the depressions, heat transfer from the strand to the mould cooling water and associated shell shrinkage reduces as the strand travels down the mould. If this results in a bigger outside dimensions of the strand relative to the inside dimensions of the distorted mould, binding occurs in the lower part of the mould leading to widening of the depressions and crack formation at the base or several millimeters below the meniscus.

(iv) About 90% of the depressions studied were preceded by a rise in metal level suggesting that metal level fluctuations, a consequence of ropey streams are critical to the formation of depressions.

(v) Observations made in mini-mills across North America reveal that depressions form when excessive oil flow rate (> 0.05 ml/min. per mm of perimeter) is used. This observation, together with a rise in metal level preceding the formation of the depressions, and the initiation of the depressions close to the meniscus indicate that exertion of pressure by trapped oil vapor beneath the meniscus on the shell is the probable cause of depressions.

(vi) The depressions are influenced by steel composition as indicated by the numerous depressions observed in the boron grades (containing titanium), few in the medium plain carbon grades and none in the high carbon grades. This observation suggests that, the nature (solid or semi-solid) of the initial shell formed, influences depression formation. The dispersion of TiN in the shell of the boron grades renders it most solid and susceptible to depression formation.

(vii) Casting speed (relative to section size) influences depression formation through the rate of superheat entry and extraction in the mould, which in turn affect the nature of skin formation at the meniscus.

(viii) Excessive mould taper in the lower part of the mould may cause binding leading to crack formation below the depressions.

(ix) The critical Lorento number, $Lo = Q_{sh}/Q_m = u_c A_m/p_m$ related to casting speed, provides a useful criterion in monitoring casting speed levels that could lead to transverse depression formation.

It is believed that finally, the various parameters influencing transverse depression formation, especially metal level fluctuations, and the location in the mould where the depressions initiate have been identified. It is recommended that, a combination of optimum mould operation parameters, and on-line monitoring of the process are important to detect any upsets that may arise during the operation and any defect that may occur as a result of an undetected upset.

In monitoring depressions on a particular face a maximum of four thermocouples is adequate - one above the meniscus to monitor the metal level fluctuations, and two or three below the meniscus. The thermocouple above the meniscus may be placed not lower than 10 mm and higher than 15 mm. Above 15 mm the response of the thermocouple to metal level fluctuations begin to diminish, and below 10 mm, there is a chance that the thermocouple may be covered by the metal. Below the meniscus the first thermocouple may be located about 15 - 20 mm from the metal surface, while the second or third should be placed away from the influence of metal level fluctuations approximately 80 mm below the meniscus. These may be used to confirm an earlier detection by the first thermocouple below the meniscus.

It is also recommended that knowledge of the character of transverse depressions in mould thermal data, the influencing factors, and the Lorento Number be tested in subsequent plant trials and optimal monitoring and controlling procedures established.

References

1. I.V. Samarasekera, and J.K. Brimacombe: "The Continuous Casting Moulds", International Metals Review, 1978, No. 6, pp. 236-299.

2. S. Chandra, Ph.D. Thesis, The University of British Columbia, Vancouver, B.C. Canada, 1992.

3. I.V. Samarasekera, and J.K. Brimacombe: "The Heat Extraction Capabilities of Continuous Casting Billet Moulds", Proceedings of the W.O. Philbrook Memorial Symposium Conference, 1988, pp. 157-171.

4. B.G. Thomas, J.K. Brimacombe, and I.V. Samarasekera: "The Formation of Panel Cracks in Steel Ingots", A State of the Art Review I, Hot Ductility of Steel, ISS Transactions, 1986, vol. 7, pp. 7-18.

5. L. Brendzy, M.A.Sc Thesis, The University of British Columbia, Vancouver, B.C., 1990.

6. S. Watanabe et al., Tetsu-to-Hagane, JISI of Japan, 1972, vol. 5B, No. 11, pp. 393-394.

7. R.J. Dippenaar, I.V. Samarasekera, and J.K. Brimacombe: "Mould Taper in Continuous Casting Billet Machines", ISS Transactions, 1986, vol. 7, pp. 31-43.

8. Y. Aketa, and K. Ushijima, Tetsu-to-Hagane Overseas, JISI of Japan, 1962, vol. 2, No. 4, pp. 334-343.

9. A. Grill, K. Sorimachi, and J.K. Brimacombe, Metall. Trans. B, 1976 7(B), pp. 211-216.

10. E.G. Zetterland, and J.K. Kristiansson, Scandinavian Journal of Metallurgy, 1983, vol. 12, pp. 211-216.

11. I.V. Samarasekera, D.L. Anderson, and J.K. Brimacombe: "The Thermal Distortion of Continuous Casting Moulds", Metall. Trans. B, March 1982, vol. 13B, pp. 91-104.

12. I.V. Samarasekera, J.K. Brimacombe, and R. Bommaraju, ISS Trans. 1984, vol. 5, pp. 79-94.

13. C.R. Taylor, Metall. Trans B, 1975, vol. 6B, pp. 359-375.

14. R. Bommaraju, and J.K. Brimacombe, Metall. Trans. 1982, vol. 13B, pp. 95-105.

15. J. Stel, J.M. Ranberg, M.C.M Cornilissen, and J. Cilisouv, 1st European Conference on Continuous Casting, Italy, 1991, pp. 2377-2386.

16. I.V. Samarasekera, and J.K. Brimacombe, International Metals review, 1978, No. 6, pp. 286-300.

17. M.M. Wolf, Mould Operation for Quality and Productivity, 1991, pp. 15-31.

18. I.G. Saucedo, and K.E. Blazek: "Characterization of the Effects of Mould Oscillation on Heat Transfer Rate and Friction During Continuous Casting", Proceedings of the 6 th International Iron and Steel Congress, Steelmaking I, Nagoya 1990, vol. 3, pp. 325-333.

19. S. Junghans: "Process Device for the Casting of Metal Strands", German Patent 750,301 of October 20, 1933.

20. D.H. Miller, and T.E. Dancy: "Continuous Casting - Past, Present, and Future", AISI, Pittsburgh, PA, 1964, pp. 38-42.

21. I.M.D. Halliday: "Continuous Casting at Barrow", Journal of the Iron and Steel Institute, 1959, vol. 191, pp. 121-1163.

22. W.J. Maddever et al., Canadian Metallurgical Quarterly, 1973, vol. 12, No. 4, pp. 79-87.

23. W.J. Maddever et al., Proceedings of the AIME Open Hearth Conference,a 1976, vol. 59, pp. 177-211.

24. L. Heaslip et al., AIME-ISS 2nd Process Technology Conference, 1981, vol. 2, pp. 54-64.

25. F. Kemeney et al., AIME-ISS 2nd Process Technology Conference, 1981, vol. 2, pp. 232-245.

26. I.V. Samarasekera, and J.K. Brimacombe: "The Thermal Field in Continuous Casting Billet Moulds", Can. Met. Quart., vol. 18, 1979, pp. 251-266.

27. I.V. Samarasekera and J.K. Brimacombe: "The Influence of Mould Behaviour on the Production of Continuously-Cast Steel Billets", Metall. Trans. B, vol. 13B, 1982, pp. 105-116.

28. I.V. Samarasekera and J.K. Brimacombe: "Thermal and Mechanical Behaviour of Continuous-Casting Billet Moulds", Ironmaking and Steelmaking, vol. 9, 1982, pp. 195-116.

29. J.K. Brimacombe, E.B. Hawbolt and F. Weinberg: "Metallurgical Investigation of Continuous Billet Moulds I. - Distortion, Fouling and Wear", ISS Trans. vol 1, 1982, pp. 29-40.

30. E.B. Hawbolt, F. Weinberg and J.K. Brimacombe: "Metallurgical Investigation of Continuous Billet Moulds II. - Microstructure, Softening Behaviour, Mechanical Properties", ISS Trans. vol 1, 1982, pp. 41-60.

31. I.V. Samarasekera and J.K. Brimacombe: "Investigation of Mould-Related Quality Problems in Billet Casting Using Mathematical Models", Third PTD Conference on Application of Mathematical and Physical Models in the Iron and Steelmaking Industry, ISS, Pittsburgh, 1982, pp. 283-295.

32. R. Bommaraju, J.K. Brimacombe and I.V. Samarasekera: "Mould Behaviour and Solidification in the Continuous Casting of Steel Billets III. - Structure, Solidification Bands, Crack Formation and Off-Squareness", ISS Trans. vol. 5, 1984, pp. 95-105.

33. J.K. Brimacombe et al., Proceedings of the 69th Steelmaking Conference, 5th International Iron and Steel Congress, April 1986, Washington D.C. U.S.A.

34. I.V. Samarasekera, J.K. Brimacombe, and R. Bommaraju: "Mould Behaviour and Solidification in the Continuous Casting of Steel Billets II. - Mould Heat Extraction, Mould-Shell Interaction, and Oscillation Mark Formation", ISS Trans 1984, vol 5. pp. 79-84.

35. P.J. Wray: "Geometric Features of Chill-Cast Surfaces", Metallurgical Trans., March 1981, vol. 12B, pp. 167-176.

36. T. Emi et al. "Properties of Continuous Casting Powders Influencing Surface Defects of Wide Slabs for Plates", Tetsu-to-Hagane, 1974, vol. 60, No. 7, pp. 981-989.

37. E. Takeuchi, and J.K. Brimacombe: "The Formation of Oscillation Marks in the Continuous Casting of Steel Slabs", Metallurgical Transactions, September 1984, vol.15B, pp. 493-509.

38. I.V. Samarasekera, R. Bommaraju, and J.K. Brimacombe: "Factors Influencing the Formation of Oscillation Marks in the Continuous Casting of Steel Billets", 24th Annual Conference of Metallurgists 15th Annual Hydrometallurgical Meeting 1985, pp. 1-11.

39. I.V. Samarasekera, and J.K. Brimacombe, Report to Stelco Edmonton Steel Works, Unpublished Work, 1987.

40. A. Tsuneoka et al.: "Measurement and Control System of Solidification in Continuous Casting Mould", 1985 ISS Steelmaking Conference Proceedings, pp. 3-10.

41. S. Itoyama et al: "Prediction and Prevention System for Sticking Type Breakout in Continuous Casting", 1988 ISS Steelmaking Conference Proceedings, pp. 97-102.

42. W.H. Emling, S.D. Mis, and D.J. Simko: "A Thermocouple-Based System for Breakout Prevention and Practice Development" 1988 ISS Steelmaking Conference Proceedings, pp. 183-188.

43. K.E. Blazek and I.G. Saucedo: "Characterization of the Formation, Propagation, and Recovery of Sticker/Hanger Type Breakouts", ISIJ International, 1990, vol. 30 No. 6, pp. 435-443.

44. A. Matsushita et al.: "Breakout Prediction and Surface Quality Analysis by Mould Diagnosis System - Development of Mould Total Diagnostics II", Transactions ISIJ, 1984, vol. 24.

45. B. Mairy et al.: "Mould Lubrication and Oscillation Monitoring for Optimising Continuous Casting", Fifth PTD Proceedings, AIME, 1985, pp. 101-117.

46. B. Mairy, et al.: "Recent Developments in Mould Monitoring", 1990 ISS PTD Conference Proceedings, pp. 73-81.

47. B. Mairy et al.: "Lubrication Control in Caster Moulds with the ML TEKTOR", Steelmaking Conference Proceedings, 1979, vol. 62, pp. 103-104.

48. H.L. Gilles and B.R. Forman: "Measurement and Analysis of Slab Caster Mould Movement", Mould Operation for Quality and Productivity, 1991, pp. 183-196.

49. B. Mairy and M. Wolf, Facherichte, vol. 20 No. r, April 1982, pp. 222-227.

50. H.L.Gilles et al.: "The Use of Instrumented Mould in the Development of High Speed Slab Casting", 9th PTD Conferences Proceedings, 1990, pp. 123-138.

51. M. Schmid, Concast News, 12, 1973, 1, p. 6-8.

52. S.G. Thornton, N. Hunter, B. Patrick, and D. Bowen: "Techniques to Achieve On-Line Total Mould Monitoring in Continuous Casting", A.T.S Stelmaking Conference, Paris, November-December 1988.

53. E.A. Parr, Industrial Control Handbook, vol. 1 Industrial Press Inc. New York.

54. R.J. Phillips, W. Salem, H.D. Baker, and W.H. Emling, "Prevention of Broadface Sticking", 1990 ISS Steelmaking Conference Proceedings, pp. 247-251.

55. A. Delhalle et al.: "New Development in Quality and Process Monitoring in Solmer's Slab Casting", 1984, ISS Steelmaking Conference Proceedings, pp. 21-35.

56. K.E. Blazek and I.G. Saucedo; "An Investigation of Sticker and Hanger Breakouts", Fourth International Conference on Continuous Casting, Preprints 2, Brussels, 1988.

57. W.H. Emling, "Mould Instrumentation for Breakout Detection and Control", Mould Operation for Quality and Productivity, 1991, pp.161-181.

58. P.J. Koening, "Measurement of the Heat Balance of Continuous Casting Moulds as a Source of Information for Process Technology", Stahl und Eisen, vol. 92, 1972, No. 14, pp. 678-688.

59. J. Savage and W.H. Pritchard, "The Problem of Rupture of the Billet in the Continuous Casting of Steel", Journal of the Iron and Steel Institute, November 1954, pp.269-277.

60. M. Yaji et al.: "Method of Controlling Continuous Casting Equipment", United States Patent, Number 4,553,604, Date of Patent: November 19, 1985.

61. Y. Miyashita et al.: "Improvement of Surface Quality of continuously Cast Slab", Nippo Kokan Technical Report, Overseas No. 36, 1982, pp. 1-10.

62. K. Koyama et al.. Tetsu-to-Hagane, vol. 69, 1983, pp. S1036.

63. I.V. Samarasekera, and J.K. Brimacombe, Ironmaking and Steelmaking, 1982, vol. 9, pp. 1-15.

64. H.L. Gilles: "Breakout Prevention by Automatic Mould Control", Proceedings of 2nd Annual AIME Process Technology Conference, Chicago, February 1982, pp. 205-212.

65. S. Itoyama et al.: "Prediction and Prevention System for Sticking Type Breakouts in Continuous Casting", 1988 ISS Steelmaking Conference Proceedings, pp. 97-102.

66. K. Kurihara et al.: "Development of Mould Diagnostic Technology - Breakout Prevention and Quality Prediction", Transaction ISIJ, vol. 25, 1985.

67. I.A. Bakshi et al.: US Patent Application 1991

68. C.D. Henning and R. Parker, Trans ASME, May 1967, pp. 146-154

69. J.K. Brimacombe et al.: "Mould Behaviour and Solidifucation in the Continuous Casting of Steel Billets I - Industrial Trials", ISS Trans, 1984, vol. 5, pp. 71-77.

70. I.A. Bakshi, E. Osinski, I.V. Samarasekera and J.K. Brimacombe, INternational Symposium on Hot Charging and Direct Rolling, eds; J.J. Jonas, R.W. Pugh and S. Yue, CIM, 1988, 10, pp. 60-69.

71. A.W. Cramb: "Steelmaking and Continuous Casting of Microalloyed Steels", Proceedings of the International Conference on Processing, MIcrostructure and Properties of Microalloyed and Other High Strength Low Alloy Steels, pp. 3-8.

72. J.L. Brendzy et al.: "Mould Strand Interaction in the Continuous Casting of Steel Billets. Part II. Lubrication and Oscillation-Mark Formation", Ironmaking and Steelmaking, 1993, vol. 20, No. 1, pp. 63-74.

73. I.A. Bakshi et al.: "Mould Strand Interaction in the Continuous Casting of Steel Billets. Part II. Industrial Trials", Ironmaking and Steelmaking, 1993, vol. 20, No. 1, pp. 54-62.

74. I.V. Samarasekera, J.K. Brimacombe, H.M. Adjei-Sarpong, P.K. Agarwal, B.N. walker, D.P. Lorento: "Basic Knowledge for the Intelligent Continuous Casting Mould" to be presented at the 2nd Canada-Japan Symposium on Steelmakin and Continuous Casting, 33rd Conference of Metallurgists, CIM, Toronto, Canada, 20-25 August 1994.

75. I.V. Samarasekera, J.K. Brimacombe, K. Wilder: "The Pursuit of Steel Billet Quality", Iron and Steelmaker, 1994, vol. 21(3), pp. 53-63.

76. S. Chandra, J.K. Brimacombe and I.V. Samarasekera: "Mould Strand Interaction in the Continuous Casting of Steel Billets. Part III. Mould Heat Transfer and Mould Taper", Iron and Steelmaking, 1993, vol. 20, pp. 104-112

77. J.K. Brimacombe: "Empowerment with Knowledge - Toward the intelligent Mould for the Continuous Casting of Steel Billets", Metall. Trans. B, 1993, vol. 24B, pp. 917-935.

78. E.T Turkdogan: "Causes and Effects of Nitrides and Carbonitride Precipitation During Continuous Casting", Iron and Steelmaker, pp. 403.

79. F.A. Pellicani, R. Szezesy and F. Vilette: "Inovative Process for Production of Contnuous Casting of Boron Steel Using Cored Wire Injection" , Electric Steelmaking and Billet Casting of Highly Deoxidized Steels, Hamilton, Ontario, Canada, 10-12 May 1988.

80. J.E. Morral and T.B. Cameron: "Boron Hardenability Mechanisms:, Proceedings of the International Symposium on Boron Steels, September 18, 1979.

81. U.B.C. Billet Quality Team, Report to Alta Steel, Unpublished Work, 1994.